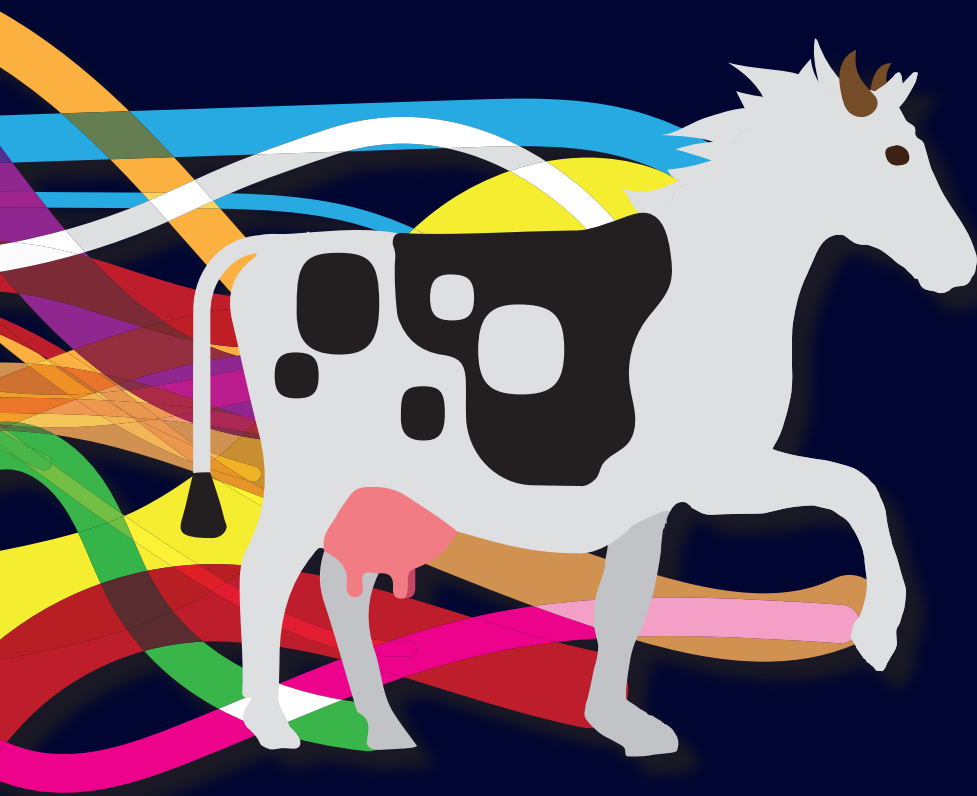


# Locomotion analysis in horses and cows based on sensor signals



Marij Tijssen

# **Locomotion analysis in horses and cows based on sensor signals**

**Marij Tijssen**

## **Colofon**

### **Locomotion analysis in horses and cows based on sensor signals**

PhD thesis with summary in Dutch

M. Tijssen

ISBN 978-94-93270-10-7

Cover Design by Proefschrift-aio.nl

Layout by Guus Gijben | Proefschrift-aio.nl

Printed by Proefschrift-aio.nl

© 2021 Marij Tijssen

No part of this publication may be reproduced or transmitted in any form or by any means without prior written permission from the author or, when appropriate, from the aforementioned publishers.

# **Locomotion analysis in horses and cows based on sensor signals**

## **Locomotie-analyse bij paarden en koeien op basis van sensor signalen**

(met samenvatting in het Nederlands)

### **Proefschrift**

ter verkrijging van de graad van doctor aan de  
Universiteit Utrecht  
op gezag van de  
rector magnificus, prof.dr. H.R.B.M. Kummeling,  
ingevolge het besluit van het college voor promoties  
in het openbaar te verdedigen op

dinsdag 5 oktober 2021 des middags te 4.15 uur

door

**Marij Tijssen**

geboren op 7 januari 1988  
te Amsterdam

**Promotoren:**

Prof. dr. M. Nielen

Prof. dr. J.A.P. Heesterbeek

**Copromotoren:**

Dr. F.M. Serra Bragança

Dr. E.L. Hernlund

**Two roads diverged in a wood, and I—  
I took the one less traveled by,  
And that has made all the difference.**

- Robert Frost



# Contents

<b>Chapter 1</b>	General introduction and outline of the thesis	9
------------------	--	---

## **Part 1: Development of signal analysis procedures**

<b>Chapter 2</b>	Automatic hoof-on and -off detection in horses using hoof-mounted inertial measurement unit sensors	21
------------------	---	----

<b>Chapter 3</b>	Automatic detection of break-over phase onset in horses using hoof-mounted inertial measurement unit sensors	51
------------------	--	----

## **Part 2: Application of signal analysis procedures to another species**

<b>Chapter 4</b>	Kinematic gait characteristics of straight line walk in clinically sound dairy cows	83
------------------	---	----

<b>Chapter 5</b>	Kinematic gait characteristic changes in induced hind limb lameness in dairy cows	123
------------------	---	-----

<b>Chapter 6</b>	General discussion	149
------------------	--------------------	-----

Nederlandse samenvatting	165
--------------------------	-----

Dankwoord	171
-----------	-----

Authors affiliations	177
----------------------	-----

Curriculum Vitae	181
------------------	-----





# 1

## General introduction

## Background

Horses and cows are both domesticated quadrupeds for which the proper functioning of their locomotor system is important for their health, well-being and performance (1-4). The performance of horses' and cows' locomotor system can be studied by observing their motion and behavior (such as standing time, lying time and eating time) as well as the specific sequence of the limb motion (e.g. walk, trot, canter etc.). Furthermore, the study of gait plays an important role in identifying deviation from normal gait patterns due to compensatory movements to avoid pain and discomfort, which is highly valuable for lameness detection, and hampers animal welfare (5, 6).

There are multiple methods to study and measure motion and gait. The most commonly used method in clinical surroundings is visual scoring during which the locomotion is visually inspected, which is often used for lameness assessment (9). Different locomotion scores and grading methods have been developed to inspect different gait characteristics such as motion asymmetry, body poses and position of the back. However, this method lacks objectivity and delivers variable accuracy and reliability due to discrepancies between observers (10, 11). To overcome these limitations, more objective and advanced methods are developed which can be subdivided in kinetic and kinematic methods. Kinetics studies the relationships between motion and forces and torques, while kinematics is the study of motion (without consideration of forces) in respect to time.

### Kinetic methods

In kinetic measurements, a device called the force plate is considered the gold standard. The main working principle of the force plate is to measure the ground reaction forces exerted under the foot of the animal when standing on the force plate. Force plates are a robust method with high accuracy (12), and they come in different sizes and complexity. There are single pedestal force plates that can measure the weight distribution during standing, in contrast to multiple pedestal force plates which can measure consecutive steps. The simplest force plate measures the force in one direction while more advanced force plates can measure the ground reaction force in all three directions. The disadvantage of force plates is that they are expensive tools and therefore limit the number of consecutive steps that can be measured. It is also very time consuming to measure consecutive strides with single pedestal force plates. Furthermore, they are heavy and can therefore only be used in a laboratory setting (13). To overcome these limitations, a force measuring treadmill (large rectangle in Fig 1) has been



designed to measure consecutive strides but it requires accustomed locomotion of the animal and is even more expensive than several force plates (14).

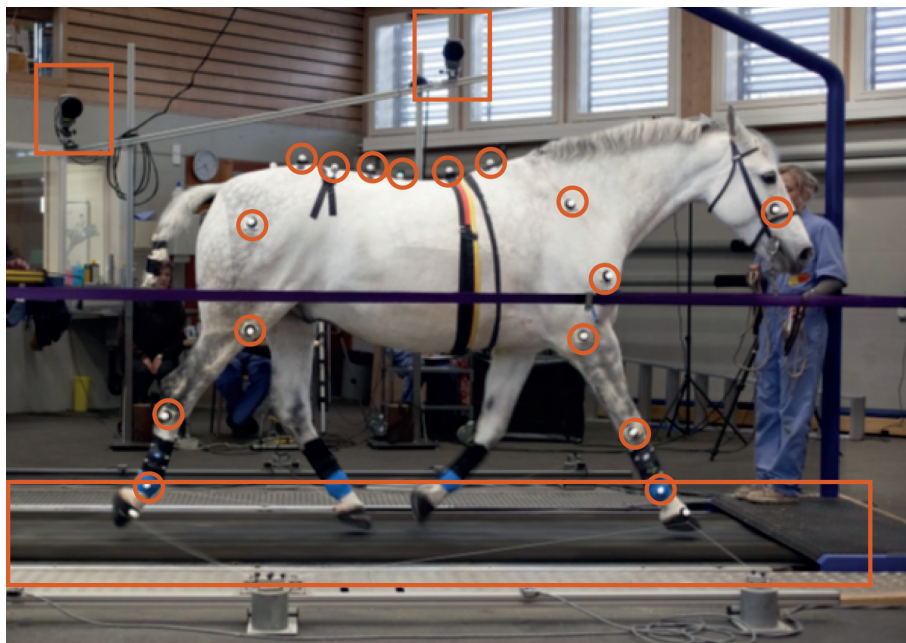


**Figure 1.** A horse equipped with reflective markers (circles) is trotting on a treadmill (large rectangle) surrounded by infrared cameras (small rectangles) (figure is obtained from (7) and made by M.A. Weishaupt (8)).

### Kinematic methods

The gold standard for kinematics is considered to be a video-based motion capture system that tracks the movements of infra-red markers. The markers (circles in Fig 1) can be placed on multiple anatomical locations of the animal and the position of the markers is measured over time with infrared cameras (small rectangles in Fig 1). The position data of the markers is used to calculate the displacement and velocity, in addition to the angle between two markers (12, 13). Measurements with these systems result in a large amount of data of multiple anatomical locations, which makes it possible to gain extensive insight in multiple gait characteristics. Furthermore, the accuracy and precision of these systems is fairly high (15, 16). However, the usefulness in the field is limited because these systems are expensive and not easy to relocate due to the number of cameras and infrastructure needed (12). Nowadays, upcoming development of computer vision

techniques are providing marker less tracking where anatomical locations can be automatically followed based on video images. This development is less precise, but the ease of use makes it an interesting approach for future incorporation in clinical settings and farms (17, 18). However, knowledge about the healthy gait characteristics and deviations from what is considered to be normal is needed before these techniques can be used accurately.

## Inertial Measurement Units

An alternative kinematic method that can more easily be used under various field conditions are Inertial Measurement Units (IMUs). These IMUs measure acceleration and angular velocity in three directions with an accuracy high enough to study changes in gait characteristics, although this is less accurate compared to optical motion capture systems (19, 20). Advantages of IMUs are that multiple IMUs can be attached to the animals on various anatomical locations (Fig 2) while being synchronized in time to make it possible to measure consecutive strides. Furthermore, the whole system is wireless and relatively cheap (12, 13). Like the optical motion capture systems, large amounts of data of multiple anatomical locations can be obtained and displacement, velocity, acceleration and angles can be calculated from the data (Fig 2).

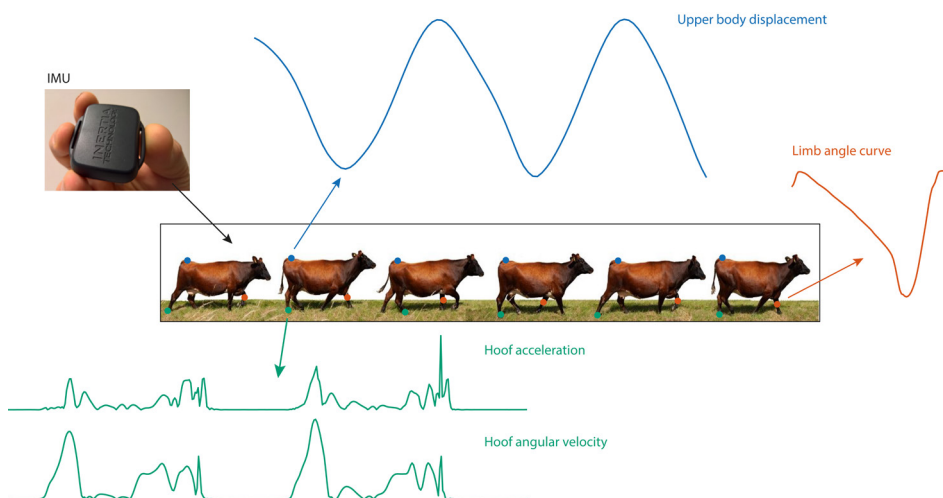


**Figure 2. An IMU is shown in the upper left part and data obtained from different anatomical locations is shown.** Different types of data can be obtained depending on the anatomical location, such as upper body displacement data from the tuber sacrale (blue), limb angle data from the left front limb (orange) and hoof acceleration and angular velocity (green).

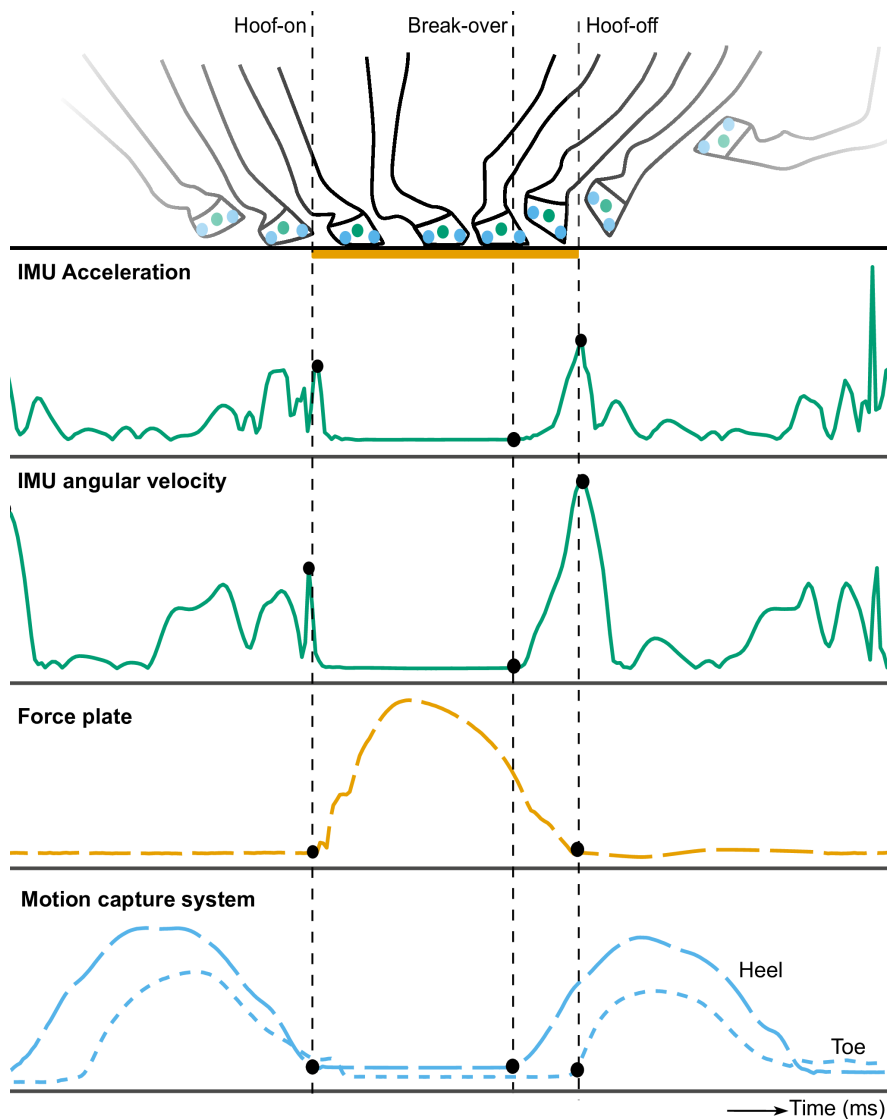


**Figure 3.** Hoof-on and hoof-off events are shown with the break-over phase onset in the upper part of the figure. The corresponding acceleration and angular velocity data of an IMU attached to the hoof are shown in green, the corresponding force plate data is shown in yellow and the corresponding motion capture data of markers placed on the heel and toe is shown in blue.

## Data processing

IMUs have a great potential to monitor sport performance of horses, and to provide objective data for evaluation of orthopedic rehabilitation and injury prevention in both horses and cows. In Fig 2, the IMU data is shown for different anatomical attachment places. Important gait characteristics for lameness detection are support durations of the limbs, limb angles and upper body displacement. Another important characteristic is the break-over phase onset (Fig 3) that gives information about the hoof-unrollment pattern and can assist the farrier. Before these characteristics can be studied, the data should be preprocessed and hoof-on and hoof-off timings should be obtained from the data (Fig 3). Depending on the method and on the anatomical location, the data shows different patterns. Furthermore, foot-fall patterns can be obtained from the hoof-events which can be used to differentiate between different gaits. This is valuable for exercise purposes in equestrian sport (21).

## Aim and outline of this thesis

Although there are many advantages of using IMUs, the analysis of the IMU data is time consuming and might be subjective when no automatic signal analysis procedures are implemented. However, these automatic analysis techniques do not yet exist and need to be developed. In addition, the performance of these analysis techniques needs to be evaluated against the gold standards (force plate and optical motion capture system). The aim of this thesis is to develop and apply different signal analysis procedures on IMU data obtained for the study of kinematic gait characteristics in horses. The performance of these signal analysis procedures is evaluated by comparison with the force plate and optical motion capture system. The second aim of this thesis is to implement IMUs and both measurement and signal analysis procedures from horse to cows with the aim to study kinematic gait characteristics since horses and cows are both quadrupeds with a similar locomotion apparatus. This is a novel approach for which knowledge about the kinematic gait characteristics in healthy cows is described first. Thereafter, a start has been made with the study to identify the changes in kinematic gait characteristics due to hindlimb lameness.

## Part 1: Development of signal analysis procedures

In the first part of this thesis, the procedures of newly developed algorithms are described for the automatic detection of hoof-events from hoof-mounted IMU signals. In **Chapter 2**, the focus will be on two algorithms to detect hoof-



on and hoof-off events. The performance of these algorithms is evaluated by comparison with results obtained with the force plate. In **Chapter 3**, the focus will be on two algorithms to detect the break-over phase onset and on evaluating the performance of these algorithms by comparison with results obtained from both the optical motion capture system and force plate.

## **Part 2: Application of signal analysis procedures to another species**

In the second part of this thesis, explorative studies are performed with IMUs attached to the upper body and limbs of dairy cows. For both chapters, horse algorithms were modified for the analysis of the cow data. In **Chapter 4**, an overview of the biomechanical gait characteristics and the appearance of IMU signals is given for clinically sound dairy cows. In **Chapter 5**, the same biomechanical gait characteristics are compared for clinically sound cows and cows with induced hind limb lameness.

In **Chapter 6**, the challenges that came with these studies are discussed, followed by a presentation of two case studies with different sensor techniques in other species. This chapter concluded on the application of sensors and development of analysis procedures.



## References

1. Egenvall A, Bonnett B, Wattle O, Emanuelson U. Veterinary-care events and costs over a 5-year follow-up period for warmblooded riding horses with or without previously recorded locomotor problems in Sweden. *Prev Vet Med.* 2008;83(2):130-43.
2. Booth CJ, Warnick LD, Gröhn YT, Maizon DO, Guard CL, Janssen D. Effect of Lameness on Culling in Dairy Cows. *Journal of Dairy Science.* 2004;87(12):4115-22.
3. Jeffcott LB, Rossdale PD, Freestone J, Frank CJ, Towers-Clark PF. An assessment of wastage in thoroughbred racing from conception to 4 years of age. *Equine Vet J.* 1982;14(3):185-98.
4. Garbarino EJ, Hernandez JA, Shearer JK, Risco CA, Thatcher WW. Effect of Lameness on Ovarian Activity in Postpartum Holstein Cows. *Journal of Dairy Science.* 2004;87(12):4123-31.
5. Leach KA, Tisdall DA, Bell NJ, Main DC, Green LE. The effects of early treatment for hindlimb lameness in dairy cows on four commercial UK farms. *Vet J.* 2012;193(3):626-32.
6. Why HR, Shearer JK. The Impact of Lameness on Welfare of the Dairy Cow. *Vet Clin North Am Food Anim Pract.* 2017;33(2):153-64.
7. Serra Braganca FM, Hernlund E, Thomsen MH, Waldern NM, Rhodin M, Bystrom A, et al. Adaptation strategies of horses with induced forelimb lameness walking on a treadmill. *Equine Vet Journal.* 2020.
8. Weishaupt MA. Equine Sports Medicine, Equine Department, Vetsuisse Faculty University of Zurich.
9. Why H. Locomotion scoring and lameness detection in dairy cattle. In *Practice.* 2002;24(8):444-9.
10. Schlageter-Tello A, Bokkers EAM, Koerkamp PWGG, Van Hertem T, Viazzi S, Romanini CEB, et al. Comparison of locomotion scoring for dairy cows by experienced and inexperienced raters using live or video observation methods. *Animal Welfare.* 2015;24(1):69-79.
11. Flower FC, Weary DM. Gait assessment in dairy cattle. *Animal.* 2009;3(1):87-95.
12. Bosch S, Serra Braganca F, Marin-Perianu M, Marin-Perianu R, van der Zwaag BJ, Voskamp J, et al. EquiMoves: A Wireless Networked Inertial Measurement System for Objective Examination of Horse Gait. *Sensors (Basel).* 2018;18(3).
13. Serra Braganca FM, Rhodin M, van Weeren PR. On the brink of daily clinical application of objective gait analysis: What evidence do we have so far from studies using an induced lameness model? *Vet J.* 2018;234:11-23.
14. Weishaupt MA, Hogg HP, Wiestner T, Denoth J, Stussi E, Auer JA. Instrumented treadmill for measuring vertical ground reaction forces in horses. *Am J Vet Res.* 2002;63(4):520-7.
15. Windolf M, Gotzen N, Morlock M. Systematic accuracy and precision analysis of video motion capturing systems--exemplified on the Vicon-460 system. *J Biomech.* 2008;41(12):2776-80.
16. Eichelberger P, Ferraro M, Minder U, Denton T, Blasimann A, Krause F, et al. Analysis of accuracy in optical motion capture - A protocol for laboratory setup evaluation. *J Biomech.* 2016;49(10):2085-8.
17. Song X, Leroy T, Vranken E, Maertens W, Sonck B, Berckmans D. Automatic detection of lameness in dairy cattle—Vision-based trackway analysis in cow's locomotion. *Computers and Electronics in Agriculture.* 2008;64(1):39-44.
18. O'Leary NW, Byrne DT, O'Connor AH, Shalloo L. Invited review: Cattle lameness detection with accelerometers. *J Dairy Sci.* 2020;103(5):3895-911.
19. Peham C. Signals from material. In: Clayton HM, Back W, editors. *Equine Locomotion.* Second Ed. ed. St. Luis, MO, USA: Saunders Elsevier; 2013. p. 61-71.
20. Clayton HM, Schamhardt HC. Measurement techniques for gait analysis. In: Clayton HM, Back W, editors. *Equine Locomotion.* Second Ed ed. St. Luis, MO, USA: Saunders Elsevier; 2013. p. 31-60.



21. Serra Braganca FM, Broome S, Rhodin M, Bjornsdottir S, Gunnarsson V, Voskamp JP, et al. Improving gait classification in horses by using inertial measurement unit (IMU) generated data and machine learning. *Sci Rep.* 2020;10(1):17785.



# **Part 1**

## **Development of signal analysis procedures**



# 2

## **Automatic hoof-on and -off detection in horses using hoof-mounted inertial measurement unit sensors**

2

Published in PLoS One, 2020, 15:6

M. Tijssen  
E. Hernlund  
M. Rhodin  
S. Bosch  
J.P. Voskamp  
M. Nielen  
F.M. Serra Bragança

## Abstract

For gait classification, hoof-on and hoof-off events are fundamental locomotion characteristics of interest. These events can be measured with inertial measurement units (IMUs) which measure the acceleration and angular velocity in three directions. The aim of this study was to present two algorithms for automatic detection of hoof-events from the acceleration and angular velocity signals measured by hoof-mounted IMUs in walk and trot on a hard surface. Seven Warmblood horses were equipped with two wireless IMUs, which were attached to the lateral wall of the right front (RF) and hind (RH) hooves. Horses were walked and trotted on a lead over a force plate for internal validation. The agreement between the algorithms for the acceleration and angular velocity signals with the force plate was evaluated by Bland Altman analysis and linear mixed model analysis. These analyses were performed for both hoof-on and hoof-off detection and for both algorithms separately. For the hoof-on detection, the angular velocity algorithm was the most accurate with an accuracy between 2.39 and 12.22 ms and a precision of around 13.80 ms, depending on gait and hoof. For hoof-off detection, the acceleration algorithm was the most accurate with an accuracy of 3.20 ms and precision of 6.39 ms, independent of gait and hoof. These algorithms look highly promising for gait classification purposes although the applicability of these algorithms should be investigated under different circumstances, such as different surfaces and different hoof trimming conditions.



## Introduction

Gait analysis is an important element for the understanding of equestrian sport and can be performed by examining gait characteristics and body segment positions of the horse while moving. Gaits can be distinguished by their foot-fall pattern in addition to knowledge about the duration of the support phase compared to the whole stride duration of one leg (1). For gait classification, the fundamental locomotion characteristic is the timing of hoof placement, i.e. hoof-on and hoof-off events from all limbs. These events can be examined visually but due to the limitations of the temporal resolution of the human eye (2) there are limitations to how well these events can be distinguished. Instead, objective measurement tools such as force plates, optical motion capture (OMC) systems and inertial measurement units (IMUs) are used (3).

In general, the force plate is considered the gold standard for kinetic gait analysis. With this method, hoof impacts can be registered from the vertical force signal by applying a threshold which is subjective. Furthermore, data collection is time consuming (4) and this method can only be used in a laboratory settings. In addition, multiple consecutive strides can only be measured with a force measuring treadmill and by force measuring shoes (3), which can alter the kinematics (5, 6). OMC systems and IMUs can also be used to measure consecutive strides and OMC systems are considered the gold standard for kinematic gait analysis. However, these systems are expensive and not easy to relocate due to the significant number of cameras and infrastructure needed. Therefore, OMC systems have limited usefulness in field conditions (7). IMUs can easily be used in field conditions because they are portable, wireless and are becoming relatively cheap. Consequently, IMUs improve the possibilities for gait analysis in field conditions.

Previous studies investigated the accuracy and precision of IMUs compared with the force plate (8, 9) and OMC systems (7, 10-12) and showed the potential of IMUs for gait analysis and classification. However, analysis of the data and extraction of hoof-events was performed manually or semi-manually which is time consuming and subjective. Time reduction and objectivity can be gained by developing an algorithm for automatic detection of hoof-on and hoof-off events from the output of the IMUs (3). The output of the IMUs consists of tri-axial acceleration and angular velocity signals. Recently, one study was performed to evaluate multiple algorithms for hoof-event detection and validation against the force plate (13). In this study, distal limb mounted IMUs were used and the best performing algorithm of this study showed an accuracy between -19.7 and 17.6 ms and a precision between



7.5 and 31.0 ms, depending on gait, limb and hoof-event (13). The accuracy found in that study was sufficient for gait classification, although the precision was less satisfactory. The performance of this algorithm might be improved by attaching the IMUs closer to the location of impact, i.e. the hoof of the horse, hence limiting the attenuation of the vibrations through the limb (14, 15).

During this study, two algorithms for automatic hoof- events detection based on the acceleration and angular velocity signals measured by hoof-mounted IMUs in walk and trot on a hard surface were developed. For gait classification, the needed accuracy and precision for hoof-event detection are not yet investigated. However, estimations of stance and swing durations in addition to knowledge about the timing of lateral and diagonal hoof placement are essential. We therefore aim for accuracies and precisions similar or better compared with the study of Bragança et al. (2017) (13).

## **Materials and Methods**

At the start of this study, force plate and IMU data were visually examined. The IMU data showed distinctive peaks coinciding with the hoof-on and hoof-off times measured with the force plates, as previous described by Olsen et al. (9) and depicted in Fig 1. During the current study, we developed two algorithms to detect these distinctive peaks from the IMU data and applied a more advanced method to determine the hoof-on and hoof-off times from the force plate. These contact times of the force plate were used for the internal validation of the algorithms.

### **Data collection**

For the current study, we used data that was collected for a previous study (13). Measurements were performed on seven Warmblood horses (*Equus ferus caballus*; for further details see S1 Appendix) in the Equine Clinic of Utrecht University at the Department Clinical Sciences.

All horses were equipped with ProMove-mini wireless IMUs (Inertia-Technology B.V., Enschede, The Netherlands; for further details see S1 Appendix) which measured the acceleration, low-*g* acceleration with a range of  $\pm 16 g$  and high-*g* acceleration with a range of  $\pm 400 g$ , and angular velocity, with a range of  $\pm 2000$  °/s, and sampling frequency of 200 Hz. Two IMUs were attached to the lateral wall of the right front (RF) and hind (RH) hooves with double sided and normal tape as can be seen in Fig 2.

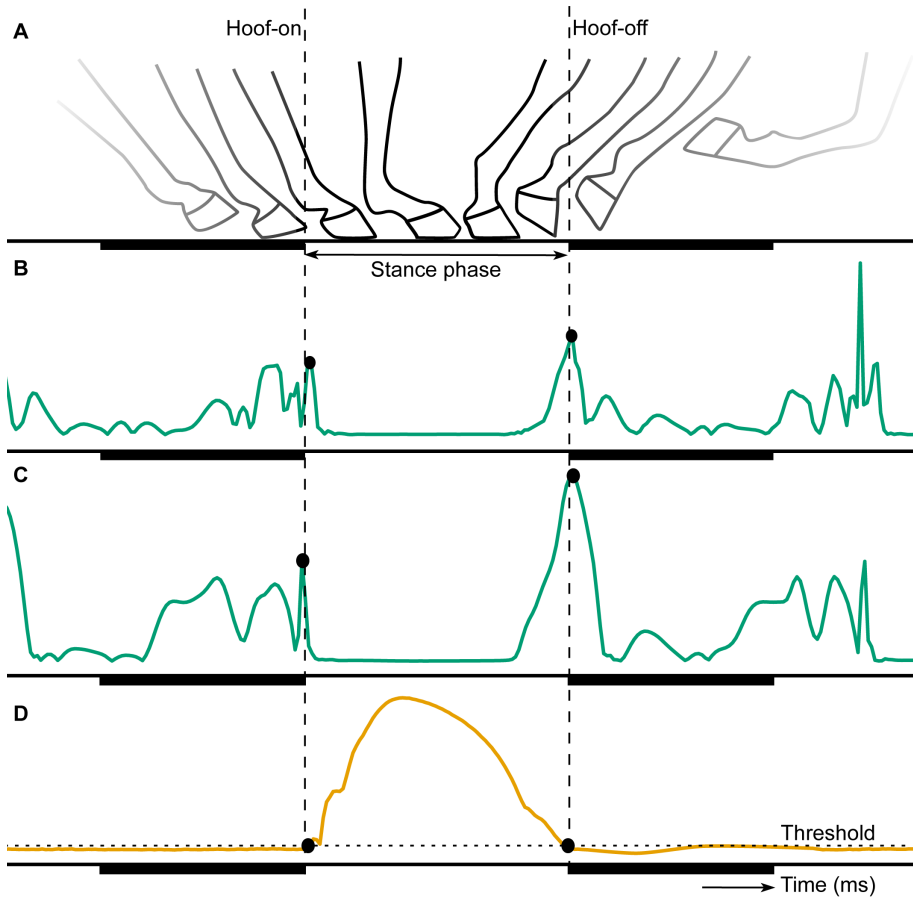


**Figure 1. Generic illustration of the movement of the hoof (A), modified from Witte et al. (8), and the signals of the acceleration (B), angular velocity (C) and vertical force (D).** The hoof-on and hoof-off events are depicted with the vertical dashed lines and the dots show the detected hoof-on and hoof-off events from the different signals. These hoof-events occur at the start and end of the stance phase, shown as the period not underlined by a dark beam. The horizontal dashed line in D shows the threshold used to detect the hoof-events from the force signal.



**Figure 2. Location of inertial measurement units (IMUs) on the hoof.** The location of the IMUs is indicated with red arrows, on the lateral quarter of the right front and hind hoof with reflective markers on both sides (lateral heel, lateral toe and lateral coronet) used for another study (13).

All horses were walked and trotted over a force plate (Z4852C, Kistler, Winterthur, Switzerland; for further details see S1 Appendix) to collect at least five valid force plate impacts for both front and hind hooves; each valid impact will be considered a trial in the further analysis. An impact was considered valid if two criteria were met: 1) only one entire hoof was placed on the force plate and 2) the horse was led in a straight line with a constant speed of 0.8 to 1.4 m/s for walk and 1.7 to 2.7 m/s for trot.

Three reflective markers of the OMC system (Qualisys AB, Motion Capture System, Göteborg, Sweden; for further details see S1 Appendix) were glued to lateral heel, lateral toe and lateral coronet of each hoof as can be seen in Fig 2. The collected OMC data were used in another study for break-over detection (16) but was needed for time synchronization in the current study.

The force plate and OMC system were time synchronized by a hardware connection ((13); for further details see S1 Appendix). Time synchronization of the OMC system and the IMUs was accomplished by calculation of a cross-correlation between the angular velocity signal of the IMUs and the position signal of the reflective markers of the OMC system ((7, 13); for further details see S1 Appendix).

The original horse measurements were performed in compliance with the Dutch Act on Animal Experimentation and approved by the local ethics committee of Utrecht University. All horses were present for teaching purposes and these measurements were not considered additional animal experiments within the Dutch law at that time. Therefore, no specific experiment number is available.

## **Data analysis**

### ***Force plate data***

The collected force plate data were preprocessed by Inertia Technology B.V.. The valid impacts were selected and cut into different trials; each trial consisted of at least one valid impact and sometimes two for consecutive impacts of the RF and RH hoof.

In Fig 1D, the vertical force signal of one valid impact can be seen. The dotted lines show the hoof-on and hoof-off time points, for the detection of which a threshold was used. This threshold value was calculated from the signal mean ( $\bar{x}$ ) and signal standard deviation ( $s$ ) of the baseline, i.e. the period before the valid impact happened. To distinguish the impacts from the baseline, the average of the force signal was calculated with a moving mean window with a length of 130



ms and the baseline was determined for average values below 100 N. For every trial, a threshold value (T) was determined by:

$$T = x + 2.58 \times s$$

The standard deviation was multiplied by 2.58 resulting in detection of the upper 0.5% of a normally distributed signal, to ensure that only high impacts are detected.

Hoof-on was determined as the first time point that the vertical force exceeded the threshold value. Hoof-off was determined as the first time point that the vertical force dropped below the threshold value.

### ***IMU data***

The collected IMU data were preprocessed by Inertia Technology B.V. and cut into different trials corresponding with the force plate trials. The collected IMU data consisted of two tri-axial acceleration signals, a low *g* acceleration signal and a high *g* acceleration signal, and one tri-axial angular velocity signal. The two acceleration signals were fused into one tri-axial acceleration signal that was used during the current study (7). Further data analysis was performed in MATLAB (version R2017a, The MathWorks Inc., Natick, Massachusetts, USA).

The preprocessed tri-axial acceleration and angular velocity signals were further prepared for analysis in two steps: 1) offset drift was removed from the acceleration signal, and 2) the root of the sum of squares, Euclidean norm, was calculated of the tri-axial acceleration and angular velocity signals resulting in a one-directional acceleration and angular velocity signal. The Euclidean norm was used to reduce the calculation time in contrast to calculating a horse specific rotation matrix (11) and to cancel out artefacts due to wrong alignment of the sensor on the hoof. This will make the algorithms better applicable in field setting.

The preprocessed signal is shown in Fig 3A. To distinguish consecutive steps from each other, the stance phase and the swing phase of a limb were estimated by calculating the variance of the acceleration and angular velocity signals. The variance was calculated by applying a moving variance function over the two signals with window length of 130 ms. The variance of the angular velocity was higher than the variance of the acceleration signal and to accommodate for this we downscaled the variance of the angular velocity with a factor of twenty-five. The stance phase was determined when both signals had a variance below five,

the remaining time points were allocated to the swing phase. The window length, downscale factor and variance threshold were kept the same for all horses and trials. These values were chosen to ensure that: 1) all time points of the swing phase were allocated to the estimated swing phase, and 2) every swing phase was succeeded by a stance phase. This procedure resulted in an estimated swing phase longer than the real swing phase to make sure that hoof-on and hoof-off events were included in the roughly estimated swing phase. The estimated swing phase is indicated by the box in Fig 3B.

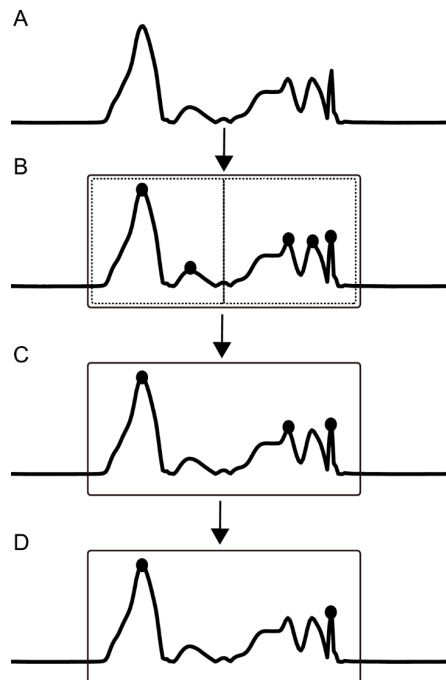


**Figure 3. Generic illustration of an IMU signal and the steps performed by both algorithms.**

The preprocessed signal is indicated in A. The estimated swing phase is indicated with the box in B. For the angular velocity signal, the peaks within one estimated swing phase are detected (B). From these peaks, peaks were selected if the peak height or prominence was bigger than the mean peak height or prominence, or both (C). Thereafter, the peak closest to the start of the estimated swing phase was selected as the hoof-off time point and the peak closest to the end of the estimated swing phase was selected as the hoof-on time point (D). For the acceleration signal, these steps were performed for the first and second half of the estimated swing phase, indicated with the dotted boxes in B.



Next, we determined the hoof-on and hoof-off from the acceleration and angular velocity signal separately by developing two algorithms.

The algorithm for the angular velocity signal assessed every swing phase separately. Peaks were detected, indicated by the dots in Fig 3B, and the mean peak height and mean peak prominence were calculated from these peaks. The peak prominence depicted how much the peak stands out due to its intrinsic height and location relative to the other peaks. Peaks were selected if the peak was higher than the mean peak height or the prominence was bigger than the mean prominence, or both. These selected peaks are indicated by the dots in Fig 3C. Hoof-off was determined as the time point corresponding with the peak closest to the start of the estimated swing phase. For hoof-on detection, only the detected peaks of the second half of the swing phase were assessed. Again, the mean peak height and mean peak prominence were calculated. Peaks were selected if the peak was higher than the mean peak height or the prominence was bigger than the mean prominence, or both. Hoof-on was determined as the time point corresponding with the peak closest to the end of the estimated swing phase. The peaks selected as hoof-off and hoof-on are indicated with dots in Fig 3D.

The algorithm for the acceleration signal assessed the signal in a similar manner as described above. However, only the peaks detected in the first half of the swing phase were assessed for hoof-off detection and the peaks detected in the second half of the swing phase were assessed for hoof-on. The first and second half of the swing phase are indicated by the dotted boxes in Fig 3B. After this step, peaks were detected, indicated by the dots in Fig 3B, and the mean peak height and mean peak prominence were calculated from these peaks. Peaks were selected if the peak was higher than the mean peak height or the prominence was bigger than the mean prominence, or both. These selected peaks are indicated by the dots in Fig 3C. Hoof-off was determined as the time point corresponding with the peak closest to the start of the estimated swing phase. Hoof-on was determined as the time point corresponding with the peak closest to the end of the estimated swing phase. The peaks selected as hoof-off and hoof-on are indicated with dots in Fig 3D.

### ***Stride parameter estimation***

With the determined hoof-on and hoof-off time points the following stride parameters were determined:

- Stance duration – time between hoof-on and hoof-off of the same hoof
- Hoof-on time difference – time difference between the hoof-on detection of both algorithms were assessed with the force plate hoof-on detection separately for a given hoof
- Hoof-off time difference – time difference between the hoof-off detection of both algorithms were assessed with the force plate hoof-off detection separately for a given hoof

### **Performance evaluation**

The normality of the stride parameters was visually checked by examining the QQ plot and histogram in R (version 1.1.414, RStudio Inc, Boston, Massachusetts, USA). Thereafter, the distribution of the hoof-on and hoof-off time differences was evaluated to interpret the results and the performance of both algorithms was evaluated by Bland Altman and linear mixed model analysis.

### ***Bland Altman***

The agreement between the acceleration algorithm and the force plate and the angular velocity algorithm and the force plate was evaluated for the stance duration. This evaluation compared two different methods to measure the stance duration and therefore a Bland Altman analysis was performed with the “BlandAltmanLeh” package (17).

The results of this analysis showed the mean difference in stance duration between the algorithms and the force plate and the standard deviation (SD) of these differences. These results were deemed better if closer to zero since this indicates a small and consistent difference between the algorithms and force plate, i.e. a good accuracy and precision. A positive mean indicates a shorter stance duration measured with the force plate and a negative mean indicates a longer stance duration measured with the force plate compared with the algorithms. In addition, the upper and lower confidence interval limits were used to calculate the width of the confidence interval. The width of the confidence interval was preferred to be small which means that the differences between the algorithms and the force plate were consistent.



### **Linear mixed model analysis**

A linear mixed model analysis was performed to estimate the effect of horse, hoof, gait and trial on the performance of the algorithms for all stride parameters. This analysis was performed with the “lme4” package (18). The independent variables of this analysis were the effect of hoof, gait, number of analyzed trials and interaction term between hoof and gait. The model is described by:

$$Y_{ijkl} \sim \mu + \text{hoof}_i + \text{gait}_j + \text{trial}_k + (\text{hoof} \times \text{gait})_{ij} + (1|\text{horse}) + \epsilon_{ijkl}$$

where  $Y_{ijkl}$  is the predicted value of the  $ijkl$ -th record,  $\mu$  is the overall mean,  $\text{hoof}_i$  is the effect of hoof ( $i$  can be RF or RH hoof),  $\text{gait}_j$  is the effect of gait ( $j$  can be walk or trot),  $\text{trial}_k$  is the effect of trial ( $k$  can be 1 until 9 depending on the number of trials collected for a horse),  $(\text{hoof} \times \text{gait})_{ij}$  is the effect of the interaction between  $\text{hoof}_i$  and  $\text{gait}_j$  and  $\epsilon_{ijkl}$  is the residual error term associated with the  $ijkl$ -th record. A random intercept for every horse was included in the model.

Model reduction was applied with the Akaike’s information criterion and the model with the lowest Akaike’s information criterion values was selected according to Occam’s Razor principle. The residuals of each selected model were visually inspected and checked for any deviations of normality and homoscedasticity. The predicted value of the stance duration and the time difference between the algorithms and the force plate ( $Y$ ) were calculated for every combination of  $\text{hoof}_i$  and  $\text{gait}_j$  (“emmeans” package (19)). In addition, the lower and upper limits were calculated of the 95% confidence interval (“MASS” package (20)).

The performance of these algorithms was evaluated based on the predicted values and width of the confidence intervals. For the stance durations, the predicted values of both algorithms were deemed better if closer to the predicted value of the force plate and the width of the confidence interval was preferred to be small, which indicates a good precision. For the hoof-on and hoof-off time differences between the algorithms and the force plate, the predicted value was deemed better if closer to zero since this indicates a small difference between the algorithms and force plate, i.e. a good accuracy. A positive predicted value indicates a delayed detection by the algorithms and a negative predicted value indicates a too early detection by the algorithms compared with the force plate measurement. The width of the 95% confidence interval was preferred to be small, which means that the differences between the algorithms and the force plate were consistent, i.e. a good precision. Schematic representations of these predicted values were used to evaluate the accuracy and precision of the algorithms.



## Results

A total of 147 trials were analyzed: 75 trials of the right front (RF) hoof (36 in walk and 39 in trot) and 72 trials of the right hind (RH) hoof (34 in walk and 38 in trot). In Table 1 an overview is given of the number of the analyzed trials and hoof and gait characteristics. Preprocessed data of one measurement in trot can be seen in Fig S1. Stance durations were calculated and can be found in Table S1. The stride parameters were normally distributed.

**Table 1. Number of analyzed trials collected per horse, gait and hoof.**

horse ID		1	2	3	4	5	6	7	total
Walk	RF	5	5	5	5	5	6	5	36
	RH	5	5	5	4	5	5	5	34
Trot	RF	5	5	6	5	8	5	5	39
	RH	7	5	5	5	5	6	5	38
		22	20	21	19	23	22	20	147

The distributions of the time differences for hoof-on detection are illustrated in Fig 4A for the acceleration algorithm and in Fig 4B for the angular velocity algorithm. The distribution in both figures show higher values for the RH hoof in walk and lower values for the RF hoof in trot. The distribution in Fig 4A has a mean around 7 ms in contrast to the distribution in Fig 4B which has a mean of 16.5 ms. Furthermore, in Fig 4A there are no outliers in contrast to Fig 4B in which the distribution has outliers around -75 and 50 ms.

The distributions of the time differences for hoof-off detection are illustrated in Fig 4C for the acceleration algorithm and in Fig 4D for the angular velocity algorithm. The distribution in Fig 4C has a lower mean, around 0.78 ms, compared to the distribution in Fig 4D which has a mean of 3.2 ms. In Fig 4C, the distribution has outliers around -57.5, 55 and 150 ms in contrast to the distribution in Fig 4D which has outliers around -50 and 50 ms. For both models, no clear distinction could be made between the different hoof/gait combinations.

### Bland Altman analysis

The results in Table 2 show that the mean difference and SD were closer to zero for the angular velocity algorithm, except for the SD of the RF hoof in trot, which was higher compared to the acceleration algorithm. Also, the confidence intervals were smaller for the angular velocity algorithm, except for the RF hoof in trot

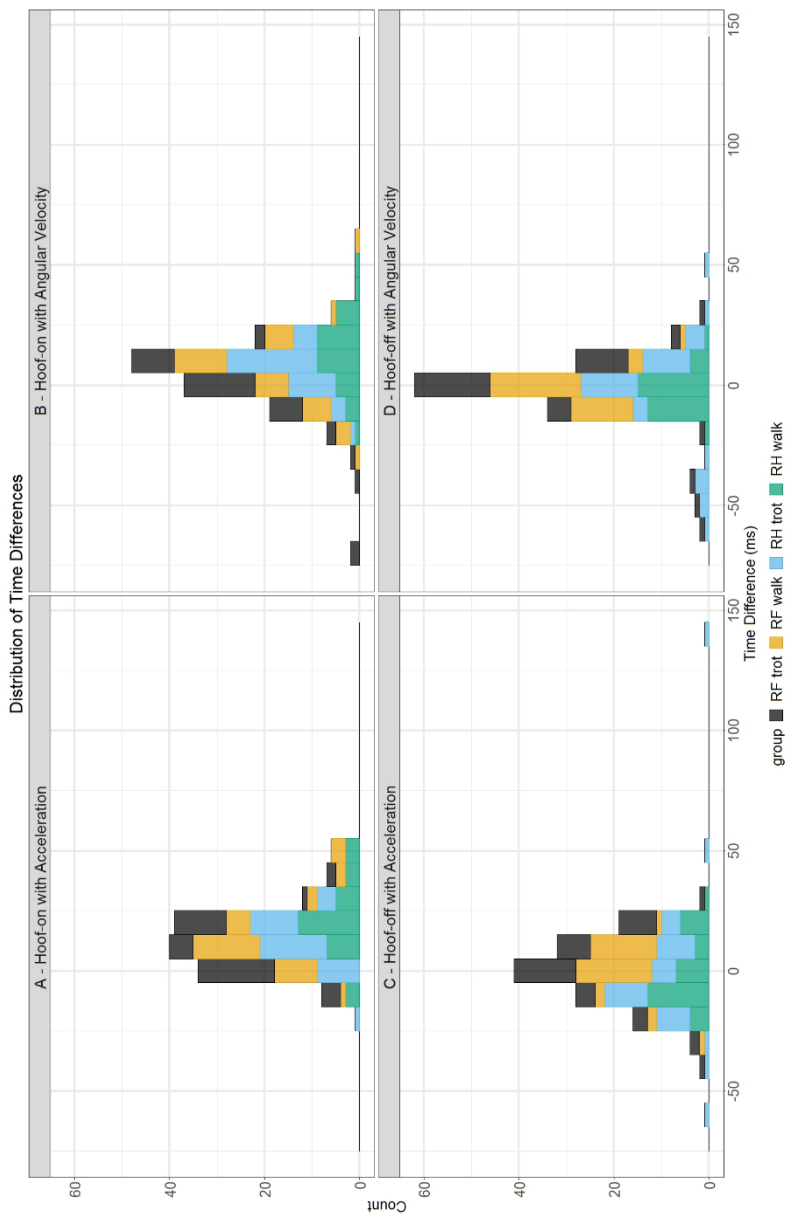


**Figure 4. Distributions of time differences between both algorithms and the force plate for hoof-on and hoof-off detection.** Time differences for hoof-on detection are depicted in the upper row and time differences for hoof-off are depicted in the bottom row. The different hoof/gait combinations are depicted with their own color.

which is caused by a higher SD. These results indicate that the agreement with the force plate was, in general, better for the angular velocity algorithm for the stance duration. Furthermore, the mean difference was negative for all groups, except for the RF hoof in trot, which means that shorter stance durations were measured with both algorithms compared to the force plate.

**Table 2. Bland Altman results for stance duration.**

			Stance duration			
			mean (ms)	SD (ms)	lower CI (ms)	upper CI (ms)
acceleration	walk	RF	-2.67	3.76	-10.05	4.71
		RH	-4.18	3.52	-11.08	2.72
	trot	RF	-1.64	3.84	-9.17	5.89
		RH	-2.39	6.18	-14.52	9.73
angular velocity	walk	RF	-1.33	3.20	-7.60	4.94
		RH	-2.88	2.86	-8.48	2.72
	trot	RF	0.74	4.98	-9.01	10.50
		RH	-1.66	4.52	-10.52	7.20

The mean differences in stance duration between the algorithms and force plate in milliseconds (ms) and the standard deviation (SD) of this mean difference in ms are deemed better if closer to zero. The 95% confidence interval was preferred to be small.

### Linear mixed model analysis

The residuals of all selected linear mixed models were normally distributed and did not show homoscedasticity.

### Hoof-on detection

The results presented in Table 3 are the models with the lowest AIC values. The predicted values of the time differences between the acceleration algorithm and the force plate (model 1) were best explained with hoof, gait, trial and interaction term as fixed effect and horse as random effect. For this model, the predicted values and lower and upper confidence interval limits were averaged over the number of analyzed trials. For the time differences between the angular velocity and the force plate (model 2), hoof and gait were needed as fixed effects and horse as random effect to explain the data best.

The results in Table 3 show that the predicted values of the time differences were smaller for the angular velocity algorithm (model 2) compared with the acceleration algorithm (model 1). All predicted values were positive which indicates a delayed detection by both algorithms compared with the force plate. Also, the confidence intervals were smaller for the angular velocity algorithm.



**Table 3. Linear mixed model results for the time differences in hoof-on and hoof-off detection.**

Hoof-on time differences					
			predicted value (ms)	lower CI (ms)	upper CI (ms)
Model 1: acceleration	walk	RF	17.93	9.33	26.52
		RH	23.96	15.35	32.57
	trot	RF	13.77	5.20	22.34
		RH	14.84	6.27	23.41
Model 2: angular velocity	walk		11.06	4.13	17.99
	trot		3.55	-3.35	10.45
		RF	2.39	-4.52	9.30
		RH	12.22	5.29	19.14

Hoof-off time differences				
		predicted value (ms)	lower CI (ms)	upper CI (ms)
Model 3: acceleration		3.20	0.05	6.34
Model 4: angular velocity		0.75	-3.83	5.32

The predicted values of the time difference between both algorithms relative to the force plate are determined in milliseconds (ms) and are deemed better if closer to zero. The 95% confidence interval was preferred to be small.

In Fig 5A, the predicted values and their confidence intervals of model 1 are shown for every hoof/gait combination because this model needs an interaction term to explain the data. In Fig 5B, the predicted values and their confidence intervals of model 2 are shown for walk versus trot and RF versus RH hoof because this model did not need an interaction term to explain the data. The predicted values are located closer to zero for model 2 and their confidence intervals are smaller.

These results indicate that the agreement with the force plate was, in general, better for the angular velocity algorithm with an accuracy between 2.39 and 12.22 ms depending on the gait and hoof and a precision of around 13.83 ms for the hoof-on detection.

### **Hoof-off detection**

The predicted values of the time differences between the acceleration algorithm and the force plate (model 3) were best explained with an empty model with no random effect. For the time differences between the angular velocity algorithm and the force plate (model 4), an empty model with random effect for horse was needed to explain the data best.

The results in Table 3 show that the predicted value was smaller for the angular velocity algorithm (model 4) compared with the acceleration algorithm (model 3). Both predicted values are positive which indicates a delayed detection by both algorithms compared with the force plate. The confidence interval was smaller for the acceleration algorithm. In Fig 5C, a schematic representation of these findings is shown.

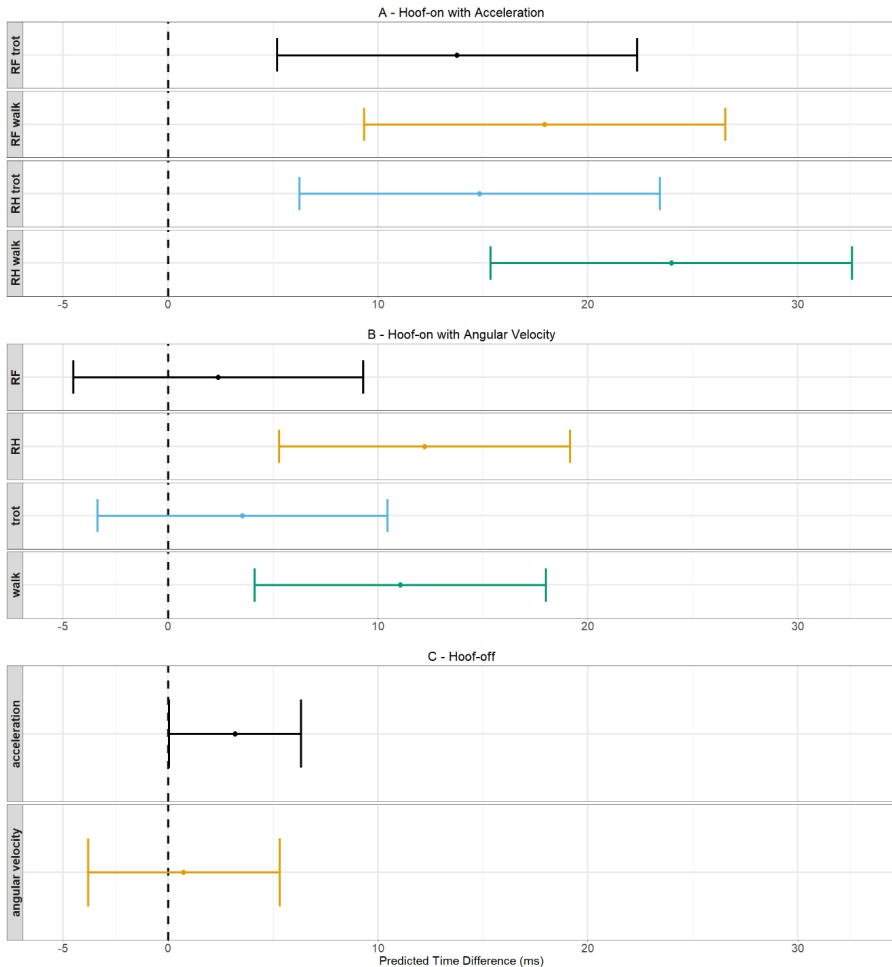


**Figure 5. Schematic representation of the predicted values of the time differences and their 95% confidence intervals.** The dots indicate the predicted value for a certain hoof/gait combination and the 95% confidence intervals are shown by the whiskers. The dashed line indicates a predicted time difference of 0 ms.



These results indicate that the agreement with the force plate was better for the acceleration algorithm with an accuracy of 3.20 ms and precision of 6.39 ms for hoof-off detection.

### **Stance duration**

For all three models, the predicted values for the stance duration were best explained when hoof, gait and interaction term were included as fixed effect and horse as random effect in the model. The results in Table 4 show that the predicted values of both algorithms are smaller compared with the force plate, except for the RF hoof in trot of the angular velocity algorithm. The predicted values determined with the acceleration algorithm are the lowest. Also, the width of the confidence intervals of both algorithms were smaller than the intervals of the force plate, except for the RF hoof in trot of the angular velocity algorithm. These results agree with the results of the Bland Altman analysis.

**Table 4. Linear mixed model results for stance duration.**

		Stance duration			
			predicted value (ms)	lower CI (ms)	upper CI (ms)
acceleration	walk	RF	779.71	759.13	800.28
		RH	777.97	757.18	798.76
	trot	RF	337.06	316.73	357.39
		RH	302.57	282.17	322.97
angular velocity	walk	RF	786.53	763.98	809.08
		RH	784.63	761.94	807.32
	trot	RF	349.01	326.61	371.41
		RH	306.32	283.88	328.76
force plate	walk	RF	793.34	771.89	814.80
		RH	799.19	777.60	820.78
	trot	RF	345.32	324.02	366.61
		RH	314.96	293.62	336.30

The predicted value for the stance duration is determined in milliseconds (ms) for both algorithms and the force plate. The 95% confidence interval was preferred to be small.

## **Discussion**

Two algorithms are presented to automatically detect hoof-events from the acceleration and angular velocity signals measured with hoof-mounted IMUs in horses walking and trotting on hard ground. Results of internal validation with the force plate showed that, for the hoof-on detection, the angular velocity algorithm

was the most accurate with an accuracy between 2.39 and 12.22 ms and a precision of around 13.80 ms, depending on gait and hoof. For hoof-off detection, the acceleration algorithm was the most accurate with an accuracy of 3.20 and precision of 6.39 ms, independent of gait and hoof.

From the results we can conclude that hoof-on is better detected by the angular velocity algorithm which might be explained by the fact that the hoof will slide forward after vertical impact on a hard surface. The forward slide results in a silent angular velocity signal while the acceleration is not silent. Also, a difference in accuracy between the RF hoof (2.39 ms) and RH hoof (12.22 ms) was found which can be explained by the fact that horses place their front and hind hooves differently on the ground. In previous studies, also different landing and braking characteristics are found for hind, front, leading and trailing limbs (21-23). Furthermore, the front hooves bounce more at impact in contrast to the hind hooves, which slide more at impact (24). For the hoof-off detection, the acceleration algorithm performed better which might be explained by the gradual hoof rotation prior to hoof-off. This gradual rotation results in an increase in the angular velocity signal while the acceleration signal is more strongly increased at the actual hoof-off moment. These phenomena could be different and variable on surfaces with other properties. Less firm surface material, such as sand would allow penetration of the hoof into the substrate. If the surface offers shear resistance the hoof would slide less forward (25). This could alter the appearance of the angular velocity versus the acceleration signal. Thomason and Peterson (2008) described a more evident forward push when the surface is smooth and firm (26). Since these algorithms are only tested on data measured on a hard surface, more extensive studies should be performed in to validate it for other surfaces.

In a previous study by Bragança et al. (2017), accuracy and precision for hoof-on were slightly better for the RH hoof and similar for the RF hoof. For hoof-off detection, the accuracy and precision found in this study were better (13). It was expected to find a better algorithm performance during this study due to the use of hoof-mounted IMUs. However, this expectation was only met for the hind hoof and not for the front hoof.

In another study, algorithms were developed to detect gait events from OMC data. Validation with the force plate showed an accuracy between -13.6 and 21.5 ms and a precision between 5.8 and 32.9 ms, depending on limb and gait (27), which is almost similar to the IMU algorithms of Bragança et al. (2017) (13). So, no clear distinction in performance could be made between algorithms developed



for OMC data and IMU data. However, both studies validated these algorithms against the force plate.

In previous studies, reservations about the use of the force plate as gold standard for lameness detection are described (28, 29). They reported that some parameters measured with the force plate should be considered less reliable than others (28, 29). Furthermore, detection of stance duration was performed by using a threshold for the force plate signal. The use of a threshold value is arbitrary; therefore a trial specific threshold was calculated in the study of Clayton et al. (1999) (30) to eliminate the horse-specific aspects, such as walking speed and weight of the horse, and the effect of noise on the signal. Stance durations determined with the IMUs were shorter than the durations determined with the force plate which is probably caused by the threshold level used for the force plate signal since stance and swing phases are estimated from the IMU signals by calculating the variance of the signals. Also, other studies described differences in stance duration according to the threshold levels used for the force plate signal (4). The reason that we chose to use the force plate as gold standard is that this system is used in most research facilities.

The OMC system used guarantees a relative precision of 1.9 mm (7) measuring the kinematics of the hoof and introduces different definitions of hoof-on and hoof-off such as toe-on, heel-on, toe-off and heel-off timings. Therefore, the OMC system might be a more appropriate technique to study the hoof movement and break-over phase more in detail. During this study, the break-over phase was also included in the analysis but is described elsewhere (16).

The needed accuracy and precision for gait classification are not yet determined. Stance duration are measured in different gaits at different speeds and the shortest stance duration reported was 103 ms in pace (31). Therefore, an algorithm with an accuracy and precision smaller than 100 ms might be sufficient to detect foot-fall pattern and thus gait classification. For lameness detection however, a more accurate and precise algorithm is needed since the stance duration increases with 1% in both the affected and contralateral limbs for mild lameness (32, 33).



## Conclusion

Two algorithms are presented to automatically detect hoof-on and hoof-off from acceleration and angular velocity data measured with hoof-mounted IMUs in walk and trot on a hard surface. Internal validation against the force plate was performed. The results showed that for the hoof-on detection, the angular velocity algorithm was the most accurate with an accuracy between 2.39 and 12.22 ms and a precision of around 13.80 ms, depending on gait and hoof. For hoof-off detection, the acceleration algorithm was the most accurate with an accuracy of 3.20 ms and precision of 6.39 ms, independent of gait and hoof. These algorithms seem promising for gait classification, although a more extensive validation process should be performed. Also, the applicability of these algorithms should be investigated under different circumstances, such as different ground surfaces, gaits, speed and different hoof trimming conditions.

## Acknowledgements

We would like to thank W. Back, M. Marin-Perianu and P.R. van Weeren for making this study possible. A special thanks to W. Back and P.R. van Weeren for the feedback on preliminary results of the current study and J. van den Broek for statistical guidance.



## References

1. Hildebrand M. The Quadrupedal Gaits of Vertebrates. *BioScience*. 1989;39(11):766-75.
2. Holcombe AO. Seeing slow and seeing fast: two limits on perception. *Trends Cogn Sci*. 2009;13(5):216-21.
3. Egan S, Brama P, McGrath D. Research trends in equine movement analysis, future opportunities and potential barriers in the digital age: A scoping review from 1978 to 2018. *Equine Vet J*. 2019;1-12.
4. Starke SD, Clayton HM. A universal approach to determine footfall timings from kinematics of a single foot marker in hooved animals. *PeerJ*. 2015;3:e783.
5. Barrey E, Galloux P, Valette JP, Auvinet B, Wolter R. Stride Characteristics of Overground versus Treadmill Locomotion in the Saddle Horse. *Acta Anat*. 1993;146:90-4.
6. Buchner HHF, Savelberg HHCM, Schamhardt HC, Merkens HW, Barneveld A. Kinematics of treadmill versus overground locomotion in horses. *Veterinary Quarterly*. 1994;16(sup2):87-90.
7. Bosch S, Serra Braganca F, Marin-Perianu M, Marin-Perianu R, van der Zwaag BJ, Voskamp J, et al. EquiMoves: A Wireless Networked Inertial Measurement System for Objective Examination of Horse Gait. *Sensors (Basel)*. 2018;18(3).
8. Witte TH, Knill K, Wilson AM. Determination of peak vertical ground reaction force from duty factor in the horse (*Equus caballus*). *J Exp Biol*. 2004;207(Pt 21):3639-48.
9. Olsen E, Andersen PH, Pfau T. Accuracy and precision of equine gait event detection during walking with limb and trunk mounted inertial sensors. *Sensors (Basel)*. 2012;12(6):8145-56.
10. Olsen E, Pfau T, Ritz C. Functional limits of agreement applied as a novel method comparison tool for accuracy and precision of inertial measurement unit derived displacement of the distal limb in horses. *J Biomech*. 2013;46(13):2320-5.
11. Pfau T, Witte TH, Wilson AM. A method for deriving displacement data during cyclical movement using an inertial sensor. *J Exp Biol*. 2005;208(Pt 13):2503-14.
12. Warner SM, Koch TO, Pfau T. Inertial sensors for assessment of back movement in horses during locomotion over ground. *Equine Vet J Suppl*. 2010(38):417-24.
13. Braganca FM, Bosch S, Voskamp JP, Marin-Perianu M, Van der Zwaag BJ, Vernooij JCM, et al. Validation of distal limb mounted inertial measurement unit sensors for stride detection in Warmblood horses at walk and trot. *Equine Vet J*. 2017;49(4):545-51.
14. Willemen MA, Jacobs MWH, Schamhardt HC. In vitro transmission and attenuation of impact vibrations in the distal forelimb. *Equine Exercise Physiology*. 1999;5(30):245-8.
15. Gustas P, Johnston C, Roepstorff L, Drevemo S. In vivo transmission of impact shock waves in the distal forelimb of the horse. *Equine Vet J*. 2001;33:11-5.
16. Tijssen M. Break-over detection using hoof-mounted inertial measurements units. Submitted to PLOS ONE. 2020b, companion paper.
17. Lehnert B. BlandAltmanLeh: Plots (Slightly Extended) Bland-Altman Plots. 2015.
18. Bates D, Mächler M, Bolker B, Walker S. Fitting Linear Mixed-Effects Models Using lme4. *Journal of Statistical Software*. 2015;67(1).
19. Lenth R. emmeans: Estimated Marginal Means, aka Least-Squares Means. 2018.
20. Venables WN, Ripley BD. *Modern Applied Statistics with S*. New York: Springer; 2002.
21. Back W, Schamhardt HC, Savelberg HHCM, Van den Bogert AJ, Bruin G, Hartman W, et al. How the horse moves: 1. Significance of graphical representation of equine forelimb kinematics. *Equine Vet J*. 1995;27(1):31-8.
22. Back W, Schamhardt HC, Savelberg HHCM, Van den Bogert AJ, Bruin G, Hartman W, et al. How the horse moves: 2. Significance of graphical representations of equine hind limb kinematics. *Equine Vet J*. 1995;27(1):39-45.

23. Hernlund E, Egenvall A, Roepstorff L. Kinematic characteristics of hoof landing in jumping horses at elite level. *Equine Vet J Suppl.* 2010(38):462-7.
24. Back W, Schamhardt HC, Hartman W, Barneveld A. Kinematic differences between the distal portions of the forelimbs and hind limbs of horses at the trot. *American Journal Veterinary Research.* 1995;56(11):1522-8.
25. Hernlund E. *Sport Surfaces in Show Jumping [Doctoral Thesis].* Uppsala: Swedish University of Agricultural Sciences; 2016.
26. Thomason JJ, Peterson ML. Biomechanical and mechanical investigations of the hoof-track interface in racing horses. *Vet Clin North Am Equine Pract.* 2008;24(1):53-77.
27. Boye JK, Thomsen MH, Pfau T, Olsen E. Accuracy and precision of gait events derived from motion capture in horses during walk and trot. *J Biomech.* 2014;47(5):1220-4.
28. Clayton HM, Lynch JA, Clayton HM, Mullineaux DR. The reliability of force platform data from trotting horses. *Equine and Comparative Exercise Physiology.* 2005;2(2):129-32.
29. Donnell JR, Frisbie DD, King MR, Goodrich LR, Haussler KK. Comparison of subjective lameness evaluation, force platforms and an inertial-sensor system to identify mild lameness in an equine osteoarthritis model. *Vet J.* 2015;206(2):136-42.
30. Clayton HM, Lanovaz JL, Schamhardt HC, Van Wessum R. The effects of a rider's mass on ground reaction forces and fetlock kinematics at the trot. *Equine Vet J.* 1999;30:218-21.
31. Robilliard JJ, Pfau T, Wilson AM. Gait characterisation and classification in horses. *J Exp Biol.* 2007;210(Pt 2):187-97.
32. Weishaupt MA, Wiestner T, Hogg HP, Jordan P, Auer JA. Compensatory load redistribution of horses with induced weight-bearing forelimb lameness trotting on a treadmill. *Vet J.* 2006;171(1):135-46.
33. Weishaupt MA, Wiestner T, Hogg HP, Jordan P, Auer JA. Compensatory load redistribution of horses with induced weightbearing hindlimb lameness trotting on a treadmill. *Equine Vet J.* 2004;36(8):727-33.



## **Additional information**

### **Horses**

The measurements were performed for a previous study performed by Bragança et al. 2017 (13). Measurements were performed with seven Warmblood horses, six mares and one gelding, with a body mass ranging from 506 to 608 kg (mean 564.4 kg), age ranging from five to twenty-one years (mean 7.5 years) and height at withers ranging from 1.58 to 1.75 m (mean 1.65 m).

### **Data collection**

The walking speed of the horses was measured with two pairs of photoelectric sensors placed before and after the force plate at a distance of two meters.

### ***Optical motion capture setup***

Three markers were used for the motion measurements; these markers were spherical passive markers with a diameter of 12.5 mm. The 3D position of the three markers was measured with six infrared cameras (ProReflex 240) of the optical motion capture (OMC) system (Qualisys AB, Motion Capture System, Göteborg, Sweden). The cameras were placed around the force plate in such way that the vertical displacement of the markers was visible. Movements of the markers was recorded with a sampling frequency of 200 Hz and with a relative precision of 1.9 mm after calibration (7). The collected OMC data was used in another study for break-over detection (34) but was needed for time synchronization in this paper.

### ***Force plate setup and synchronization***

The force plate (Z4852C, Kistler, Winterthur, Switzerland) was covered with a five mm rubber mat. The analogue force plate signal was fed to an A/D converter with a sampling frequency of 1000 Hz and connected to the Qualisys Track Manager (QTM) software (Qualisys AB, Motion Capture System, Göteborg, Sweden) of the OMC system. The QTM software down sampled the force plate signal with a frequency of 200 Hz and removed the response time lag to obtain time synchronization with the OMC system ((13); for further details see page 134 of the QTM manual (35)).

### ***Inertial measurement unit setup and synchronization***

The ProMove-mini wireless inertial measurement units (IMUs) (Inertia-Technology B.V., Enschede, The Netherlands) weighted 20 g and were set to a sampling frequency of 200 Hz. The sensors measured the tri-axial acceleration, angular velocity (gyroscope) and magnetic field intensity (compass) over time with a

precision of 100 ns (7). The collected data was stored on the onboard 2 Gb microSD card during measurements and was retrieved after each trial.

Time synchronization between the IMUs and OMC system is described by Bosch et al. (7). In short, two reflective markers were attached above and below the IMU attached to the cannon bone of the horse (data is used for another study (13)). The correlation coefficient was calculated between the position data of these reflective markers and the angular velocity signal measured with this IMU. The time shift between the OMC system and the IMU was indicated by a maximum in the correlation coefficient. To improve this calculation, interpolation was used which resulted in a time synchronization estimated better than 500  $\mu$ s (7).



## References

1. Hildebrand M. The Quadrupedal Gaits of Vertebrates. *BioScience*. 1989;39(11):766-75.
2. Holcombe AO. Seeing slow and seeing fast: two limits on perception. *Trends Cogn Sci*. 2009;13(5):216-21.
3. Egan S, Brama P, McGrath D. Research trends in equine movement analysis, future opportunities and potential barriers in the digital age: A scoping review from 1978 to 2018. *Equine Vet J*. 2019;1-12.
4. Starke SD, Clayton HM. A universal approach to determine footfall timings from kinematics of a single foot marker in hooved animals. *PeerJ*. 2015;3:e783.
5. Barrey E, Galloux P, Valette JP, Auvinet B, Wolter R. Stride Characteristics of Overground versus Treadmill Locomotion in the Saddle Horse. *Acta Anat*. 1993;146:90-4.
6. Buchner HHF, Savelberg HHCM, Schamhardt HC, Merkens HW, Barneveld A. Kinematics of treadmill versus overground locomotion in horses. *Veterinary Quarterly*. 1994;16(sup2):87-90.
7. Bosch S, Serra Braganca F, Marin-Perianu M, Marin-Perianu R, van der Zwaag BJ, Voskamp J, et al. EquiMoves: A Wireless Networked Inertial Measurement System for Objective Examination of Horse Gait. *Sensors (Basel)*. 2018;18(3).
8. Witte TH, Knill K, Wilson AM. Determination of peak vertical ground reaction force from duty factor in the horse (*Equus caballus*). *J Exp Biol*. 2004;207(Pt 21):3639-48.
9. Olsen E, Andersen PH, Pfau T. Accuracy and precision of equine gait event detection during walking with limb and trunk mounted inertial sensors. *Sensors (Basel)*. 2012;12(6):8145-56.
10. Olsen E, Pfau T, Ritz C. Functional limits of agreement applied as a novel method comparison tool for accuracy and precision of inertial measurement unit derived displacement of the distal limb in horses. *J Biomech*. 2013;46(13):2320-5.
11. Pfau T, Witte TH, Wilson AM. A method for deriving displacement data during cyclical movement using an inertial sensor. *J Exp Biol*. 2005;208(Pt 13):2503-14.
12. Warner SM, Koch TO, Pfau T. Inertial sensors for assessment of back movement in horses during locomotion over ground. *Equine Vet J Suppl*. 2010(38):417-24.
13. Braganca FM, Bosch S, Voskamp JP, Marin-Perianu M, Van der Zwaag BJ, Vernooij JCM, et al. Validation of distal limb mounted inertial measurement unit sensors for stride detection in Warmblood horses at walk and trot. *Equine Vet J*. 2017;49(4):545-51.
14. Willemen MA, Jacobs MWH, Schamhardt HC. In vitro transmission and attenuation of impact vibrations in the distal forelimb. *Equine Exercise Physiology*. 1999;5(30):245-8.
15. Gustas P, Johnston C, Roepstorff L, Drevemo S. In vivo transmission of impact shock waves in the distal forelimb of the horse. *Equine Vet J*. 2001;33:11-5.
16. Tijssen M. Break-over detection using hoof-mounted inertial measurements units. Submitted to PLOS ONE. 2020b, companion paper.
17. Lehnert B. BlandAltmanLeh: Plots (Slightly Extended) Bland-Altman Plots. 2015.
18. Bates D, Mächler M, Bolker B, Walker S. Fitting Linear Mixed-Effects Models Using lme4. *Journal of Statistical Software*. 2015;67(1).
19. Lenth R. emmeans: Estimated Marginal Means, aka Least-Squares Means. 2018.
20. Venables WN, Ripley BD. *Modern Applied Statistics with S*. New York: Springer; 2002.
21. Back W, Schamhardt HC, Savelberg HHCM, Van den Bogert AJ, Bruin G, Hartman W, et al. How the horse moves: 1. Significance of graphical representation of equine forelimb kinematics. *Equine Vet J*. 1995;27(1):31-8.

22. Back W, Schamhardt HC, Savelberg HHCM, Van den Bogert AJ, Bruin G, Hartman W, et al. How the horse moves: 2. Significance of graphical representations of equine hind limb kinematics. *Equine Vet J*. 1995;27(1):39-45.
23. Hernlund E, Egenvall A, Roepstorff L. Kinematic characteristics of hoof landing in jumping horses at elite level. *Equine Vet J Suppl*. 2010(38):462-7.
24. Back W, Schamhardt HC, Hartman W, Barneveld A. Kinematic differences between the distal portions of the forelimbs and hind limbs of horses at the trot. *American Journal Veterinary Research*. 1995;56(11):1522-8.
25. Hernlund E. *Sport Surfaces in Show Jumping [Doctoral Thesis]*. Uppsala: Swedish University of Agricultural Sciences; 2016.
26. Thomason JJ, Peterson ML. Biomechanical and mechanical investigations of the hoof-track interface in racing horses. *Vet Clin North Am Equine Pract*. 2008;24(1):53-77.
27. Boye JK, Thomsen MH, Pfau T, Olsen E. Accuracy and precision of gait events derived from motion capture in horses during walk and trot. *J Biomech*. 2014;47(5):1220-4.
28. Clayton HM, Lynch JA, Clayton HM, Mullineaux DR. The reliability of force platform data from trotting horses. *Equine and Comparative Exercise Physiology*. 2005;2(2):129-32.
29. Donnell JR, Frisbie DD, King MR, Goodrich LR, Haussler KK. Comparison of subjective lameness evaluation, force platforms and an inertial-sensor system to identify mild lameness in an equine osteoarthritis model. *Vet J*. 2015;206(2):136-42.
30. Clayton HM, Lanovaz JL, Schamhardt HC, Van Wessum R. The effects of a rider's mass on ground reaction forces and fetlock kinematics at the trot. *Equine Vet J*. 1999;30:218-21.
31. Robilliard JJ, Pfau T, Wilson AM. Gait characterisation and classification in horses. *J Exp Biol*. 2007;210(Pt 2):187-97.
32. Weishaupt MA, Wiestner T, Hogg HP, Jordan P, Auer JA. Compensatory load redistribution of horses with induced weight-bearing forelimb lameness trotting on a treadmill. *Vet J*. 2006;171(1):135-46.
33. Weishaupt MA, Wiestner T, Hogg HP, Jordan P, Auer JA. Compensatory load redistribution of horses with induced weightbearing hindlimb lameness trotting on a treadmill. *Equine Vet J*. 2004;36(8):727-33.
34. Tijssen M. Break-over detection using hoof-mounted inertial measurements units. Submitted to *Journal of Experimental Biology*. 2020b, companion paper.
35. Qualisys AB. *Qualisys Track Manager - User Manual*. Gothenborg, Sweden 2011.



**S1 Table. Table with stance durations.** Mean and standard deviation of detected stance duration as detected with the algorithms for acceleration, angular velocity and force plate.

			Detected stance duration	
			mean (ms)	SD (ms)
acceleration	walk	RF	779.72	50.18
		RH	777.79	53.49
	trot	RF	338.85	30.94
		RH	302.63	43.63
angular velocity	walk	RF	786.39	53.55
		RH	784.26	48.87
	trot	RF	350.77	33.00
		RH	306.32	32.89
force plate	walk	RF	793.06	46.46
		RH	798.68	54.11
	trot	RF	347.05	29.37
		RH	314.61	33.48

The mean stance duration and the standard deviation (SD) of this mean in milliseconds (ms) are determined for the acceleration and angular velocity signals, and force plate signal.



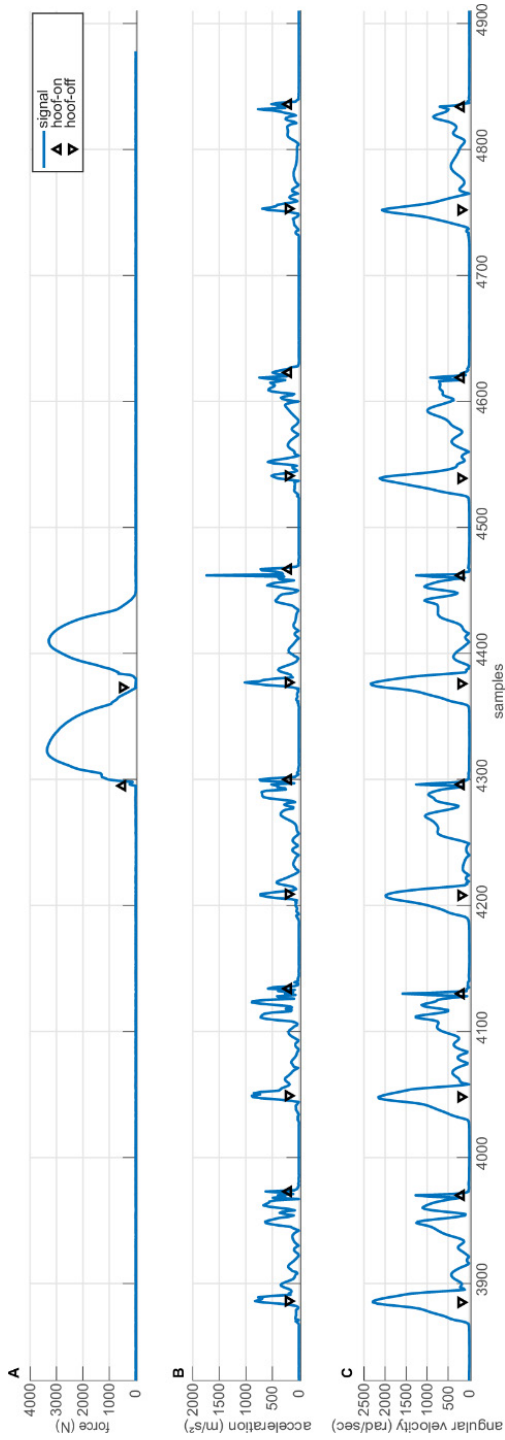


**Figure S1. Preprocessed signals of the vertical force (A), the acceleration (B) and angular velocity (C) signals of the IMU for one hoof from one measurement in trot.** The hoof-on events are depicted with upward-pointing triangle markers and hoof-off events are depicted with downward-pointing triangle markers.





# 3

## **Automatic detection of break-over phase onset in horses using hoof-mounted inertial measurement unit sensors**

3

Published in PLoS One, 2020, 15:5

M. Tijssen

E. Hernlund

M. Rhodin

S. Bosch

J.P. Voskamp

M. Nielen

F.M. Serra Bragança

## Abstract

A prolonged break-over phase might be an indication of a variety of musculoskeletal disorders and can be measured with optical motion capture (OMC) systems, inertial measurement units (IMUs) and force plates. The aim of this study was to present two algorithms for automatic detection of the break-over phase onset from the acceleration and angular velocity signals measured by hoof-mounted IMUs in walk and trot on a hard surface. The performance of these algorithms was evaluated by internal validation with an OMC system and a force plate separately. Seven Warmblood horses were equipped with two wireless IMUs which were attached to the lateral wall of the right front (RF) and hind (RH) hooves. Horses were walked and trotted over a force plate for internal validation while simultaneously the 3D position of three reflective markers, attached to lateral heel, lateral toe and lateral coronet of each hoof, were measured by six infrared cameras of an OMC system. The performance of the algorithms was evaluated by linear mixed model analysis. The acceleration algorithm was the most accurate with an accuracy between -9 and 23 ms and a precision around 24 ms (against OMC system), and an accuracy between -37 and 20 ms and a precision around 29 ms (against force plate), depending on gait and hoof. This algorithm seems promising for quantification of the break-over phase onset although the applicability for clinical purposes, such as lameness detection and evaluation of trimming and shoeing techniques, should be investigated more in-depth.



## Introduction

The break-over phase starts after the loading phase when the horse lifts its heel, causing a rotational movement around the toe, and ends with hoof-off (1, 2) as can be seen in Fig 1A. During this rotation, the body weight moves towards the toe; reducing the contact area with the ground and increasing the force on the toe and navicular bone. This increase in force results in high tensile forces on the muscles, ligaments and tendons (3, 4). The ease of rotation of the hoof is affected by the toe length and hoof angle (4-6). The break-over phase duration is the time between the start of the rotation and hoof-off. In general, this duration is around 20% of the stance duration in walk (7) but will be influenced by the gait and velocity of the horse, hoof shape and different surface properties. A prolonged break-over phase might increase the risk for development of navicular disease and tendon injury (3, 4, 8). Prolongation can also be a result of a mechanical restriction or pain and thus an indication of an orthopedic disorder or lameness (4).

The break-over phase can be measured with kinematic methods such as optical motion capture (OMC) systems, and inertial measurement units (IMUs) since the rotation of the hoof can be derived from the output of these methods. The OMC systems measure the position of markers, placed on the hoof, over time and give information about the displacement of these markers. The IMUs can also be attached to the hoof and measure the acceleration and angular velocity in three directions over time (9, 10). The displacement can be calculated by integration, although some noise in the input data and unknown initial conditions might affect the integration and lead to inaccurate results (11). In a previous study by Clayton et al. (2000), the vertical force, measured by a force plate, was used to determine the loading rate on a limb (12). The loading rate was defined as the slope of the vertical force right after hoof impact, in which the longitudinal force was decreasing. However, the slope of the decreasing vertical force, unloading rate, was not assessed in this study. In another study by Weishaupt et al. 2004, the typical shape of the vertical force curve was described in trot and a discrete kink after midstance was allocated to the breakover of the hoof (13).

In the current study, the three abovementioned techniques (IMU, OMC and force plate) are used to detect the start of the break-over phase. While OMC and force plate can be considered established methods, neither can be considered a perfect gold standard, as both measure different quantities (force versus position). The aim of this study was to present two algorithms for automatic detection of the break-over phase onset from the acceleration and angular velocity data measured

by hoof-mounted IMUs in walk and trot on a hard surface. The performance of these algorithms was evaluated through internal validation with the OMC system and the vertical force separately.

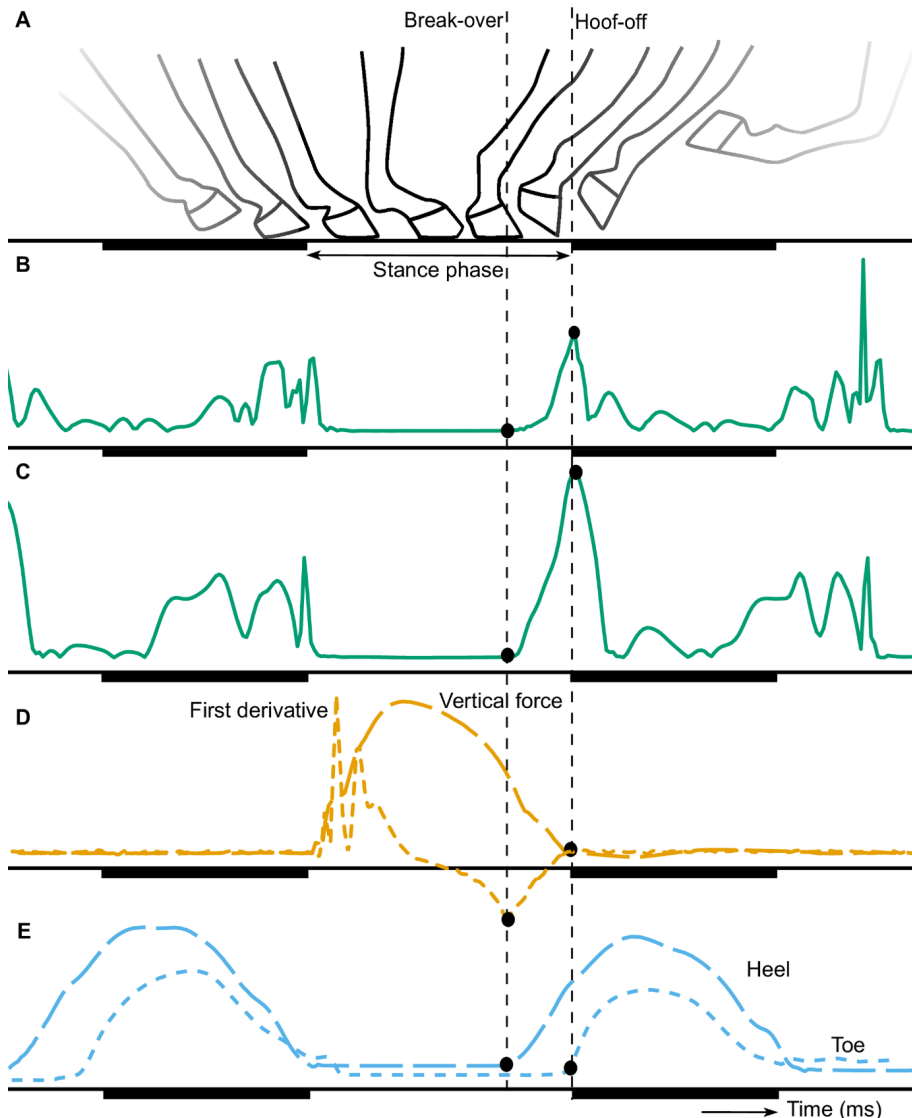


**Figure 1. Generic illustration of the movement of the hoof (A), modified from Witte et al. (15), the signals of the acceleration (B), angular velocity (C), vertical force and first derivative of the vertical force (D), and vertical displacement of the heel and toe markers of the OMC system.** The start of the break-over is depicted with the vertical dashed lines and the dots show the detected break-over from the different signals. The swing phase is underlined with a dark beam.



## Materials and Methods

### Data collection

The same data collection procedure was performed as described earlier (10, 14). In short, measurements were performed with seven Warmblood horses (*Equus ferus caballus*; for further details see S1 Appendix).

These horses were equipped with two ProMove-mini wireless IMUs (Inertia-Technology B.V., Enschede, The Netherlands; for further details see S1 Appendix) which measured the low-*g* acceleration with a range of  $\pm 16$  *g*, high-*g* acceleration with a range of  $\pm 400$  *g*, angular velocity with a range of  $\pm 2000$  °/s, and sampling frequency of 200 Hz. These IMUs were attached to the lateral wall of the right front (RF) and hind (RH) hooves with double sided and normal tape.

All horses were walked and trotted over a force plate (Z4852C, Kistler, Winterthur, Switzerland; for further details see S1 Appendix) to collect at least five valid force plate impacts for both front and hind hooves; each valid impact will be considered a trial in the further analysis.

Three reflective markers of the OMC system (Qualisys AB, Motion Capture System, Göteborg, Sweden; for further details see S1 Appendix) were attached to lateral heel, lateral toe and lateral coronet of each hoof with super glue. The 3D position of three reflective markers were measured with a sampling frequency of 200 Hz by six infrared cameras (ProReflex 240) of the OMC system (Qualisys AB, Motion Capture System, Göteborg, Sweden). The position of these markers and the acceleration and angular velocity signal measured by the IMU sensors was obtained simultaneously.

The systems were time synchronized as described earlier (10), for more details see S1 Appendix.

The original horse measurements were performed in compliance with the Dutch Act on Animal Experimentation and approved by the local ethics committee of Utrecht University. All horses were present for teaching purposes and these measurements were not considered additional animal experiments within the Dutch law at that time. Therefore, no specific experiment number is available.



## **Data analysis**

At the start of this study, data of the force plate, OMC system and IMUs were visually evaluated and a change in unloading rate of the vertical force signal was seen prior to hoof-off. To depict the unloading rate, the first derivative of the vertical force signal with respect to time was calculated and used during this study. The vertical force signal and the first derivative are depicted in Fig 1D.

### ***OMC data***

The collected OMC data were preprocessed by Inertia Technology B.V. and segmented in different trials corresponding with the force plate trials. The OMC data were analyzed and heel-off and toe-off time points, corresponding with the valid impact on the force plate, were selected by an algorithm described by Bragança et al. (14). In short, the data from the toe and heel markers were filtered with a 'maxflat filter' with a cut-off frequency of 8 Hz. Then, the stance phase was detected by calculating the average variance of the signal using a moving window of 40 frames and allocating the moments with the lowest variance to the stance phase. Thereafter, the elevation of the markers was detected by performing a forward search to find the first frame where the marker was elevated by 1 mm, using the stance phase as a reference. This frame was allocated as the toe- and heel-off moments respectively. The same steps were performed with a backward search to find the toe- and heel-on moments. For this study, the break-over phase onset was determined as the heel-off time point.

### ***Force plate data***

The collected force plate data were preprocessed by Inertia Technology B.V.. The valid impacts were selected and cut into different trials; each trial consisted of at least one valid impact and sometimes two for consecutive impacts of the RF and RH hoof. The first derivative of the vertical force signal was calculated with a fourth order differentiator FIR filter with a passband frequency of 40 Hz and a stopband frequency of 100 Hz. The break-over phase onset was determined as the time point that the first derivative of the vertical force changed from decreasing to increasing values as can be seen in Fig 1D.

### ***IMU data***

The collected IMU data were preprocessed by Inertia Technology B.V. and cut into different trials corresponding with the force plate trials. The tri-axial acceleration and angular velocity signals were preprocessed by removing the offset drift and calculation of the Euclidean norm resulting in a one-directional acceleration and angular velocity signal. Thereafter, the swing phase was estimated to distinguish



between consecutive steps by allocating the time points with a low variance as stance phase and the remaining time points as swing phase (for further details see companion paper (10)).

Next, we determined the break-over phase onset from the acceleration and angular velocity signal separately but by the same procedure. For both algorithms a threshold was developed to detect the start of the break-over phase. This threshold value was calculated from the signal mean ( $x$ ) and signal standard deviation ( $s$ ) of the stance phases. For every trial, this threshold value ( $T$ ) was determined by:

$$T = x + 1.96 \times s$$

The standard deviation was multiplied by 1.96 resulting in detection of the upper 2.5% of a normally distributed signal, to make sure that no random noise was detected.

The break-over phase onset was determined as the last time point that the signal was below the threshold value before hoof-off was detected.

### **Performance evaluation**

The time differences between the detection of the break-over phase onset of both algorithms were assessed with the OMC and force derivative separately as reference. The normality of the time differences was visually checked by examining the QQ plot and histogram in R (version 1.1.414, RStudio Inc, Boston, Massachusetts, USA). Thereafter, the distribution of the time differences was visualized to interpret the results and the performance of both algorithms was evaluated by a linear mixed model analysis.

For the linear mixed model analysis, the same model building and reduction procedure was performed as described previously (10). In short, a linear mixed model analysis was performed with hoof, gait, number of trials and interaction term between hoof and gait as independent variables. A random intercept for every horse was included in the model. Model reduction was applied based on the AIC and residuals of each selected model were visually checked for any deviations of normality and homoscedasticity. The predicted value of the time difference between both algorithms with the OMC and force derivative separately were calculated for every combination of hoof and gait. The same procedure was performed for the time differences between the force derivative and the OMC system.

The performance of the algorithms was evaluated based on the predicted values and the width of the 95% confidence intervals of the time differences. The predicted value was deemed better if closer to zero which indicates a small difference between the algorithm and the reference measurement, i.e. a good accuracy. A positive predicted value indicates a delayed detection by the algorithm and a negative predicted value indicates a too early detection by the algorithm compared with the reference measurement. The width of the 95% confidence interval of the time difference was preferred to be small, which means that the time difference is measured precisely, i.e. a good precision. Schematic representations of these predicted values were used to visualize the accuracy and precision of the algorithms compared with the reference.

## Results

A total of 147 trials were analyzed: 75 trials of the right front (RF) hoof (36 in walk and 39 in trot) and 72 trials of the right hind (RH) hoof (34 in walk and 38 in trot). An overview of the analyzed trials is given elsewhere (10). Preprocessed data of one measurement in trot can be seen in Fig S1. The time differences between the detection of the break-over phase onset of both algorithms and the two reference methods (OMC and force plate) were normally distributed.

Time differences between both algorithms and the OMC system are depicted in the upper row of Fig 2. The distribution of the acceleration algorithm versus OMC system (Fig 2A) shows a bell shape curve ranging from -70 to 135 ms and a mean of 3.12 ms with higher values found for RH. The distribution of the angular velocity algorithm versus OMC system (Fig 2B) shows a smaller half bell shape curve, ranging from -100 to 10 ms, and a mean of -32.77 ms with lower values found for RF in trot. Time differences between both algorithms and the force derivative are depicted in the bottom row of Fig 2. The distribution of the acceleration algorithm versus force derivative (Fig 2C) shows a bell shape curve ranging from -155 to 125 ms and a mean of -12.18 ms with lower values found for RH in walk and higher values found for RF in walk. The distribution of the angular velocity algorithm versus force derivative (Fig 2D) shows a smaller right skewed curve ranging from -195 to 30 ms with a mean of -48.27 ms.

Time differences between both reference methods are depicted in Fig 3A and show a bell shape curve, ranging from -75 to 120 ms and mean of 16.11 ms. Lower values were found for RH in walk and higher values for RF in walk.

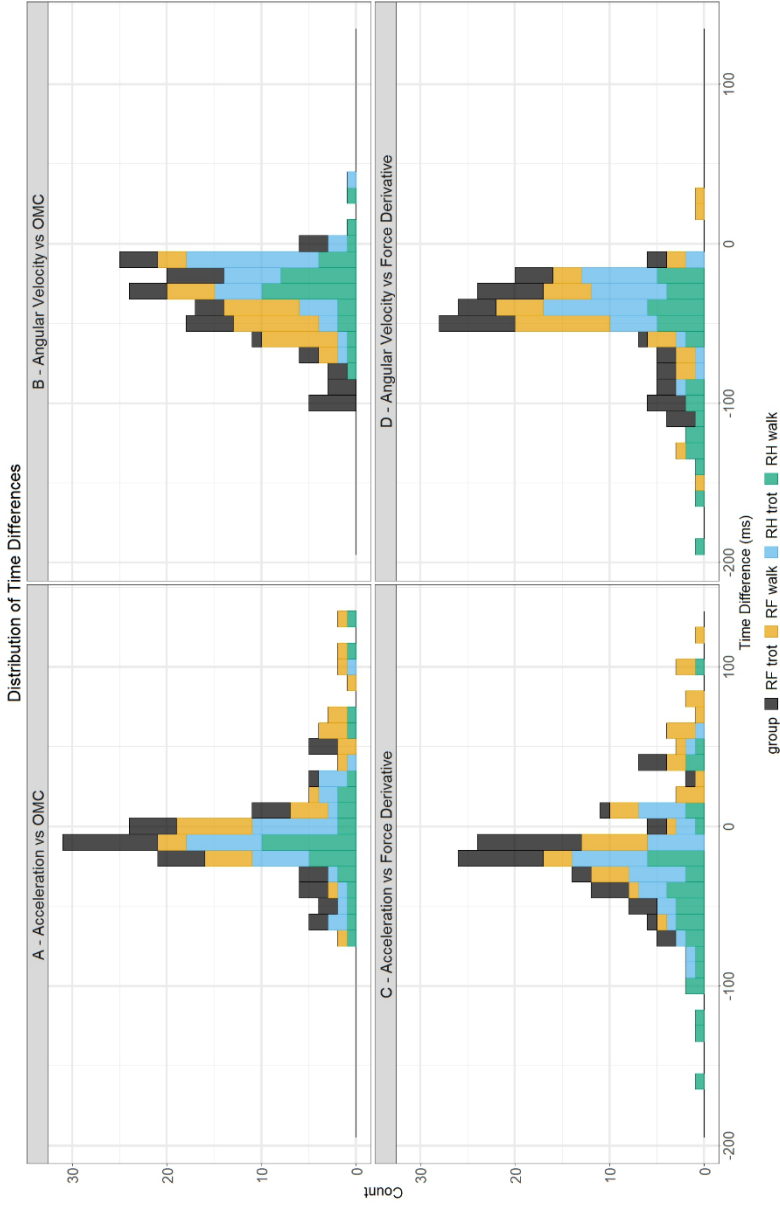


**Figure 2. Distributions of time differences between both algorithms and reference methods for the break-over phase onset detection.** Time differences with the OMC system are depicted in the upper row and time differences with the force derivative are depicted in the bottom row. The different hoof/gait combinations are depicted with their own color.

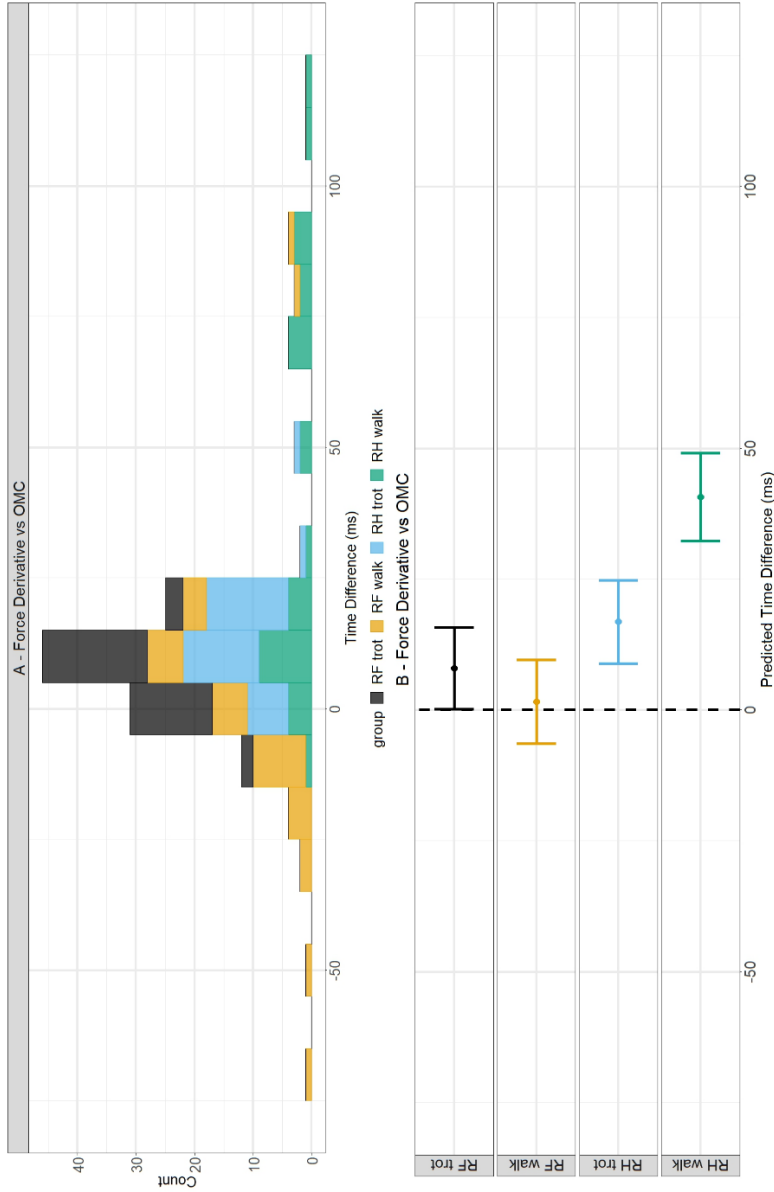


**Figure 3. Time differences and predicted values of time differences between force derivative and OMC system for break-over phase onset detection.** Time differences between the two reference methods are depicted in the upper figure with the different hoof/gait combinations depicted in their own color. In the bottom, the predicted values are indicated with dots for a certain hoof/gait combination and their 95% confidence intervals are shown by the whiskers. The dashed line indicates a predicted time difference of 0 ms.



**Table 1. Linear mixed model results for the acceleration and angular velocity algorithm.**

<b>OMC system as reference</b>					
			<b>predicted value (ms)</b>	<b>lower CI (ms)</b>	<b>upper CI (ms)</b>
Model 1: acceleration	walk	RF	22.57	10.43	34.72
		RH	2.03	-10.67	14.73
	trot	RF	-8.42	-20.08	3.23
		RH	-2.64	-14.61	9.34
Model 2: angular velocity	walk	RF	-33.51	-47.08	-19.95
		RH	-31.56	-45.10	-18.02
	trot	RF	-43.57	-57.11	-30.02
		RH	-21.50	-35.07	-7.94
<b>Force derivative as reference</b>					
			<b>predicted value (ms)</b>	<b>lower CI (ms)</b>	<b>upper CI (ms)</b>
Model 3: acceleration	walk	RF	20.25	5.76	34.74
		RH	-36.86	-51.65	-22.07
	trot	RF	-16.51	-30.65	-2.38
		RH	-16.73	-30.97	-2.50
Model 4: angular velocity	walk	RF	-43.39	-59.28	-27.50
		RH	-65.13	-81.15	-49.10
	trot	RF	-52.13	-67.87	-36.39
		RH	-34.48	-50.26	-18.69

The predicted values are determined in milliseconds (ms) and are deemed better if closer to zero. The upper and lower limits of the 95% confidence interval are determined in milliseconds (ms) and were preferred to be small.

## Linear mixed model analysis

The residuals of all selected linear mixed models were normally distributed and did not show homoskedasticity. Table 1 gives a summary of the results of the linear mixed model analysis.

### **OMC as a reference**

The models with the lowest AIC are presented in Table 1. The predicted values of the time difference between the acceleration algorithm and the OMC system (model 1) were best explained when hoof, gait and interaction term were included as fixed effect in the model with no random effect. The predicted values of the time difference between the angular velocity algorithm and the OMC system (model 2) were best explained when hoof and gait were included as fixed effect and horse as random effect in the model.

The results in Table 1 show that the predicted values of the time differences were closer to zero for the acceleration algorithm (model 1) compared with the angular velocity algorithm (model 2). For model 1, the predicted values were positive in walk and negative in trot indicating a delayed detection in walk and a too early detection in trot in contrast to model 2 for which all predicted values were negative indicating a too early detection. Also, the confidence intervals are smaller for the acceleration algorithm (model 1) compared with the angular velocity algorithm (model 2).

In Fig 4, the predicted values and their 95% confidence intervals are shown for all models. For model 1 (Fig 4A), these values are shown for every hoof/gait combination because this model needs an interaction term to explain the data. The predicted values and their 95% confidence intervals of model 2 (Fig 4B) are shown for walk versus trot and the RF hoof versus the RH hoof because this model did not need an interaction term to explain the data. For model 1, the predicted values for RH are located closer to zero compared with the RF. All confidence intervals contain both positive and negative values except for the interval of the RF in walk. For model 2, the predictive values of the gaits are located closer to each other than the values of both hooves. The predictive value of RH is located closest to zero and the value of RF is located most distant from zero.

These results indicate that the agreement with the OMC was better for the acceleration algorithm with an accuracy of between -8.42 and 22.57 ms depending on the gait and hoof and a precision around 24.24 ms.

### ***Force derivative as a reference***

The predicted values of the time differences between the acceleration algorithm and the force plate (model 3) and the angular velocity algorithm and the force plate (model 4) were best explained when in the model hoof, gait and interaction term were included as fixed effect and horse as random effect.

The results in Table 1 show that the predicted values were smaller for the acceleration algorithm (model 3) compared with the angular velocity algorithm (model 4). The predictive values of both models were all negative, indicating a too early detection, except for RF in walk of model 3. Also, the widths of the 95% confidence intervals were smaller for the acceleration algorithm (model 3).

For model 3 (Fig 4C) and model 4 (Fig 4D), these values are shown for every hoof/gait combination because this model needs an interaction term to explain the



data. For model 3, the predictive values and confidence intervals are negative except for the RF in walk which has a positive predictive values and completely positive confidence interval. The values of both hooves are located closer to zero in trot compared to walk. For model 4, the predictive values and all confidence intervals are completely negative. The predictive value of RH in trot is located the closest to zero and the value of RH in walk is located the most distant from zero.

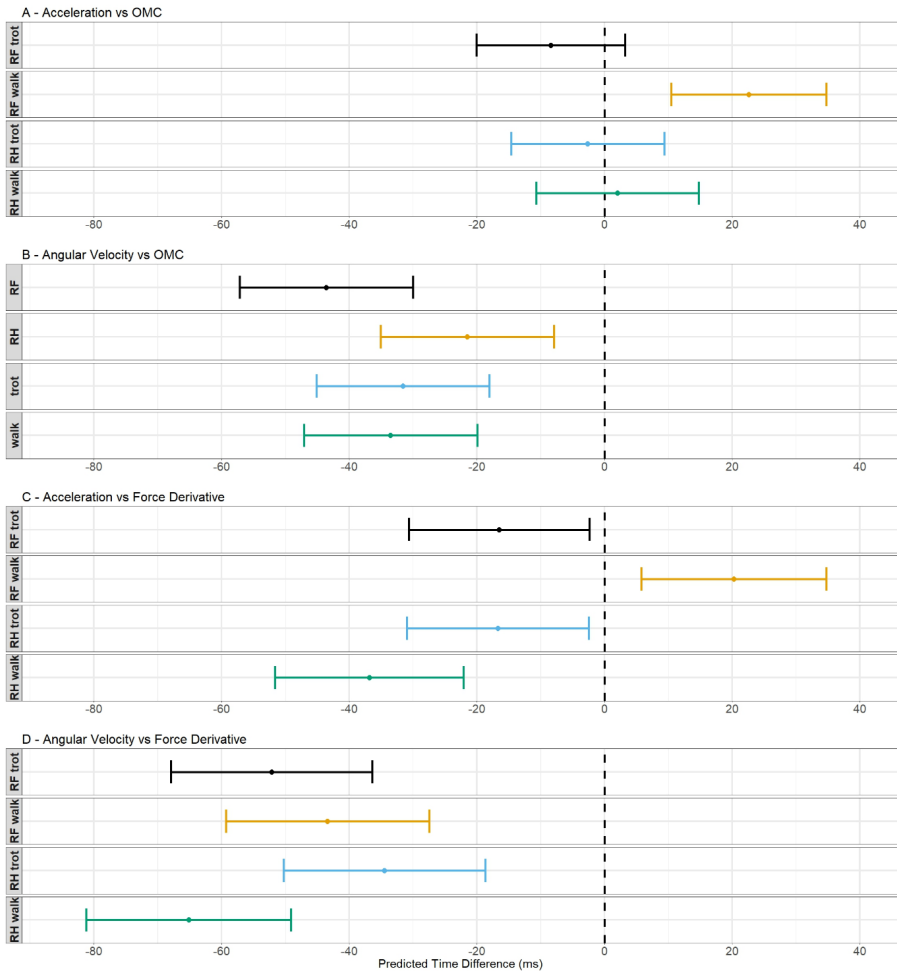


**Figure 4. Schematic representation of the predicted values of the time differences and their 95% confidence intervals.** The dots indicate the predicted value for a certain hoof/gait combination and the 95% confidence intervals are shown by the whiskers. The dashed line indicates a predicted time difference of 0 ms.



These results indicate that the agreement with the force derivative was better for the acceleration algorithm, which agrees with the results found for the validation with the OMC system. The accuracy of this algorithm was found between -36.86 and 20.25 ms, depending on gait and hoof, and the precision was around 28.83 ms.

### **Force derivative versus OMC system**

The predicted values of the time differences between the two references methods, force derivative and OMC system, were best explained when the model contained a fixed effect for hoof and gait, an interaction term and no random horse effect.

The results in Table 2 show that all predicted values are positive, indicating a delayed detection with the force derivative compared to the OMC system. The value for RH in walk was the most located from zero. The confidence intervals were all completely positive, except for the interval of the RF in walk.

**Table 2. Linear mixed model results for the reference methods, OMC system and force derivative.**

Force derivative vs OMC system				
		predicted values (ms)	lower CI (ms)	upper CI (ms)
walk	RF	1.57	9.56	-6.44
	RH	40.62	49.01	32.24
trot	RF	7.97	15.77	0.18
	RH	16.81	24.71	8.90

The predicted values are determined in milliseconds (ms) and are deemed better if closer to zero. The lower and upper limits of the 95% confidence interval are determined in milliseconds (ms) and were preferred to be small.

In Fig 3B, the predicted values and their 95% confidence intervals are shown for every hoof/gait combination because this model needs an interaction term to explain the data. For the RF hoof in both gaits, the predicted values were closer to zero in contrast to the RH in walk for which the predicted value was the most distant from zero. All the confidence intervals were completely positive except for the interval of the RF in walk.

## **Discussion**

Two algorithms are described to automatically detect the break-over phase onset from the acceleration and angular velocity signals measured with hoof-mounted IMUs in walk and trot on a hard surface. Results of the internal validation show



that the acceleration algorithm was the most accurate with an accuracy between -9 and 23 ms and a precision around 24 ms with assessment against the OMC system and an accuracy between -37 and 20 ms and a precision around 29 ms with assessment against the force plate, depending on gait and hoof.

Both models needed a hoof, gait and interaction term to explain the predicted values of the time differences. The hoof effect might be explained by the fact that the shape of the hind- and front hooves are different; the hind hoof angle is steeper and the hoof is narrower, which results in a different hoof-unrollment pattern compared with the front hoof (6, 16). The hoof-unrollment pattern might be affected by the velocity of the horse which explained the gait effect. The interaction term might be explained by the fact that hoof-unrollment patterns of hind- and front hooves might change differently over different gaits.

This is the first study that reports the use of the slope of the decreasing vertical force, unloading rate, for detection of the break-over phase onset. When the two established methods, OMC system and force plate, were assessed with each other, the predicted values of the time difference showed a time difference of 7.97 and 16.81 ms for respectively RF and RH in trot and 1.57 and 40.62 ms for respectively RF and RH in walk. This shows that the break-over phase onset detection based on the first derivative of the vertical force signal did not agree closely to the OMC system for all hoof/gait combinations. Based on the results of the current study, it's not possible to conclude which method detects the break-over phase onset most accurately. However, the OMC system might be better suited for detecting of rotational movement around the toe while the force plate might be better suited for detection of sudden hoof contact moments (10). Although, to determine toe-off and heel-off timings with the OMC system, an arbitrary threshold is needed in contrast to the force derivative.

During this study, no clear effect of stance duration on the performance of the break-over phase onset detection was seen. Stance durations can be found in Table S1 of the companion paper (10). With the force derivative as reference, the angular velocity algorithm did not show a better performance in walk or trot, although the acceleration algorithm did show a better performance in trot compared to walk. With the OMC system as reference, the angular velocity algorithm did show a better performance in trot compared to walk, although the acceleration algorithm did not show a better performance in walk or trot.

The results of this study show that the acceleration algorithm was the most accurate algorithm to detect the break-over phase onset which was not as expected since the hoof was not yet lifted from the ground and no big acceleration change occurred. This might be a result of calculation of the Euclidean norm; an increasing angular velocity in one direction might become concealed by a decrease in angular velocity in another direction. For clinical applications, such as evaluation of hoof trimming, testing different shoeing techniques (6, 17-19) and lameness detection (20), it might be beneficial to investigate the acceleration and angular velocity in three directions separately since rotation direction and maximal angle of rotation change with different hoof shapes and when horses are lame.

Besides measuring the rotation direction, the break-over duration might be a helpful addition for these applications. An increased break-over duration was found at mild lameness, even before lameness could be detected with the naked eye and before the stance duration of the lame limb increased (21). In the current study, break-over durations were not evaluated by statistical analysis because calculation of these durations depends on the break-over onset as well as hoof-off detection per measurement method. Both detections are performed with their corresponding accuracy and precision, where the accuracy and precision of hoof-off detections is discussed in the companion paper (10). An overview of the break-over durations within each measurement method is given in Table S1-S4 with their relative duration as percentage of the corresponding stance duration.

Break-over onset timing relative to the stance phase might also be of importance. In a previous study by Clayton et al. (2000), coffin joint moment and force plate data showed that the center of pressure began to move forward in a relatively early stage of the stance phase, initiating an early break-over phase onset in the lame limb (12). Further research should be performed to investigate the possible wider applicability of these algorithms, for instance on different surfaces. On a hard surface, the hoof remains flat on the ground until heel-off, in contrast to a soft surface on which the toe rotates into the surface before heel-off (22). This will probably make break-over phase onset detection more difficult with these algorithms. Furthermore, reliability of these algorithms should be revalued in different situations, such as sound and lame conditions or before and after hoof trimming.



## Conclusion

Two algorithms were presented to automatically detect the start of the break-over phase from the acceleration and angular velocity data measured with hoof-mounted IMUs in walk and trot on a hard surface. Internal validations against the OMC system and unloading rate, measured by the force derivative, were performed separately. The acceleration algorithm appeared to perform best with an accuracy between -9 and 23 ms and a precision around 24 ms (with the OMC system as reference), and an accuracy between -37 and 20 ms and a precision around 29 ms (with the force plate as reference), depending on gait and hoof. These algorithms seem promising for the onset of the break-over phase quantification. However, a more extensive validation process should be performed with more data and additional horses. Furthermore, the applicability of these algorithms for clinical purposes, such as lameness detection and evaluation of trimming and shoeing techniques, should be investigated more in-depth, including on different surfaces.

3

## Acknowledgements

We would like to thank W. Back, M. Marin-Perianu and P.R. van Weeren for making this study possible. A special thanks to W. Back and P.R. van Weeren for the feedback on preliminary results of the current study and J. van den Broek for statistical guidance.

## References

1. Thomason JJ, Peterson ML. Biomechanical and mechanical investigations of the hoof-track interface in racing horses. *Vet Clin North Am Equine Pract.* 2008;24(1):53-77.
2. Starke SD, Clayton HM. A universal approach to determine footfall timings from kinematics of a single foot marker in hoofed animals. *PeerJ.* 2015;3:e783.
3. Clayton HM. Comparison of the stride of trotting horses trimmed with a normal and a broken-back hoof axis. *Proceedings 7th American Association of Equine Practitioners 1987.* p. 289-98.
4. Clayton HM, Sigafoos R, Curle RD. Effect of three shoe types on the duration of breakover in sound trotting horses. *Journal of Equine Veterinary Science.* 1990;11(2):129-32.
5. Wilson A, Agass R, Vaux S, Sherlock E, Day P, Pfau T, et al. Foot placement of the equine forelimb: Relationship between foot conformation, foot placement and movement asymmetry. *Equine Vet J.* 2016;48(1):90-6.
6. Keegan KG, Satterley JM, Skubic M, Yonezawa Y, Cooley JM, Wilson DA, et al. Use of gyroscopic sensors for objective evaluation of trimming and shoeing to alter time between heel and toe lift-off at end of the stance phase in horses walking and trotting on a treadmill. *American Journal of Veterinary Research.* 2005;66(12):2046-54.
7. Chateau H, Degueurce C, Denoix JM. Three-dimensional kinematics of the equine distal forelimb: effects of a sharp turn at the walk. *Equine Vet J.* 2005;37(1):12-8.
8. Glade MJ, Salzman RA. Effects of toe angle on hoof growth and contraction in the horse. *Journal of Equine Veterinary Science.* 1985;5(1):45-50.
9. Bosch S, Serra Braganca F, Marin-Perianu M, Marin-Perianu R, van der Zwaag BJ, Voskamp J, et al. *EquiMoves: A Wireless Networked Inertial Measurement System for Objective Examination of Horse Gait.* Sensors (Basel). 2018;18(3).
10. Tijssen M. A method for automatic hoof-event detection in horses based on hoof-mounted inertial measurement units. Submitted to PLOS ONE. 2020a, companion paper.
11. Pfau T, Witte TH, Wilson AM. A method for deriving displacement data during cyclical movement using an inertial sensor. *J Exp Biol.* 2005;208(Pt 13):2503-14.
12. Clayton HM, Schamhardt HC, Willemsen MA, Lanovaz JL, Colborne GR. Kinematics and ground reaction forces in horses with superficial digital flexor tendinitis. *American Journal of Veterinary Research.* 2000;61(2):191-6.
13. Weishaupt MA, Wiestner T, Hogg HP, Jordan P, Auer JA. Vertical ground reaction force-time histories of sound Warmblood horses trotting on a treadmill. *Vet J.* 2004;168(3):304-11.
14. Braganca FM, Bosch S, Voskamp JP, Marin-Perianu M, Van der Zwaag BJ, Vernooij JCM, et al. Validation of distal limb mounted inertial measurement unit sensors for stride detection in Warmblood horses at walk and trot. *Equine Vet J.* 2017;49(4):545-51.
15. Witte TH, Knill K, Wilson AM. Determination of peak vertical ground reaction force from duty factor in the horse (*Equus caballus*). *J Exp Biol.* 2004;207(Pt 21):3639-48.
16. Van Heel MCV, Moleman M, Barneveld A, Van Weeren PR, Back W. Changes in location of centre of pressure and hoof-unrollment pattern in relation to an 8-week shoeing interval in the horse. *Equine Vet J.* 2005;37(6):536-40.
17. Page BT, Hagen TL. Breakover of the hoof and its effect on structures and forces within the foot. *Journal of Equine Veterinary Science.* 2002;22(6):258-64.
18. Spaak B, van Heel MC, Back W. Toe modifications in hind feet shoes optimise hoof-unrollment in sound Warmblood horses at trot. *Equine Vet J.* 2013;45(4):485-9.
19. Van Heel MCV, Van Weeren PR, Back W. Shoeing sound Warmblood horses with a rolled toe optimises hoof-unrollment and lowers peak loading during breakover. *Equine Vet J.* 2006;38(3):258-62.



20. Moorman VJ, Reiser RF, 2nd, Mahaffey CA, Peterson ML, Mcllwraith CW, Kawcak CE. Use of an inertial measurement unit to assess the effect of forelimb lameness on three-dimensional hoof orientation in horses at a walk and trot. *Am J Vet Res.* 2014;75(9):800-8.
21. Moorman VJ, Reiser RF, 2nd, Peterson ML, Mcllwraith CW, Kawcak CE. Effect of forelimb lameness on hoof kinematics of horses at a walk. *Am J Vet Res.* 2013;74(9):1192-7.
22. Hernlund E, Egenvall A, Roepstorff L. Kinematic characteristics of hoof landing in jumping horses at elite level. *Equine Vet J Suppl.* 2010(38):462-7.

## **Additional information**

### **Horses**

The measurements were performed for a previous study performed by Bragança et al. 2017 (14). Measurements were performed with seven Warmblood horses, six mares and one gelding, with a body mass ranging from 506 to 608 kg (mean 564.4 kg), age ranging from five to twenty-one years (mean 7.5 years) and height at withers ranging from 1.58 to 1.75 m (mean 1.65 m).

### **Data collection**

The walking speed of the horses was measured with two pairs of photoelectric sensors placed before and after the force plate at a distance of two meters.

### ***Optical motion capture setup***

Three markers were used for the motion measurements; these markers were spherical passive markers with a diameter of 12.5 mm. The 3D position of the three markers was measured with six infrared cameras (ProReflex 240) of the optical motion capture (OMC) system (Qualisys AB, Motion Capture System, Göteborg, Sweden). The cameras were placed around the force plate in such way that the vertical displacement of the markers was visible. Movements of the markers was recorded with a sampling frequency of 200 Hz and with a relative precision of 1.9 mm after calibration (9). The collected OMC data was used in another study for break-over detection (23) but was needed for time synchronization in this paper.

### ***Force plate setup and synchronization***

The force plate (Z4852C, Kistler, Winterthur, Switzerland) was covered with a five mm rubber mat. The analogue force plate signal was fed to an A/D converter with a sampling frequency of 1000 Hz and connected to the Qualisys Track Manager (QTM) software (Qualisys AB, Motion Capture System, Göteborg, Sweden) of the OMC system. The QTM software down sampled the force plate signal with a frequency of 200 Hz and removed the response time lag to obtain time synchronization with the OMC system ((14); for further details see page 134 of the QTM manual (24)).

### ***Inertial measurement unit setup and synchronization***

The ProMove-mini wireless inertial measurement units (IMUs) (Inertia-Technology B.V., Enschede, The Netherlands) weighted 20 g and were set to a sampling frequency of 200 Hz. The sensors measured the tri-axial acceleration, angular velocity (gyroscope) and magnetic field intensity (compass) over time with a



precision of 100 ns (9). The collected data was stored on the onboard 2 Gb microSD card during measurements and was retrieved after each trial.

Time synchronization between the IMUs and OMC system is described by Bosch et al. (9). In short, two reflective markers were attached above and below the IMU attached to the cannon bone of the horse (data is used for another study (14)). The correlation coefficient was calculated between the position data of these reflective markers and the angular velocity signal measured with this IMU. The time shift between the OMC system and the IMU was indicated by a maximum in the correlation coefficient. To improve this calculation, interpolation was used which resulted in a time synchronization estimated better than 500  $\mu$ s (9)).

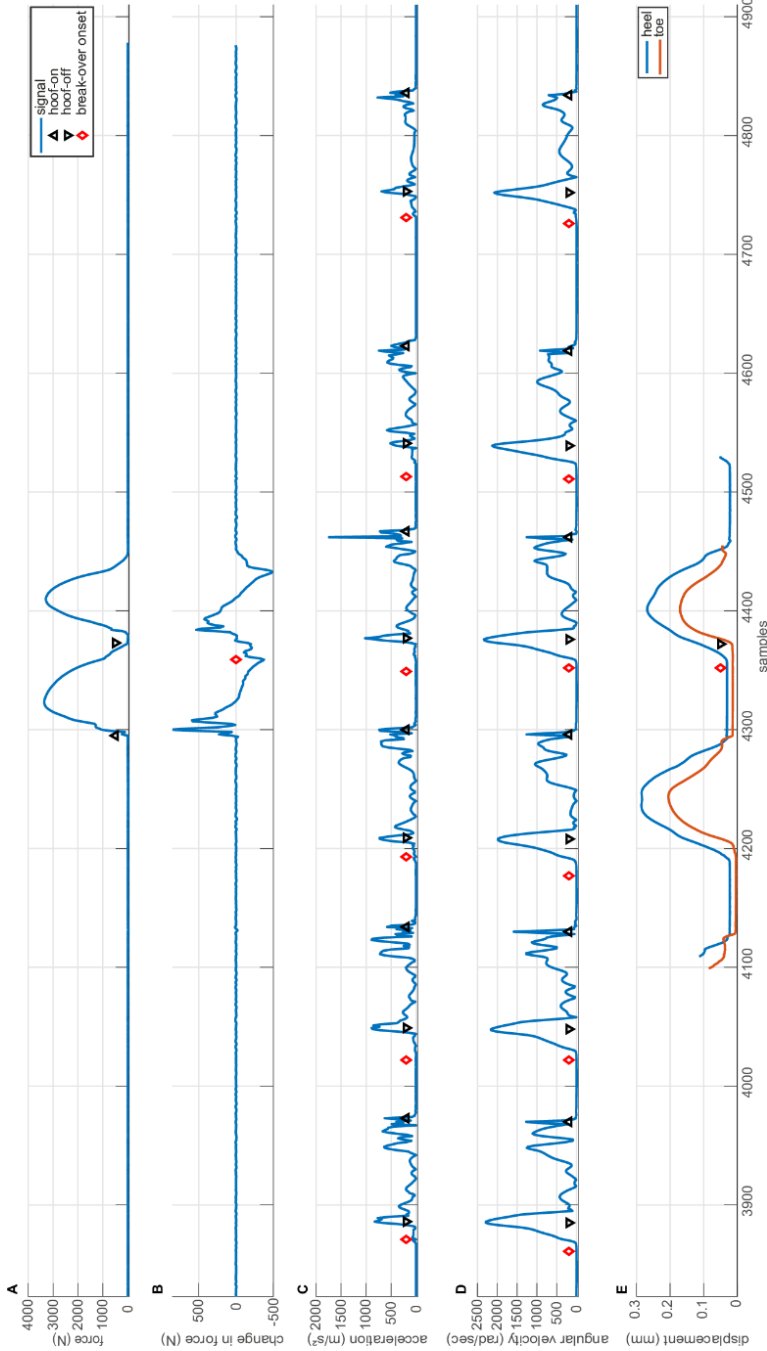


## References

1. Thomason JJ, Peterson ML. Biomechanical and mechanical investigations of the hoof-track interface in racing horses. *Vet Clin North Am Equine Pract.* 2008;24(1):53-77.
2. Starke SD, Clayton HM. A universal approach to determine footfall timings from kinematics of a single foot marker in hoofed animals. *PeerJ.* 2015;3:e783.
3. Clayton HM. Comparison of the stride of trotting horses trimmed with a normal and a broken-back hoof axis. *Proceedings 7th American Association of Equine Practitioners 1987.* p. 289-98.
4. Clayton HM, Sigafoos R, Curle RD. Effect of three shoe types on the duration of breakover in sound trotting horses. *Journal of Equine Veterinary Science.* 1990;11(2):129-32.
5. Wilson A, Agass R, Vaux S, Sherlock E, Day P, Pfau T, et al. Foot placement of the equine forelimb: Relationship between foot conformation, foot placement and movement asymmetry. *Equine Vet J.* 2016;48(1):90-6.
6. Keegan KG, Satterley JM, Skubic M, Yonezawa Y, Cooley JM, Wilson DA, et al. Use of gyroscopic sensors for objective evaluation of trimming and shoeing to alter time between heel and toe lift-off at end of the stance phase in horses walking and trotting on a treadmill. *American Journal of Veterinary Research.* 2005;66(12):2046-54.
7. Chateau H, Degueurce C, Denoix JM. Three-dimensional kinematics of the equine distal forelimb: effects of a sharp turn at the walk. *Equine Vet J.* 2005;37(1):12-8.
8. Glade MJ, Salzman RA. Effects of toe angle on hoof growth and contraction in the horse. *Journal of Equine Veterinary Science.* 1985;5(1):45-50.
9. Bosch S, Serra Braganca F, Marin-Perianu M, Marin-Perianu R, van der Zwaag BJ, Voskamp J, et al. *EquiMoves: A Wireless Networked Inertial Measurement System for Objective Examination of Horse Gait.* Sensors (Basel). 2018;18(3).
10. Tijssen M. A method for automatic hoof-event detection in horses based on hoof-mounted inertial measurement units. Submitted to PLOS ONE. 2020a, companion paper.
11. Pfau T, Witte TH, Wilson AM. A method for deriving displacement data during cyclical movement using an inertial sensor. *J Exp Biol.* 2005;208(Pt 13):2503-14.
12. Clayton HM, Schamhardt HC, Willemsen MA, Lanovaz JL, Colborne GR. Kinematics and ground reaction forces in horses with superficial digital flexor tendinitis. *American Journal of Veterinary Research.* 2000;61(2):191-6.
13. Weishaupt MA, Wiestner T, Hogg HP, Jordan P, Auer JA. Vertical ground reaction force-time histories of sound Warmblood horses trotting on a treadmill. *Vet J.* 2004;168(3):304-11.
14. Braganca FM, Bosch S, Voskamp JP, Marin-Perianu M, Van der Zwaag BJ, Vernooij JCM, et al. Validation of distal limb mounted inertial measurement unit sensors for stride detection in Warmblood horses at walk and trot. *Equine Vet J.* 2017;49(4):545-51.
15. Witte TH, Knill K, Wilson AM. Determination of peak vertical ground reaction force from duty factor in the horse (*Equus caballus*). *J Exp Biol.* 2004;207(Pt 21):3639-48.
16. Van Heel MCV, Moleman M, Barneveld A, Van Weeren PR, Back W. Changes in location of centre of pressure and hoof-unrollment pattern in relation to an 8-week shoeing interval in the horse. *Equine Vet J.* 2005;37(6):536-40.
17. Page BT, Hagen TL. Breakover of the hoof and its effect on structures and forces within the foot. *Journal of Equine Veterinary Science.* 2002;22(6):258-64.
18. Spaak B, van Heel MC, Back W. Toe modifications in hind feet shoes optimise hoof-unrollment in sound Warmblood horses at trot. *Equine Vet J.* 2013;45(4):485-9.
19. Van Heel MCV, Van Weeren PR, Back W. Shoeing sound Warmblood horses with a rolled toe optimises hoof-unrollment and lowers peak loading during breakover. *Equine Vet J.* 2006;38(3):258-62.



20. Moorman VJ, Reiser RF, 2nd, Mahaffey CA, Peterson ML, Mcllwraith CW, Kawcak CE. Use of an inertial measurement unit to assess the effect of forelimb lameness on three-dimensional hoof orientation in horses at a walk and trot. *Am J Vet Res.* 2014;75(9):800-8.
21. Moorman VJ, Reiser RF, 2nd, Peterson ML, Mcllwraith CW, Kawcak CE. Effect of forelimb lameness on hoof kinematics of horses at a walk. *Am J Vet Res.* 2013;74(9):1192-7.
22. Hernlund E, Egenvall A, Roepstorff L. Kinematic characteristics of hoof landing in jumping horses at elite level. *Equine Vet J Suppl.* 2010(38):462-7.
23. Tijssen M. Break-over detection using hoof-mounted inertial measurements units. Submitted to *Journal of Experimental Biology.* 2020b, companion paper.
24. Qualisys AB. Qualisys Track Manager - User Manual. Gothenborg, Sweden 2011.



**S1 Figure. Preprocessed signals of the force plate, vertical force (A) and the first derivative of the vertical force (B), the acceleration (C) and angular velocity (D) signals of the IMU, and vertical displacement signals of the heel and toe markers of the OMC system (E) from one hoof from one measurement in trot.** The hoof-on events are depicted with upward-pointing triangle markers, hoof-off events are depicted with downward-pointing triangle markers and break-over onset events are depicted with diamond shaped markers. For the OMC data, break-over onset events are depicted were the heel of the hoof leaves the ground and hoof-off events are depicted were the toe of the hoof leaves the ground.



**S1-S4 Table. Tables with break-over durations.** Tables with break-over durations per trial in milliseconds (ms) and relative to corresponding stance duration (%) as detected with the acceleration and angular velocity algorithms, force derivative and OMC system for every hoof and gait combination.

**Table S1. Break-over durations per trial in milliseconds (ms) and relative to stance duration (%) for right front hoof in walk**

Break-over duration in ms (%) for right front hoof in walk									
horse ID	trial	Acceleration		Angular Velocity		Force Derivative		OMC	
1	1	140	(18.92)	170	(22.97)	145	(19.33)	90	(12.59)
	2	150	(21.13)	170	(23.78)	140	(19.18)	60	(8.82)
	3	150	(20.00)	175	(23.33)	165	(21.71)	60	(8.76)
	4	110	(14.57)	210	(27.63)	160	(20.78)	80	(11.68)
	5	155	(19.75)	195	(25.16)	150	(19.23)	70	(9.59)
2	1	140	(17.50)	175	(21.74)	130	(16.15)	110	(13.84)
	2	90	(11.11)	170	(20.99)	125	(15.53)	100	(12.74)
	3	25	(3.05)	185	(22.02)	135	(16.56)	135	(17.09)
	4	115	(13.69)	185	(21.76)	135	(16.07)	120	(14.20)
	5	215	(24.43)	175	(19.89)	150	(17.14)	50	(6.17)
3	1	80	(10.13)	170	(21.79)	125	(15.82)	65	(8.72)
	2	70	(8.97)	175	(22.15)	50	(6.29)	100	(12.99)
	3	140	(19.18)	160	(21.62)	115	(15.65)	105	(14.29)
	4	105	(14.09)	160	(20.78)	120	(15.29)	125	(15.82)
	5	55	(7.75)	175	(22.88)	135	(17.53)	100	(13.89)
4	1	175	(23.18)	225	(29.80)	170	(21.66)	45	(6.98)
	2	165	(19.88)	230	(27.38)	170	(20.00)	30	(4.35)
	3	190	(23.60)	200	(24.24)	170	(20.00)	20	(2.94)
	5	155	(18.90)	240	(27.75)	170	(19.54)	35	(4.73)
	6	155	(19.38)	240	(28.40)	175	(20.59)	90	(11.69)
	5	1	45	(5.81)	185	(24.18)	135	(17.42)	35
5	2	185	(22.16)	200	(23.95)	165	(19.53)	55	(7.80)
	3	45	(5.70)	185	(23.42)	150	(18.99)	100	(14.18)
	4	145	(16.67)	190	(21.84)	160	(18.39)	15	(2.10)
	5	95	(11.24)	205	(24.12)	55	(6.43)	30	(4.23)
	6	1	140	(17.61)	180	(21.95)	115	(14.38)	45
4		135	(17.31)	175	(22.88)	100	(12.90)	95	(12.58)
5		145	(17.47)	185	(22.70)	105	(12.65)	55	(7.24)
7		45	(5.39)	170	(19.88)	115	(13.94)	105	(12.96)

	8	100	(14.29)	155	(20.81)	180	(24.66)	35	(5.43)
	9	135	(17.88)	175	(23.49)	210	(27.63)	60	(8.70)
7	1	95	(13.01)	100	(13.79)	85	(11.49)	30	(4.41)
	2	110	(15.38)	105	(15.00)	90	(12.59)	0	-
	3	30	(3.92)	105	(13.91)	90	(11.61)	30	(4.38)
	4	35	(4.93)	105	(15.00)	95	(13.19)	35	(5.56)
	5	115	(16.79)	120	(17.78)	80	(10.88)	25	(3.91)

The break-over duration is determined as the time between break-over phase onset and hoof-off for the force plate, acceleration and angular velocity algorithms. For the OMC system, the break-over duration is determined as the time between heel-off and toe-off. The stance duration is determined as the time between hoof-on and hoof-off for the force plate, acceleration and angular velocity algorithms. For the OMC system, the stance duration is determined as the time between heel-on and toe-off. Break-over duration as percentage of the corresponding stance duration is given between brackets.

**Table S2. Break-over durations per trial in milliseconds (ms) and relative to stance duration (%) for right hind hoof in walk**

Break-over duration in ms (%) for right hind hoof in walk									
horse ID	trial	Acceleration		Angular Velocity		Force Derivative		OMC	
1	1	150	(19.74)	165	(21.85)	55	(7.14)	60	(8.76)
	2	145	(19.59)	160	(21.19)	105	(13.64)	60	(8.82)
	3	165	(21.85)	190	(24.84)	80	(10.26)	50	(7.30)
	4	90	(12.00)	125	(16.56)	85	(10.97)	65	(9.29)
	5	175	(23.18)	135	(17.65)	130	(16.46)	65	(9.29)
2	1	130	(16.99)	190	(25.00)	60	(8.00)	25	(3.70)
	2	160	(21.05)	165	(21.57)	70	(8.75)	145	(18.01)
	3	135	(17.20)	185	(23.57)	60	(7.45)	40	(5.67)
	4	120	(15.19)	210	(25.93)	60	(7.32)	55	(7.48)
	5	225	(25.86)	240	(28.40)	55	(6.08)	125	(15.15)
3	1	125	(16.67)	155	(20.53)	120	(16.00)	45	(6.52)
	2	140	(18.54)	160	(21.05)	110	(14.67)	45	(6.57)
	3	125	(17.48)	125	(17.24)	115	(15.75)	40	(6.02)
	4	130	(17.69)	150	(20.41)	115	(15.65)	40	(5.88)
	5	130	(18.31)	140	(19.86)	100	(13.70)	35	(5.30)
4	1	145	(18.71)	140	(17.95)	125	(15.82)	65	(8.78)
	2	200	(25.00)	170	(21.25)	120	(15.00)	55	(7.43)
	5	55	(6.67)	190	(22.49)	135	(15.88)	55	(7.19)
	6	200	(25.32)	170	(20.99)	135	(16.46)	55	(7.24)
5	1	100	(12.66)	165	(20.75)	120	(15.09)	0	-
	2	150	(18.07)	170	(20.24)	130	(15.20)	45	(6.04)
	3	175	(21.60)	185	(22.70)	140	(16.87)	65	(8.78)
	4	170	(20.12)	170	(19.88)	125	(14.20)	0	-
	5	25	(2.91)	175	(20.47)	65	(7.30)	45	(5.84)



6	1	155	(20.26)	195	(24.84)	170	(21.79)	130	(17.11)
	5	160	(18.71)	175	(20.11)	100	(11.24)	115	(14.02)
	7	215	(22.51)	205	(22.16)	130	(13.76)	0	-
	8	185	(24.50)	195	(25.49)	65	(8.44)	160	(21.19)
	9	165	(22.15)	165	(21.43)	60	(7.64)	160	(20.38)
7	1	50	(6.71)	160	(20.92)	105	(13.46)	65	(9.15)
	2	130	(17.69)	140	(19.18)	100	(13.42)	40	(5.97)
	3	75	(10.07)	135	(17.76)	105	(13.46)	30	(4.35)
	4	160	(22.07)	130	(18.06)	90	(12.24)	40	(5.97)
	5	95	(13.57)	130	(17.57)	85	(10.97)	35	(5.11)

The break-over duration is determined as the time between break-over phase onset and hoof-off for the force plate, acceleration and angular velocity algorithms. For the OMC system, the break-over duration is determined as the time between heel-off and toe-off. The stance duration is determined as the time between hoof-on and hoof-off for the force plate, acceleration and angular velocity algorithms. For the OMC system, the stance duration is determined as the time between heel-on and toe-off. Break-over duration as percentage of the corresponding stance duration is given between brackets.

**Table S3. Break-over durations per trial in milliseconds (ms) and relative to stance duration (%) for right front hoof in trot**

Break-over duration in ms (%) for right front hoof in trot									
horse ID	trial	Acceleration		Angular Velocity		Force Derivative		OMC	
1	1	140	(36.36)	120	(30.00)	70	(17.95)	60	(16.22)
	3	95	(27.54)	120	(33.33)	70	(19.44)	45	(14.52)
	4	125	(34.72)	125	(33.33)	70	(20.00)	30	(9.09)
	6	150	(42.86)	125	(35.21)	70	(20.00)	25	(9.26)
	7	90	(25.71)	125	(34.25)	60	(17.14)	50	(14.49)
2	1	35	(12.96)	180	(57.14)	70	(22.22)	20	(7.69)
	4	90	(26.47)	195	(52.70)	65	(20.63)	20	(7.27)
	5	50	(15.87)	200	(56.34)	75	(21.74)	30	(10.34)
	6	55	(19.64)	180	(48.65)	65	(20.31)	20	(7.27)
	7	110	(32.35)	195	(52.70)	70	(21.21)	25	(9.43)
3	1	75	(22.39)	80	(24.24)	55	(16.92)	20	(6.90)
	2	110	(32.84)	80	(23.19)	75	(21.74)	65	(19.12)
	3	100	(27.40)	95	(22.35)	70	(19.72)	60	(17.39)
	4	110	(31.88)	100	(29.85)	65	(19.40)	40	(12.70)
	5	75	(23.08)	80	(23.88)	60	(18.46)	60	(18.46)
	7	45	(14.75)	80	(23.88)	65	(19.40)	60	(19.35)
4	1	75	(22.73)	185	(50.00)	75	(20.83)	45	(15.25)
	2	105	(31.82)	120	(39.34)	75	(21.74)	10	(4.17)
	3	105	(30.43)	130	(41.27)	70	(20.00)	0	-
	4	115	(31.94)	175	(46.05)	80	(21.62)	15	(5.56)
	5	75	(23.81)	100	(30.77)	80	(21.33)	15	(5.00)

5	1	55	(16.67)	95	(24.36)	65	(19.40)	0	-
	2	75	(23.44)	120	(36.36)	65	(18.84)	20	(8.16)
	3	105	(27.63)	125	(34.25)	75	(20.27)	20	(7.55)
	4	100	(25.00)	140	(35.90)	90	(22.50)	20	(6.90)
	5	65	(18.06)	130	(34.21)	75	(19.48)	0	-
	6	50	(12.99)	140	(35.90)	80	(20.78)	35	(12.96)
	7	60	(14.81)	170	(42.50)	95	(23.46)	30	(9.84)
	8	105	(26.92)	145	(37.18)	90	(23.08)	10	(3.92)
6	1	95	(30.65)	95	(31.67)	70	(23.73)	20	(10.26)
	4	50	(15.87)	100	(31.75)	70	(22.22)	25	(10.20)
	5	120	(40.00)	140	(46.67)	75	(24.19)	60	(22.64)
	6	135	(43.55)	150	(50.00)	70	(23.73)	30	(12.50)
	7	45	(14.75)	75	(25.42)	65	(22.41)	30	(11.76)
7	1	115	(32.86)	75	(21.13)	55	(14.86)	20	(7.27)
	2	70	(22.58)	60	(19.05)	40	(12.50)	15	(5.66)
	3	110	(31.88)	75	(21.74)	50	(13.89)	20	(7.14)
	4	60	(18.18)	70	(20.59)	55	(14.67)	25	(9.62)
	5	125	(36.23)	80	(23.19)	55	(15.94)	15	(5.17)

The break-over duration is determined as the time between break-over phase onset and hoof-off for the force plate, acceleration and angular velocity algorithms. For the OMC system, the break-over duration is determined as the time between heel-off and toe-off. The stance duration is determined as the time between hoof-on and hoof-off for the force plate, acceleration and angular velocity algorithms. For the OMC system, the stance duration is determined as the time between heel-on and toe-off. Break-over duration as percentage of the corresponding stance duration is given between brackets.

**Table S4. Break-over durations per trial in milliseconds (ms) and relative to stance duration (%) for right hind hoof in trot**

Break-over duration in ms (%) for right hind hoof in trot									
horse ID	trial	Acceleration		Angular Velocity		Force Derivative		OMC	
1	1	105	(30.43)	140	(40.00)	80	(23.19)	25	(9.09)
	2	80	(24.24)	130	(36.62)	60	(17.65)	20	(7.41)
	3	100	(31.25)	135	(40.91)	80	(24.24)	25	(9.80)
	4	105	(31.34)	135	(39.71)	80	(23.53)	30	(10.91)
	5	190	(52.05)	165	(42.31)	105	(27.63)	30	(10.53)
	6	100	(33.33)	155	(50.82)	70	(22.95)	40	(19.05)
	7	125	(37.88)	125	(36.23)	85	(25.00)	50	(17.24)
2	1	70	(25.93)	85	(30.91)	55	(18.97)	30	(12.00)
	2	55	(22.00)	160	(53.33)	45	(15.79)	40	(14.81)
	3	45	(17.65)	90	(30.51)	40	(13.56)	70	(22.58)
	4	25	(10.87)	80	(28.57)	60	(21.05)	70	(22.95)
	7	35	(14.00)	105	(35.00)	60	(20.69)	65	(23.64)



3	2	50	(17.86)	85	(30.36)	60	(21.05)	25	(11.11)
	3	85	(28.81)	85	(29.31)	55	(19.30)	25	(11.63)
	5	90	(33.96)	80	(29.09)	60	(21.43)	20	(8.51)
	6	105	(38.89)	90	(31.58)	55	(19.64)	20	(8.70)
	7	90	(32.73)	85	(30.36)	60	(21.05)	20	(8.51)
4	1	85	(27.87)	120	(38.71)	65	(19.70)	15	(6.00)
	2	85	(28.33)	120	(39.34)	55	(18.03)	15	(6.25)
	3	75	(25.42)	120	(38.71)	60	(19.05)	15	(5.77)
	4	30	(10.91)	115	(35.94)	65	(20.31)	20	(8.16)
	5	80	(26.67)	100	(31.75)	60	(18.75)	20	(8.16)
5	3	90	(28.13)	85	(26.98)	60	(19.67)	0	-
	4	165	(40.74)	240	(59.26)	240	(55.17)	0	-
	5	90	(31.03)	95	(30.16)	70	(22.22)	35	(15.56)
	7	15	(5.00)	95	(28.79)	80	(24.24)	70	(35.90)
	8	95	(31.15)	60	(22.64)	70	(21.54)	30	(13.04)
6	2	90	(32.14)	90	(31.58)	65	(21.67)	85	(27.87)
	3	20	(7.69)	70	(26.42)	45	(16.07)	45	(17.65)
	4	40	(18.60)	90	(30.51)	55	(19.64)	75	(25.42)
	5	30	(11.76)	70	(25.45)	50	(18.52)	35	(14.89)
	6	270	(66.67)	80	(30.19)	55	(20.00)	70	(25.93)
	8	185	(51.39)	140	(40.58)	55	(17.74)	50	(17.24)
7	1	80	(22.22)	70	(23.33)	75	(20.55)	55	(19.30)
	2	90	(28.13)	60	(21.05)	65	(20.00)	30	(11.76)
	3	105	(30.88)	60	(21.05)	70	(20.59)	35	(11.29)
	4	95	(28.36)	65	(22.81)	70	(20.90)	50	(18.18)
	5	75	(24.19)	65	(22.41)	65	(19.40)	20	(7.41)

The break-over duration is determined as the time between break-over phase onset and hoof-off for the force plate, acceleration and angular velocity algorithms. For the OMC system, the break-over duration is determined as the time between heel-off and toe-off. The stance duration is determined as the time between hoof-on and hoof-off for the force plate, acceleration and angular velocity algorithms. For the OMC system, the stance duration is determined as the time between heel-on and toe-off. Break-over duration as percentage of the corresponding stance duration is given between brackets.





## **Part 2**

# **Application of signal analysis procures to another species**



# 4

## **Kinematic gait characteristics of straight line walk in clinically sound dairy cows**

Published in PlosOne, 2021, 16(7)

M. Tijssen  
F. M. Serra Bragança  
K. Ask  
M. Rhodin  
P. H. Andersen  
E. Telezhenko  
C. Bergsten  
M. Nielen  
E. Hernlund

## **Abstract**

The aim of this study is to describe the kinematic gait characteristics of straight line walk in clinically sound dairy cows using body mounted Inertial Measurement Units (IMUs) at multiple anatomical locations. The temporal parameters used are speed and non-speed normalized stance duration, bipedal and tripedal support durations, maximal protraction and retraction angles of the distal limbs and vertical displacement curves of the upper body.

Gait analysis was performed by letting 17 dairy cows walk in a straight line at their own chosen pace while equipped with IMU sensors on tubera sacrale, left and right tuber coxae (LTC and RTC), back, withers, head, neck and all four lower limbs. Data intervals with stride by stride regularity were selected based on video data. For temporal parameters, the median was calculated and 95% confidence intervals (CI) were estimated based on linear mixed model (LMM) analysis, while for limb and vertical displacement curves, the median and most typical curves were calculated.

The temporal parameters and distal limb angles showed consistent results with low variance and LMM analysis showed non-overlapping CI for all temporal parameters. The distal limb angle curves showed a larger and steeper retraction angle range for the distal front limbs compared with the hind limbs. The vertical displacement curves of the sacrum, withers, LTC and RTC showed a consistent sinusoidal pattern while the head, back and collar curves were less consistent and showed more variation between and within cows.

This kinematic description might allow to objectively differentiate between normal and lame gait in the future and determine the best anatomical location for sensor attachment for lameness detection purposes.



## Introduction

The kinematic study of gait characteristics in dairy cows can provide important insight into the normal walking gait patterns, allowing us to objectively differentiate normal from abnormal gait (1, 2). Lameness can be defined as a deviation from the normal gait pattern due to compensatory movements to avoid any pain or discomfort (3). Despite intense research, lameness still is one of the most important welfare issues in dairy cows since its prevalence is high and it often remains undetected until the lameness degree worsens (4-6). Therefore, recognition and treatment of lameness at an early stage improves welfare for the cow and also reduces the economical and unwanted consequences for the farmer (7, 8).

Currently, lameness detection is based on visual assessment using subjective locomotion scoring to recognize alterations in the gait patterns (9-12). These locomotion scales mainly make use of stride change, body poses and abnormal position of the back. However, studies show that farmers visually recognize only a third of the lame cows in their herd, which are assessed as severely lame cows by researchers (12, 13). A method with high sensitivity for subtle lameness is therefore warranted (2, 14). Research has been focused on refinement of behavioral methods, based on quantification of lying and standing behaviors, which also proved insensitive for early detection of subtle lameness (15, 16). Several works are describing the kinematic gait characteristics of both lame and clinically sound cows (17-19). And, only recently, gait characteristics were introduced in combination with the behavioral-based methods (2, 14), revealing a need for more knowledge on kinematic gait characteristics in cows to allow objectively differentiation of the normal gait from abnormal gait.

In equine practice, quantitative lameness detection has matured into a practical clinical tool, and is routinely performed using optical motion systems or Inertial Measurement Units (IMUs) (3). These techniques have overcome the low accuracy inherent to the human visual assessment by measuring subtle changes in kinematic gait characteristics (20-22). The most reliable and clinically used characteristics for lameness assessment in trot is the vertical excursion of the head, withers and tubera sacrale measured by IMUs attached to the upper body (20, 23, 24). This vertical excursion is also useful for detection of lameness at the walk, together with temporal stride parameters (e.g. stride and stance duration) and joint angles of the limbs (23, 25-27).

Since many cows already wear single low-resolution accelerometers around their neck or limb, it is most obvious to focus on accelerometer based techniques, such as IMUs, to overcome major barriers for adoption on dairy farms (2). In a previous study, the gait characteristics of walking dairy cows were based on data from two accelerometers attached to the lateral claw and metatarsus (1). This study showed promising results and a description of gait characteristics that differ between lame and non-lame cows (1). However, vertical excursion of the upper body has not yet been described of the walking gait in dairy cows. Given the visibility of these body landmarks, even for a cow among herd mates, it would be of future interest to explore if asymmetries in the vertical excursions of the upper body could prove sensitive for detection of lame animals. This can be of particular interest in the development on automated lameness detection systems based on computer vision, where challenging sensor attachment is superfluous, but optical occlusion of limbs is a challenge. Prerequisite for such studies is the knowledge of normal walking gait.

The aim of this study is to describe the kinematic gait characteristics and their normal variation of straight line walk in clinically sound dairy cows using body mounted IMUs at multiple anatomical locations. This detailed kinematic description might allow us to objectively differentiate between normal and lame gait characteristics in the future and determine the best anatomical location for sensor attachment for lameness detection purposes.

## **Materials and Methods**

### **Ethical statement**

The study was approved by the Swedish Ethics Committee and according to the Swedish legislation on animal experiments (diary number 5.8.18-10570/2019).

### **Study protocol**

Gait analysis was performed during straight line locomotion by letting cows walk on a 72 meter concrete corridor in their own chosen pace while equipped with IMU sensors on different anatomical landmarks. Intervals with stride by stride regularity were selected from the data based on video data for further analysis. Subsequently, temporal parameters as well as distal limb angles and vertical displacement curves were extracted from respectively the limb and upper body IMUs. The temporal parameters used are the stance duration, speed normalized stance duration, bipedal and tripedal support durations, speed normalized



bipedal and tripedal support durations, maximal protraction and retraction angles of the distal limbs.

### **Experimental animals**

For the study, 17 early or mid-lactation cows were selected from the Swedish Livestock Research Centre Lövsta at the Swedish University of Agricultural Sciences (nine Swedish Red and eight Swedish Holstein cows), for more details see S1 Table. The cows were selected if they met the following inclusion criteria: i. they were claw trimmed within the last three months prior to the measurements during which no clinically significant claw disorders were recorded, ii. they showed no signs of pain, nervous or stressed behavior, iii. they were assessed as clinically healthy and scored zero on the Sprecher lameness scale (9) as evaluated by two experienced raters (CB and ET), iv. they had a body exterior within normal range and a normal limb exterior without major visible deviations.

4

### **IMUs and sensor placement**

The measurements were performed with the equine gait analysis system EquiMoves® (28). The cows were equipped with 11 ProMove-mini wireless IMU sensors (Inertia-Technology B.V., Enschede) as can be seen in Fig 1. The sensors were placed on the following anatomical landmarks; just caudal to the nuchal crest (further called head), the highest point of the withers (further called withers), the spinal process of the 13<sup>th</sup> thoracic vertebra (further called back), between the tubera sacrale of the pelvis (further called sacrum), right and left tuber coxae (further called RTC and LTC respectively), lateral aspect of the mid metatarsus/metacarpus of each limb (further called limb or LF (left front), RF (right front), LH (left hind), RH (right hind)) and one sensor was attached to the inner right side of neck collar (further called collar). The upper body sensors were attached to the skin with cyanoacrylate glue, and limb and collar sensors were attached with straps. After the measurements, the sensors were removed with acetone from the upper body.

The IMU sensors attached to the upper body were set to a range of  $\pm 8 g$  for the low-*g* acceleration,  $\pm 100 g$  for the high-*g* acceleration and 2000 degrees/s for the angular velocity. The IMU sensors attached to the limbs were set to a range of 16 *g* for the low-*g* acceleration, 200 *g* for the high-*g* acceleration and 2000 degrees/s for the angular velocity. All sensors were set to a sampling rate of 200 Hz and synchronized in time with an accuracy of  $< 100$  ns.



The IMU sensors were calibrated when every measurement was started with a period of five seconds of silent signal in which the cow was completely standing still. After each measurement, the acceleration and angular velocity data (further described as IMU data) were wirelessly transmitted via the Inertia Gateway to the Inertia Studio software (version 3.5.2)



**Figure 1. Cow equipped with IMU sensors on predefined anatomical landmarks.** IMUs are indicated with orange circles; just caudal to the nuchal crest, the highest point of the withers, the spinal process of the 13<sup>th</sup> thoracic vertebra, between the tubera sacrale of the pelvis, right and left tuber coxae, lateral aspect of the metatarsus/metacarpus of each limb and one sensor was attached on the inner right side of neck collar.

### **Data collection**

At each day of the measurements, two cows were moved to the stable where the measurements took place to familiarize themselves with the surroundings. The cows were allowed to walk freely and had access to hay and water ad libitum.

For the measurements, each cow was walked through a corridor of 72 meters long with diamond grooved solid concrete flooring and cubicles and fences on both sides. The cows had to walk this corridor up and down twice (in total 288 meters) with a self-chosen calm and constant pace to obtain data of a natural walking

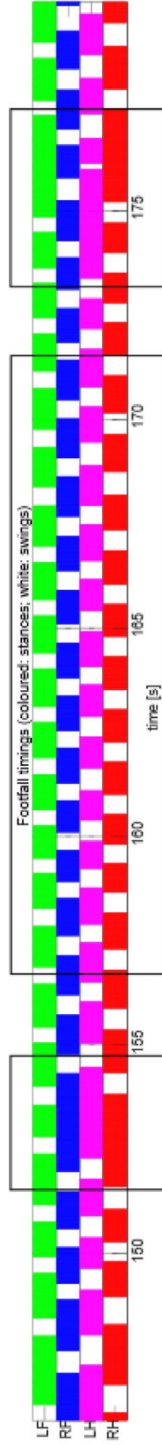


**Fig 2. Footfall figure of selected interval of a measurement.** Limbs are indicated by separate colors (green: LF, blue: RF, purple: LH, red: RH); colored areas indicate stances and white areas indicate swing phases as adapted from horses (29). The first box shows an excluded epoch in which three limbs have a prolonged stance duration compared with the LH limb, the second box indicates an included epoch of stride-by-stride regularity in which all limbs have comparable stance and swing durations and the third box indicates an excluded epoch in which three limbs have longer stance durations but not at the same moment in time.

flow. One or two researchers walked behind the cow from a distance to prevent the cow from turning around, while handling the cow as little as possible to not disturb the measurements. No other animals were present in the corridor during measurements.

Each measurement was video recorded from the side by a researcher walking alongside the cow with a handheld camera (Canon Legria HF R78, Canon, Tokyo, Japan). The handheld camera had a frame rate of 50 fps and a resolution of 1280x720 pixels. The camera was synchronized with the IMUs by tapping the withers sensor twice at the start of the measurement while filming.

### **Data selection**

From each measurement, selection of IMU data for further analysis was based on video images of the handheld camera and footfall figures (Fig 2; adapted from horses (29)). Intervals were selected when they met the following criteria: i. the cows were walking in a straight line up and down the corridor (no turns), ii. the cows were physical handled to walk by the driver (to avoid selection of intervals with anomalous walking patterns or body postures), iii. stride by stride regularity was seen in the footfall figures (the second box of Fig 2). A maximum of four intervals per measurement was used for analysis.

### **Data analysis**

The selected intervals from the IMU data were exported to MATLAB (version R2017a, The MathWorks Inc., Natick, Massachusetts, USA) for analysis by the following steps which are also shown in S1 Fig.

Claw-on and claw-off timings were detected with already existing algorithms developed for horses (30) and these timings were used for stride segmentation of the limb data. Stride segmentation was performed based on the claw-on moment of the LH limb as previously described (28).

For the limb data, the sagittal orientation of the IMU was calculated as described in the EquiMoves data analysis framework (28) and based on the quaternion-based complementary filter (31). This resulted in stride segmented distal limb angle curves from which the maximal distal limb angles were calculated. Maximal protraction is the maximal forward extension (positive angle) from midstance and maximal retraction is the maximal backward extension (negative angle) from midstance of a distal limb in the sagittal plane (S2 Fig; adapted from horses (32)). These distal limb angles and stride segmented limb angle curves were used for distal limb angle analysis.



For the not stride segmented upper body IMU signals, the orientation on a global coordinate frame was calculated based on the quaternion-based complementary filter (31). Thereafter, the vertical displacement signals were determined based on a cyclic double integration of the acceleration signal (33) and used for the vertical displacement analysis. Stride segmentation of these signals was performed with a novel method as described in the vertical displacement analysis section.

### ***Temporal analysis***

From the stride segmented limb data, the stance duration was calculated for all limbs separately while the bipedal and tripedal support durations were calculated for all possible limb (pairs). The definitions of these durations can be found Table 1. Since the cows were walking in their own chosen pace, speed normalization was performed for all these durations by dividing the duration with the entire stride duration of the corresponding stride of the LH limb resulting in a fraction (i.e. duty factor). All the calculated durations and fractions were evaluated and durations shorter than zero seconds and fractions bigger than one or smaller than zero were excluded from further analysis.

Distributions of these parameters were visualized in boxplots for every cow and limb (pairs) separately. The median duration of each parameter and their 95% confidence interval was calculated by bootstrapping. Differences between limbs, for stance duration, and limb pair combinations, for bipedal and tripedal support durations, were evaluated based on the stride level data by linear mixed model analysis with the “lme4” package (34) in R (version 1.1.442, RStudio Inc., Boston, Massachusetts, USA). For these models, limb (pairs) and deviations from the median stride duration was taken as fixed effects, except for the speed normalized data, and cow as random effect. Deviations of normality and homoscedasticity of the residuals was visually checked by examining the QQ plot and residual plot. Thereafter, 95% confidence intervals were evaluated with the “confint” package (35) and used for hypothesis testing.

**Table 1. Detailed description of the calculated parameters used in this study.** Limbs are indicated by LF (left front), RF (right front), LH (left hind) and RH (right hind). These definitions are adapted from horses (25).

Name	Abbreviation	Description
Stance duration (sec)		Time between claw-on and subsequent claw-off
Stride duration (sec)		Time between claw-on and subsequent claw-on
Bipedal support phase duration (sec)		Duration of simultaneous stance phase of two limbs:
	LF-RH	left diagonal
	RF-LH	right diagonal
	LF-LH	left ipsilateral
	RF-RH	right ipsilateral
Tripedal support phase duration (sec)		Duration of simultaneous stance phase of three limbs:
	not LF	RF-LH-RH
	not RF	LF-LH-RH
	not LH	LF-RF-RH
	not RH	LF-RF-LH
Speed normalization		Duration divided by entire stride duration of LH (resulting in a fraction between 0 and 1).
Distal limb angles (degrees)	max protraction	Maximal forward protraction of the distal limb measured at the metacarpus/-tarsus in the sagittal plane
	max retraction	Maximal backward retraction of the distal limb measured at the metacarpus/-tarsus in the sagittal plane
Vertical displacement (mm)		Upwards and downwards displacement of the sensor in the sagittal plane

### ***Distal limb angle analysis***

The determined distal limb angles were evaluated; maximal retraction angles larger than zero degrees and maximal protraction angles smaller than zero degrees were excluded. Visualization and estimation of the confidence intervals was performed in the same manner as described for the temporal parameters.

The stride segmented distal limb angle curves were linear interpolated to 100 samples to ensure that all curves were of the same length, allowing comparison between and within cows since the cows were walking in their own chosen pace. The following analysis steps were performed over all cows and steps for every limb separately: i) the differences between all the curves was calculated and the curve with the least difference is further called the most typical curve, ii) the median curve and median absolute deviation (MAD), mean claw-on timing and mean claw-off timing were calculated, and iii) the curves were depicted on a scale from zero to 100; where zero indicated the start of the stride (first claw-on moment) and 100 the end of the stride (next claw-on moment).



### **Vertical displacement analysis**

The vertical displacement signals of the upper body sensors (sacrum, RTC, LTC, back, withers, head and collar) were cut into intervals from claw-on to claw-on timing of the left hind limb. Before and after these timings, ten percent of the entire stride duration was added, to make visual inspection of the intervals more intuitive, and every interval was linear interpolated to 100 samples allowing comparison between and within cows. The following analysis steps were performed over all steps for every cow and sensor location separately: i) the most typical curve, median curve and MAD were calculated, ii) the mean claw-on and claw-off timings were calculated for every limb, to indicate the stance and swing phase for every limb in the figures (further called footfalls), and iii) the curves and footfalls were depicted on a scale from zero to 100; zero indicates the start of the stride (first claw-on moment of the left hind limb) and 100 indicates the end of the stride (second claw-on moment of the left hind limb).

## **Results and Discussion**

### **Data description**

In total, 32 measurements were performed in 17 cows, with on average two measurements per cow. The characteristics of the cows are displayed in S1 Table. The number of selected strides per cow ranged between 72 and 286 with a median of 204.

For the temporal analysis, a total of two stance durations, one stride duration and 63 normalized stance durations were excluded. The high number of excluded normalized stance durations was caused by an unequal number of strides per limb within one interval, as can be seen in Fig 2. The temporal data were not normally distributed on a cow level. No data was excluded during the distal limb angle and vertical displacement analysis.

### **Temporal and distal limb angle analysis**

The distribution of the stance duration, in seconds, is shown on the left side and the speed normalized stance duration, as fraction of the entire stride duration, is shown on the right side of Fig 3.

Fig 3 suggests similar and consistent stance durations between 0.5 and 1 s and speed normalized stance duration between 0.50 and 0.75 for all cows. For the stance duration, a median value of 0.87 s was found over all cows and limbs, with a longer

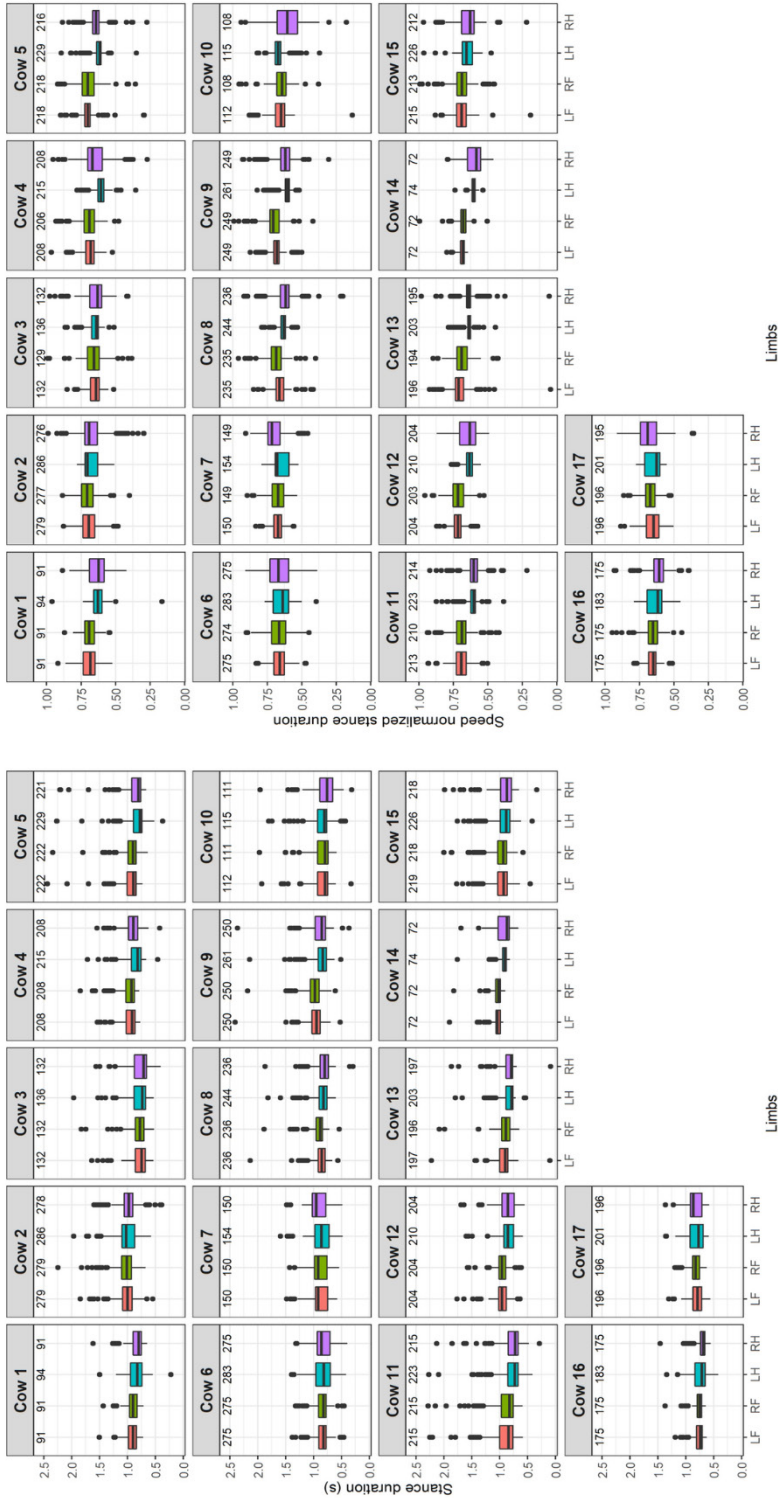


Figure 3. Distributions of stance durations (left panel) and speed normalized stance durations (right panel) for every cow and limb separately. In red: LF, green: RF, blue: LH and purple: RH. The number of selected strides per limb is shown above the boxes. The spacing of the boxplot shows the range between the first and third quartile, the median is indicated with the black line, the whiskers show the range of the maxima and minima and the outliers are indicated with dots.



median around 0.91 s for the front limbs and 0.86 s for the hind limbs (Table 2). On a cow level, the boxes overlap, and the width of the boxes seem to be rather similar for most cows and their limbs, which indicates that the variance in stance duration might be fairly consistent for all cows and limbs. For the speed normalized stance duration, a median value of 0.66 was found over all cows and limbs, with a longer median around 0.68 for the front limbs and 0.64 for the hind limbs (Table 2). On a cow level, the differences between the front and hind limbs seem to become more obvious after speed normalization, while some cows show a large variation with wider boxes.

The differences in stance duration between the front and hind limbs might suggest a difference in protraction and retraction angle of the distal limbs. In a previous study in cows (1) and in horses (25), a duty factor of around 0.63 was found, which is in agreement with the fraction of the entire stride duration found for the hind limbs in this study.

The distribution of the bipedal support durations, in seconds, is shown on the left side and the speed normalized bipedal durations, as fraction of the entire stride duration, is shown on the right side of Fig 4.

For the bipedal support durations (Fig 4), the figure suggests slightly longer support durations for diagonal limb pairs, although this difference does not seem obvious for all cows. On a group level, a median value of 0.13 s was found, with a longer median value 0.14 s for the diagonal limb pairs and 0.10 s for the ipsilateral limb pairs (Table 2). Furthermore, a greater variation in the ipsilateral durations might be seen for most cows, indicated by wider boxes, which might suggest less consistent ipsilateral support durations for most cows. For the speed normalized bipedal support durations, the differences between the diagonal and ipsilateral limb pairs seems not to become more obvious and the variation in the ipsilateral support durations seems not to become clearer. On a group level, a median fraction of 0.10 was found, with a median around 0.11 for the diagonal limb pairs and 0.8 for the ipsilateral limb pairs.



**Table 2. Summary of the temporal parameters and distal limb angles.** The median values and 95% confidence intervals based on the LMM analysis are estimated over all cows and steps for every limb (pair) separately. The median values are given in seconds for the non-speed normalized conditions, in fractions of the entire stride duration (i.e. duty factor), and in degrees for the distal limb angles.

Parameter	Non-speed normalized (s)	Speed normalized (duty factor)
<b>Stance duration</b>		
Overall	0.87 (0.86-0.87)	0.66 (0.66-0.66)
LF	0.91 (0.90-0.92)	0.68 (0.67-0.69)
RF	0.92 (0.90-0.93)	0.69 (0.68-0.70)
LH	0.86 (0.84-0.87)	0.64 (0.63-0.65)
RH	0.86 (0.84-0.88)	0.64 (0.63-0.65)
<b>Bipedal support phase duration</b>		
Overall	0.13 (0.13-0.13)	0.10 (0.10-0.10)
LF-RH	0.14 (0.13-0.15)	0.11 (0.10-0.12)
RF-LH	0.14 (0.13-0.15)	0.11 (0.10-0.12)
LF-LH	0.10 (0.10-0.11)	0.08 (0.07-0.09)
RF-RH	0.11 (0.10-0.12)	0.08 (0.08-0.09)
<b>Tripedal support phase duration</b>		
Overall	0.21 (0.21-0.21)	0.16 (0.16-0.16)
no LF	0.18 (0.18-0.19)	0.14 (0.13-0.14)
no RF	0.19 (0.17-0.20)	0.14 (0.13-0.14)
no LH	0.24 (0.23-0.25)	0.18 (0.17-0.19)
no RH	0.24 (0.23-0.25)	0.18 (0.17-0.19)
<b>Maximal protraction (degrees)</b>		
Overall	25 (25 - 25)	
LF	25 (24 - 26)	
RF	26 (25 - 27)	
LH	24 (23 - 25)	
RH	23 (22 - 24)	
<b>Maximal retraction (degrees)</b>		
Overall	-36 (-37 - -36)	
LF	-46 (-44 - -48)	
RF	-46 (-44 - -48)	
LH	-29 (-28 - -30)	
RH	-30 (-28 - -31)	

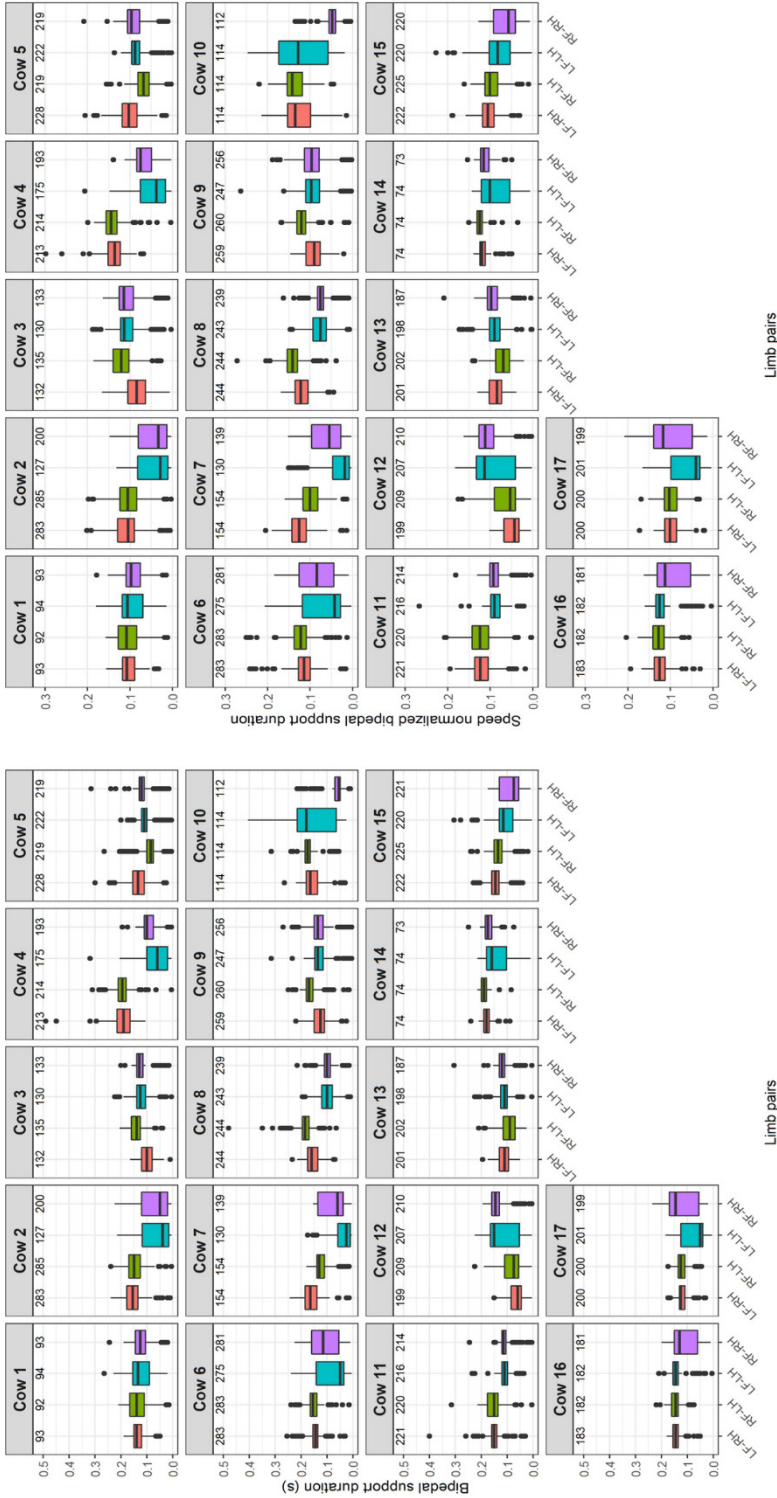


**Figure 4. Distributions of bipedal support durations (left panel) and speed normalized bipedal support durations (right panel) for every cow and limb pairs separately.** In red: LF-RH, green: RF-LH and purple: LF-LH. The number of selected strides per limb is shown above the boxes. The spacing of the boxplot shows the range between the first and third quartile, the median is indicated with the black line, the whiskers show the range of the maxima and minima and the outliers are indicated with dots.

The difference between the diagonal and ipsilateral support durations are in contrast to observations in horses for which slightly shorter diagonal support durations were found compared with ipsilateral durations (0.12 versus 0.13 respectively) in the walk (25).

The distribution of the tripedal support durations, in seconds, is shown on the left side and the speed normalized tripedal support durations, as fraction of the entire stride duration, is shown on the right side of Fig 5.

For the tripedal support durations (Fig 5), the figure suggests that the durations might be shorter when only a single front limb is involved in most cows, although these durations seem to show the largest variation, indicated by the differences in width of the boxes. On a group level, a median duration of 0.21 s was found, with a median duration around 0.18 s for involvement of a single front limb and 0.24 s for involvement of a single hind limb (Table 2). For the speed normalized tripedal support durations, the same differences in durations and variations seem to be found. On a group level, a median fraction of 0.16 was found, with a median fraction around 0.14 for involvement of a single front limb and 0.18 for involvement of a single hind limb, indicating again that cows tend to stand longer when both front limbs are on the ground. In horses in the walk, all support durations were shorter, around 0.12 of the entire stride duration (25).

In summary, the LMM analysis showed non-overlapping confidence intervals between the front and hind limbs, diagonal and ipsilateral limb pairs and single front limb and single hind limb involvement for all speed normalized and non-speed normalized durations. All previous temporal analyses included walking speed normalization to compare temporal parameters between cows. As the cows were not walking on a treadmill or with a handler in a constant speed, fluctuation in walking speed occurred, which is known to influence the durations of these temporal parameters (36). Walking speed normalization improved illustration of stance duration patterns between the front and hind limbs although for the bipedal and tripedal support durations, less effect was observed. Whether walking speed normalization is needed in the future depends on the changes due to lameness and whether we want to compare between cows or between limbs, for the latter no walking speed normalization is needed. The variance was found to be low indicated by the small confidence intervals for all the temporal parameters due to the high number of analyzed steps.

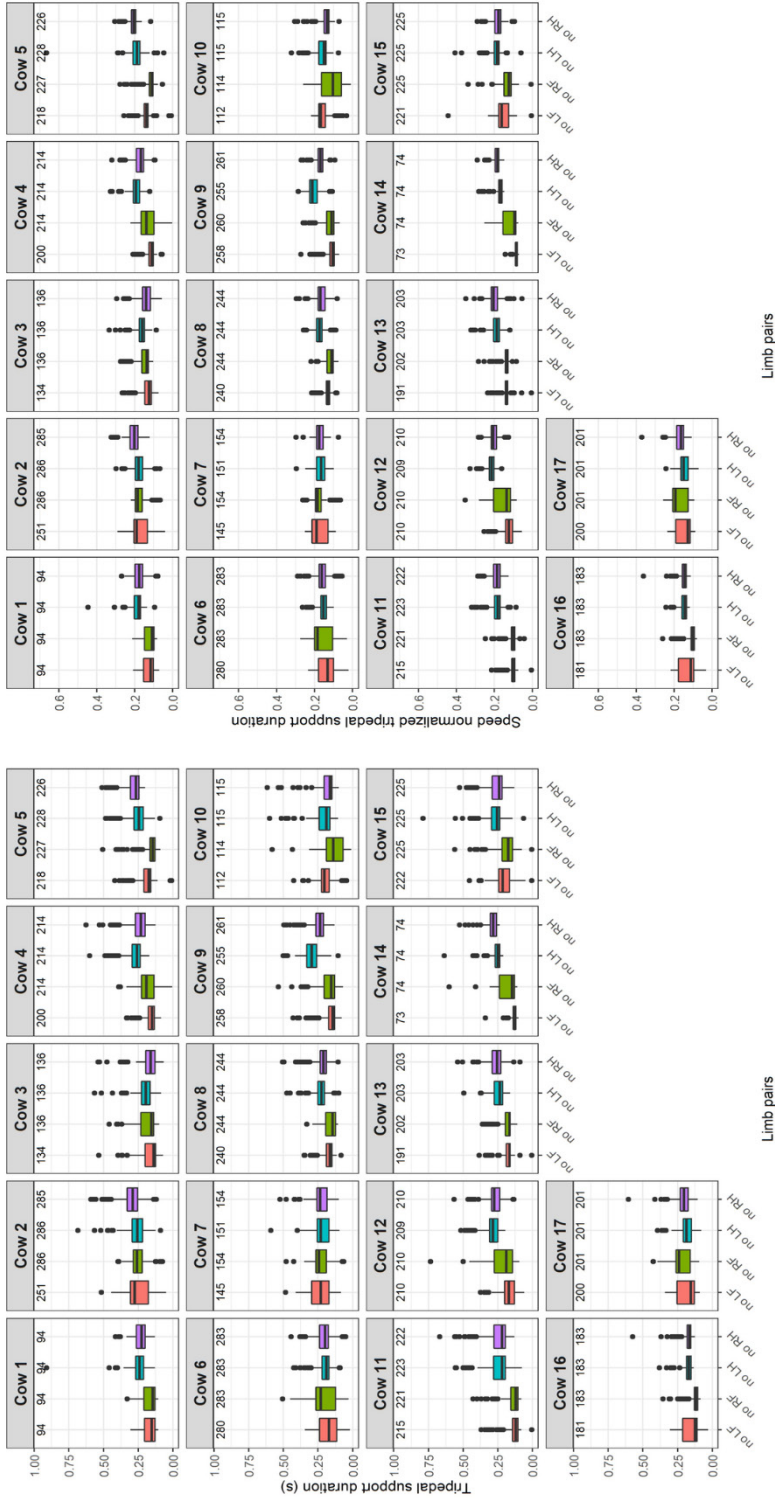


**Figure 5. Distributions of tripod support durations (left panel) and speed normalized tripod support durations (right panel) for every cow and limb pair combinations separately.** In red: no LF, green: no RF, blue: no LH and purple: no RH. The number of selected strides per limb is shown above the boxes. The spacing of the boxplot shows the range between the first and third quartile, the median is indicated with the black line, the whiskers show the range of the maxima and minima and the outliers are indicated with dots.

The distributions of the maximal protraction angles (left) and maximal retraction angles (right) is shown in degrees for every cow and limb separately in Fig 6.

Fig 6 suggest rather similar protraction angles in most of the cows with little variance, indicated by the width of the boxes. On a group level, a median protraction angle of 25 degrees is found over all limbs, with a somewhat comparable angle around 25 degrees for the front limbs and around 23 degrees for the hind limbs (Table 2). For the retraction angles, smaller angles are found for the front limb compared with the hind limbs indicated by the non-overlapping boxes. On a group level, a median retraction angle of -36 degrees is found, with a clear difference between -45 degrees for the front limbs and around -29 degrees for the hind limbs. The estimated confidence intervals of the LMM shows non-overlapping intervals between the front and hind limbs for the retraction angles while the intervals of the protraction angle are almost indifferent. On a cow level, the width of the boxes seems consistent for most cows and their limbs, which indicates that the variance is low, and the angles might be fairly consistent.

Cows show a similar protraction pattern as horses in walk, where the maximal protraction was reported an equal 19.6 degrees for both the front and hind legs. Retraction angles in horses differed between front and hind legs as well, but in contrast to cows a larger retraction has been observed for the hind legs (28.2 versus 23.0 degrees) (25). This difference might be caused by the more sickle-hocked posture of the hind limbs in cows.

### **Distal limb angle curve analysis**

The distal limb angle curves were displayed both as median over all cows and steps, and as most typical curves per cow (Fig 7). The most typical distal limb angle curves were very similar between cows, as the cow specific curves overlap nicely, and the median curves show small MAD areas. The front and hind limbs show somewhat different patterns; the front limbs have a larger range (80 versus 60 degrees) and show a steeper decline just before and a steeper incline just after claw-off compared with the hind limbs.

In summary, the distal limb angle analyses show a larger retraction for the front limbs with a larger distal limb angle range and a steeper distal limb angle curve which might also explain the differences in stance duration between the front and hind limbs. A possible explanation might be the anatomical conformation of the front and hind limbs. The steeper decline just before claw-off of the front limbs might be caused by flexion of the carpal joints just before full toe off. The steeper

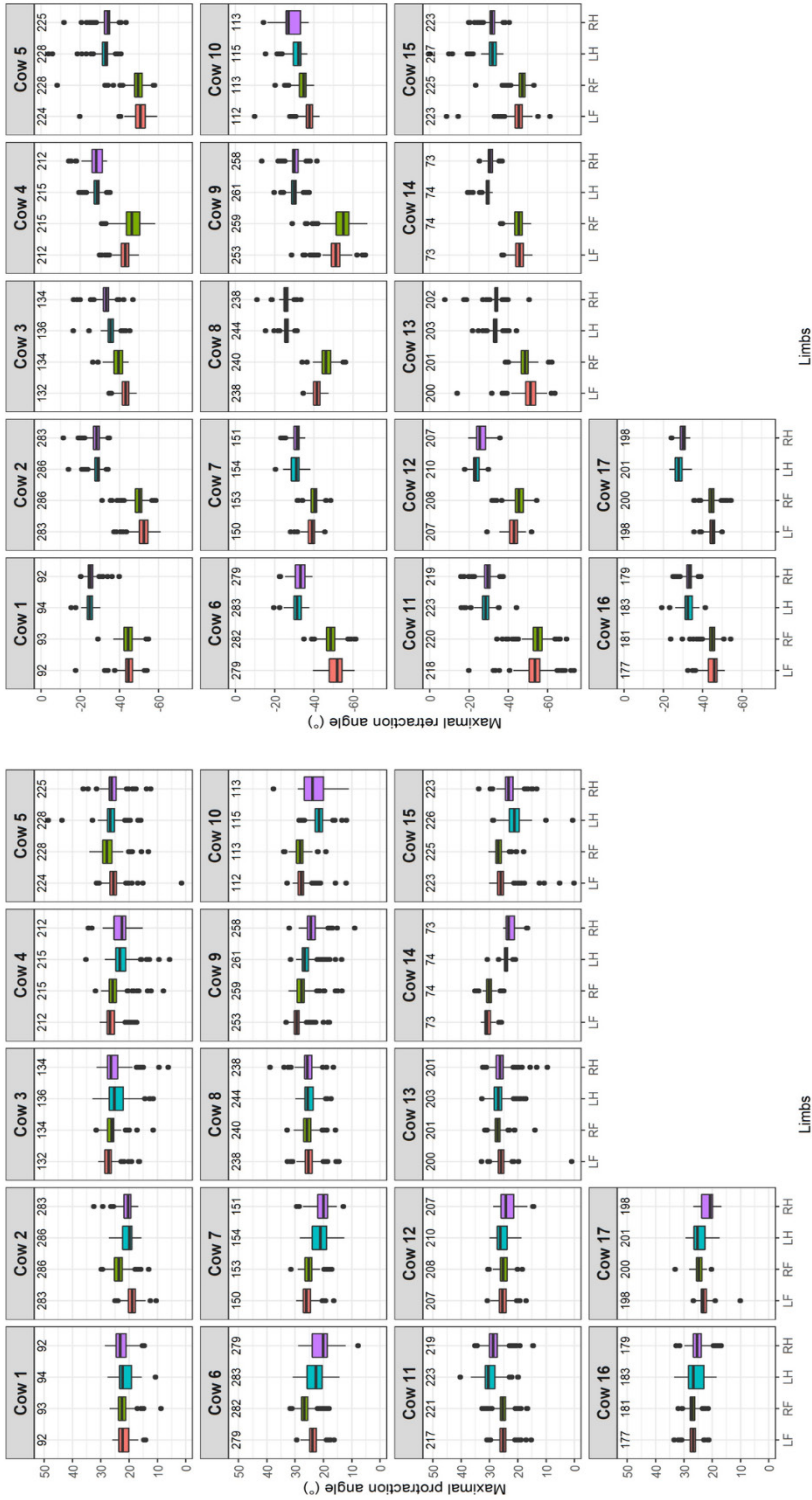


**Figure 6. Distribution of distal limb maximal protraction (left panel) and maximal retraction (right panel) angles in degrees for every cow and limb separately.** In red: LF; green: RF; blue: LH and purple: RH. The number of selected strides per limb is shown above the boxes. The spacing of the boxplot shows the range between the first and third quartile, the median is indicated with the black line, the whiskers show the range of the maxima and minima and the outliers are indicated with dots.

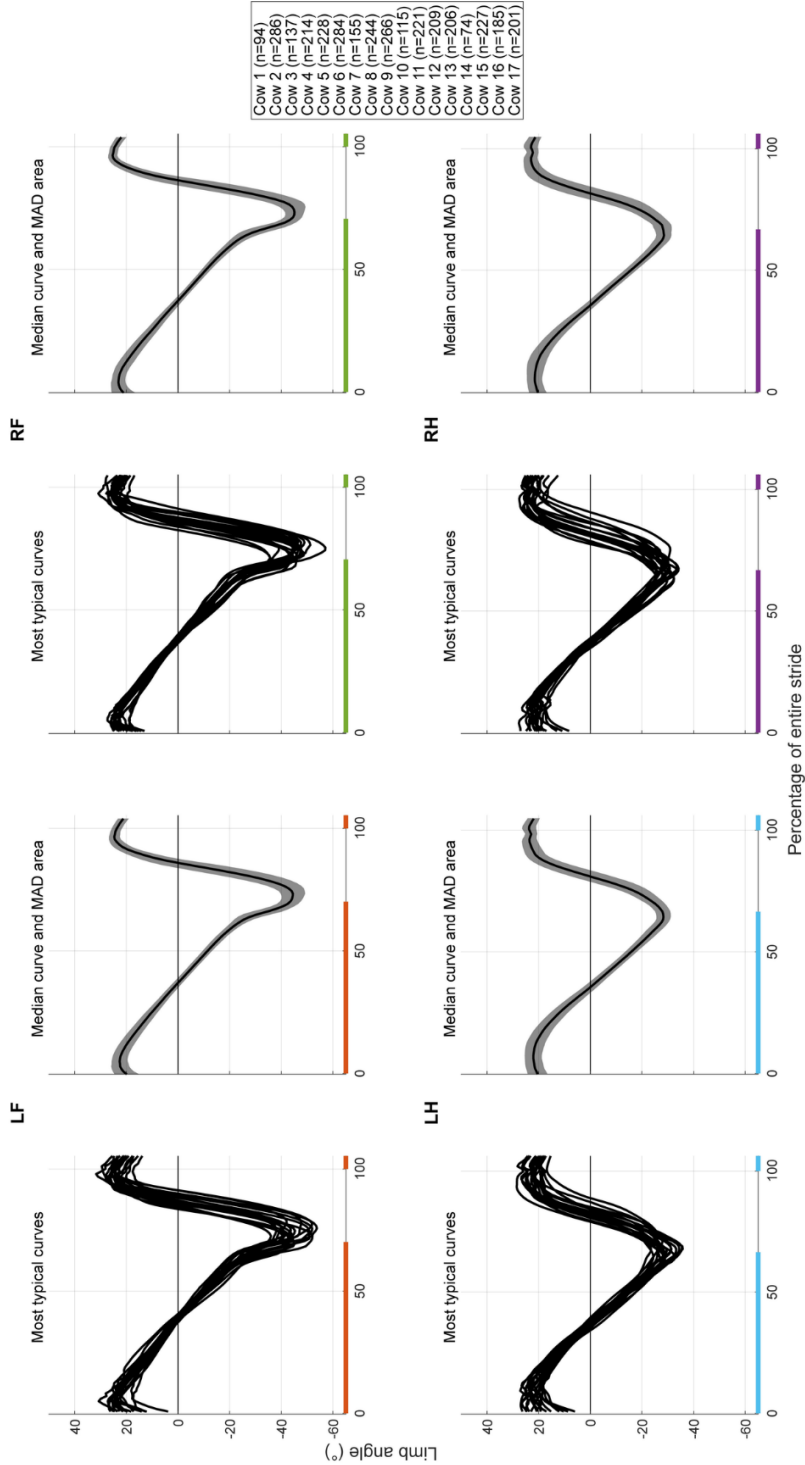


**Figure 7. Distal limb angle curves per limb.** For all limbs, the most typical curves per cow is shown on the left, and the median curve (black) with the MAD area (grey), calculated over all cows and steps, is shown on the right. The curves are shown on a scale from zero to 100 % of the entire stride duration. The stance phases are indicated for every limb by the horizontal lines underneath the curves (orange: LF, green: RF, blue: LH, purple: RH).



angle increase during swing phase of the front limbs follows from the similar swing phase duration for the hind and front limbs combined with a larger angle to cover.

### Vertical displacement analysis

The vertical displacement curves of the sacrum are shown in Fig 8, of the withers in S3 Fig and of the back in S4 Fig.

All the curves show one complete sinusoidal cycle per stride. For the sacrum (Fig 8), two peaks are found with the first peak around 25 and the second around 75% of the stride, which coincides with midstance of the LH limb and the RH limb respectively. This can be expected since the sacrum should be at its highest point during midstance of one of the hind limbs (Fig 9). For the withers (S3 Fig), the peaks around zero and 100% coincides with midstance of the RF limb and the peak around 50% coincides with midstance of the LF limb, which again can be anatomically expected. For the back (S4 Fig), the first peak is located just before zero, the second peak just before 50 and the third peak just before 100% of the stride, which happens to be just after the peaks of the sacrum and just before the peaks in of the withers. This can be explained by the attachment location on the 13<sup>th</sup> thoracic vertebra between the sacrum and the withers.

For the sacrum, most cows seem to have equal height peaks, which indicate a symmetrical gait pattern, and show a stable pattern, with small MAD area and very similar median and most typical curves. For the withers, the curves seem less symmetrical, indicated by less similar peak height and seem to show more variation between and within cows, indicated by less similar typical and median curves (37). For the back, not all the cows seem to show three distinctive peaks and the curves are less smooth and show more variation, compared with the curves of the sacrum and the withers, which might be caused by the attachment of the sensor on the spinal process resulting in a rolling motion of the sensor over the spinal process in the more skinny cows.

The amplitude of the sacrum and withers curves is variable between 0.04 and 0.05 m in contrast to 0.02 and 0.03 m for the back.

The vertical displacement curves of the left (red) and right (green) tuber coxae seem to show one sinusoidal cycle per stride for each side in Fig 10. The peaks of the sinusoidal curve are located around 25 and 75% of the stride. For some cows, the locations of these peaks seem to happen a bit later during the stride, for example



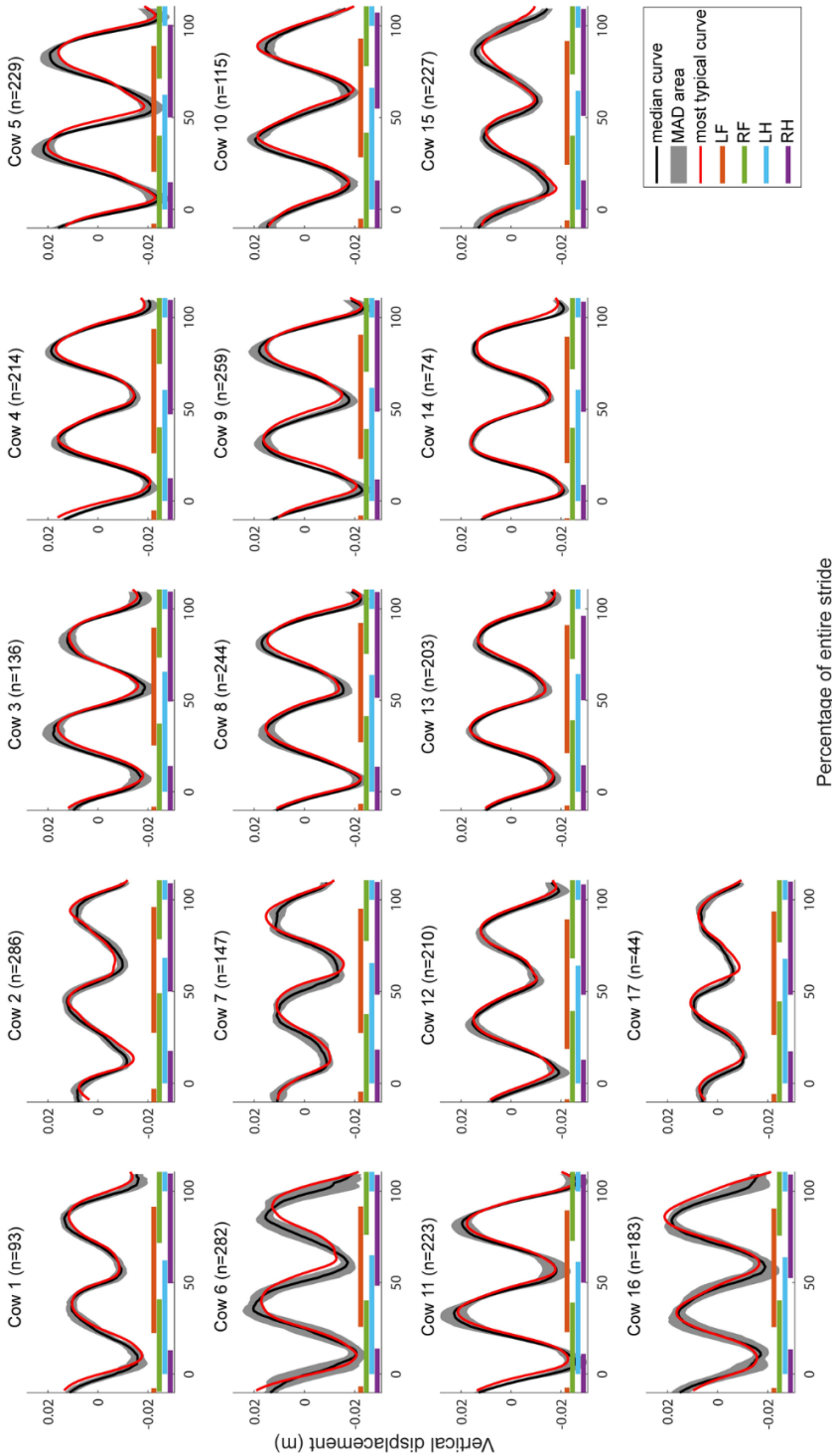


**Figure 8. Vertical displacement curves of the sacrum.** Per cow, the median curve (black), the MAD area (grey), and most typical curve (red) is shown on a scale from zero to 100 % of the entire stride duration. The stance phases of the limbs are indicated by the horizontal lines underneath the curves (orange: LF, green: RF, blue: LH, purple: RH).



Cow 2, and are shifted towards 50 and 100% of the stride respectively. For the LTC, the first peak is the highest peak and coincides with midstance of the LH limb while the second and lowest peak coincides with midstance of the RH limb. The opposite is found for the RTC (38). This finding seems obvious since the cow is pushing herself over the standing limb causing the hip to move over the standing limb and tilting the hip resulting in a higher vertical displacement for the side of the standing limb compared with the opposite side. All cows show a smooth and consistent pattern with a small MAD area around the median curve and the most typical curve seems almost similar to the median curve, except for Cow 7. The amplitude seems to be similar for all cows, around 0.1 m, except for Cow 7, which seems to have a flatter

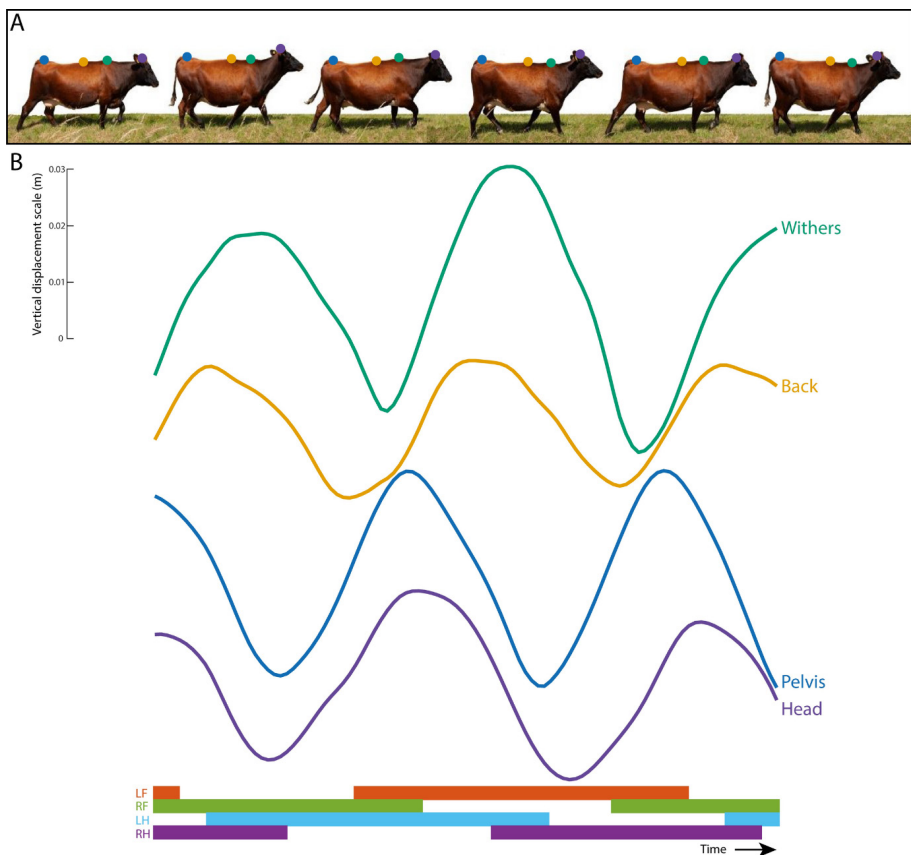


**Figure 9. Upper body displacement curve and footfall pattern of normal walking gait.** In A, different phases of a walking cow are shown with dots indicating the different sensor locations and their corresponding vertical signal pattern (green: withers, yellow: back, blue: sacrum and purple: head). In B, the median vertical displacement curves for the different sensor locations are shown from one cow, except for the head signal, which is selected from another cow for illustrative purposes. The synchronized footfall pattern is indicated underneath for all four limbs (orange: LF, green: RF, blue: LH and purple: RH). The scale of the signals is based on the true scale.

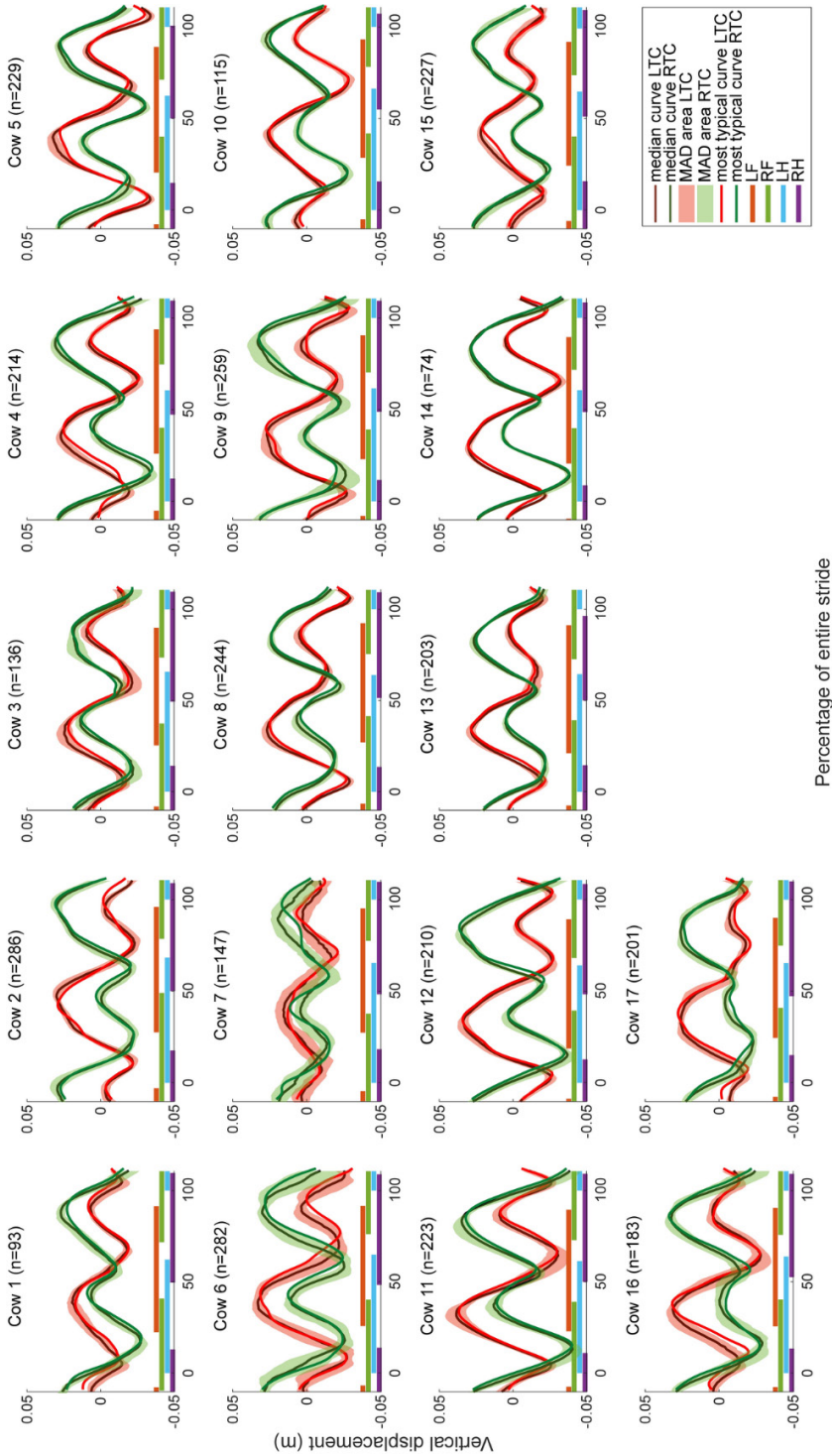


**Figure 10. Vertical displacement curves of the left and right tuber coxae.** Per cow, the median curve, MAD area and most typical curve is shown for the LTC (red) and RTC (green) on a scale from zero to 100 % of the entire stride duration. The stance phases of the limbs are indicated by the horizontal lines underneath the curves (orange: LF, green: RF, blue: LH, purple: RH).



curve with small vertical differences between the two tuber coxae indication a low range of pelvic axial rotation. Overall, the curves seem smooth and similar between and within cows.

The vertical displacement curves of the head (S5 Fig) and collar (S6 Fig) show a less consistent sinusoidal pattern in about half of the cows for the head, and very unclear sinusoidal patterns for the collar, if present at all. For the cows with a sinusoidal pattern, the peaks are located around zero, 50 and 100% of the stride. The peak around or just before 50% of the stride coincide with claw-off of the RF and claw-on of the LF limb. For the head, the sinusoidal patterns are less consistent than the patterns of the previous discussed locations and seem to differ more clearly between and within cows, with broader MAD areas and clear differences between the median and most typical curves for all cows. For the collar, the curves are even less consistent with even more variation within and between cows. The amplitude seems to differ between cows; between 0.02 and 0.04 m for the collar and between 0.02 and 0.1 m for the head.

When comparing the curves of the different locations, it becomes clear that the sacrum, RTC and LTC show smooth sinusoidal curves without much variation between and within cows. The withers seem to have a bit more variation between and within cows although the sinusoidal patterns were still clearly visible. The back sensor seems to show slightly more variation between and within cows and the pattern seem to become less clearly visible. For the head and collar sensor, the curves seem to be less consistent and to show more variation between and within cows and for some cows, the sinusoidal pattern seem to have vanished for some cows completely.

An explanation for these differences might be that the cows were free to look around while walking resulting in head movements obscuring the stride related double sinusoidal vertical displacement curve. For the collar sensor, noise might have been introduced by the swinging movement of the sensor while walking because the collar was attached loosely around the cows' neck or because the sensor came loose during the measurement which happened in two measurements. Other signal processing technique might be more appropriate to evaluate the main frequency components from the noisy signal, for example using frequency component analysis methods such as Fourier series analysis (39-41).

Peaks were found around 25 and 75% of the stride for the sacrum, RTC and LTC, while the peaks of the withers were found around 0, 50 and 100%. This difference was also found in horses and the optimal phase shift observed in horses was found

around 25% (42), which is in agreement with the phase shift found in this study. The phase shift of the vertical displacement curves between the different locations can be explained by the limb spread of the front and hind limbs (42). In Fig 9, the footfalls and vertical displacement curves are illustrated of one non-existing ideal cow to make this phenomena clearly visible. During midstance of the limbs, the body part above these limbs is at its highest point in contrast to the body part above the limbs in limb spread, which is at its lowest point. The phase shift between the front and hind part of the upper body can be explained by the asynchrony of the front and hind limbs at walk, where only one pair is in limb spread while one limb of the other pair is at midstance. The back sensor is located in between the front part (withers) and hind part (sacrum) of the upper body and therefore this curve shows peaks just before the withers and just after the sacrum (23). The head is raised and lowered out of phase with the withers and is discussed as an energy saving mechanism of the walk which is seen in a majority of hoofed mammals (42).

The differences in height and depth of the peaks and valleys can be interpreted as an asymmetry of the vertical displacement. Such asymmetries are also described in horses and might be an indication of lameness (25), although asymmetries in vertical displacement of the sacrum and withers were also found in sound horses, in both walk and trot, and linked to differences in maximal protraction and retraction angles of the legs and motor laterality (37). However, a sinusoidal pattern is needed to determine whether a symmetrical gait pattern is present and the absence of this, as in the head and collar curves, might therefore be problematic as indication for lameness using this approach. Nevertheless, modern signals analysis methods, including machine learning techniques, might be able to help to better further explore these complex signals in the near future.

The algorithm used for the claw-on and claw-off detection was developed and validated against the force plate and optical motion capture in horses (30). No validation study was performed to evaluate the performance of this algorithm in cows since this involves letting the cows walk over a force plate, which was not possible. However, the signal appearance for cow and horse signals is quite similar and claw-on and claw-off detection were checked for consistence, as can be seen in S7 and S8 Figs. Temporal parameters might be affected when the claw-on and claw-off moments are not precisely detected, especially bipedal and tripedal support durations might be affected because these durations are short. It is not expected that the curve analysis of the upper body data is affected by the quality of claw-on and off detection since the curves are evaluated by adding a small interval around the claw-on and -off moments of the left hind limb and timing of footfalls is not a prerequisite for integration of the



IMU data. Extreme outliers were manually removed when parameters were exceeding a threshold level, as described in the method section, to prevent these from obscuring our results.

## Conclusion

This is the first study that describes the kinematic gait characteristics of straight line walk in clinically sound dairy cows using body mounted IMUs at multiple anatomical locations. The method used in this study shows consistent results with low variance and speed normalization resulted in clearer differences between front and hind limbs for the stance duration. Furthermore, clear differences in distal limb angles between the front and hind limbs were found, as well as consistent and clear sinusoidal pattern for the vertical displacement curves of the tubera sacrale, withers, and left and right tuber coxae. For the head, back and collar sensors, signals with a sinusoidal pattern were found although they were less consistent and showed more variation between and within cows. These sensor locations are therefore less suitable for future exploration of lameness metrics in cows.

Even though the instrumentation used in this study might not be practical for daily implementation on farms, it allowed us to explore in unprecedented detail the kinematic gait characteristics of cows at walk. Future analysis of these signals in lame cows will allow us to identify the best features that can be used from IMU data to objectively quantify lameness and might be useful for the development of an automatic recognition method and extensions to computer vision techniques.

## Acknowledgments

We acknowledge that cooperation of the cows was vital to collect these data. Furthermore, we would like to thank J. Lundblad, C. Frisk and the animal caretakers of the Swedish Livestock Research Centre Lövsta for their contribution to the data collection. And at last, J. van den Broek for statistical guidance.

## References

1. Alsaad M, Luternauer M, Hausegger T, Kredel R, Steiner A. The cow pedogram-Analysis of gait cycle variables allows the detection of lameness and foot pathologies. *J Dairy Science*. 2017;100(2):1417-26.
2. O'Leary NW, Byrne DT, O'Connor AH, Shalloo L. Invited review: Cattle lameness detection with accelerometers. *J Dairy Sci*. 2020;103(5):3895-911.
3. Serra Braganca FM, Rhodin M, van Weeren PR. On the brink of daily clinical application of objective gait analysis: What evidence do we have so far from studies using an induced lameness model? *Vet J*. 2018;234:11-23.
4. Fabian J, Laven RA, Whay HR. The prevalence of lameness on New Zealand dairy farms: a comparison of farmer estimate and locomotion scoring. *Vet J*. 2014;201(1):31-8.
5. Leach KA, Paul ES, Whay HR, Barker ZE, Maggs CM, Sedgwick AK, et al. Reducing lameness in dairy herds--overcoming some barriers. *Res Vet Sci*. 2013;94(3):820-5.
6. Bicalho RC, Machado VS, Caixeta LS. Lameness in dairy cattle: A debilitating disease or a disease of debilitated cattle? A cross-sectional study of lameness prevalence and thickness of the digital cushion. *J Dairy Sci*. 2009;92(7):3175-84.
7. Leach KA, Tisdall DA, Bell NJ, Main DC, Green LE. The effects of early treatment for hindlimb lameness in dairy cows on four commercial UK farms. *Vet J*. 2012;193(3):626-32.
8. Thomas HJ, Remnant JG, Bollard NJ, Burrows A, Whay HR, Bell NJ, et al. Recovery of chronically lame dairy cows following treatment for claw horn lesions: a randomised controlled trial. *Veterinary Record*. 2016;178(5):116-.
9. Sprecher DJ, Hostetler DE, Kaneene JB. A lameness scoring system that uses posture and gait to predict dairy cattle reproductive performance. *Theriogenology*. 1997;47(6):1179-87.
10. Engel B, Bruin G, Andre G, Buist W. Assessment of observer performance in a subjective scoring system: visual classification of the gait of cows. *The Journal of Agricultural Science*. 2003;140(3):317-33.
11. Thomsen PT, Munksgaard L, Togersen FA. Evaluation of a lameness scoring system for dairy cows. *J Dairy Sci*. 2008;91(1):119-26.
12. Flower FC, Weary DM. Effect of hoof pathologies on subjective assessments of dairy cow gait. *J Dairy Sci*. 2006;89(1):139-46.
13. Leach KA, Whay HR, Maggs CM, Barker ZE, Paul ES, Bell AK, et al. Working towards a reduction in cattle lameness: 1. Understanding barriers to lameness control on dairy farms. *Res Vet Sci*. 2010;89(2):311-7.
14. Alsaad M, Fadul M, Steiner A. Automatic lameness detection in cattle. *Vet J*. 2019;246:35-44.
15. Ito K, von Keyserlingk MA, Leblanc SJ, Weary DM. Lying behavior as an indicator of lameness in dairy cows. *J Dairy Sci*. 2010;93(8):3553-60.
16. Thorup VM, Munksgaard L, Robert PE, Erhard HW, Thomsen PT, Friggens NC. Lameness detection via leg-mounted accelerometers on dairy cows on four commercial farms. *Animal*. 2015;9(10):1704-12.
17. Telezhenko E, Bergsten C. Influence of floor type on the locomotion of dairy cows. *Applied Animal Behaviour Science*. 2005;93(3-4):183-97.
18. Flower FC, Sanderson DJ, Weary DM. Hoof pathologies influence kinematic measures of dairy cow gait. *J Dairy Sci*. 2005;88(9):3166-73.
19. Thorup VM, do Nascimento OF, Skjoth F, Voigt M, Rasmussen MD, Bennedsgaard TW, et al. Short communication: Changes in gait symmetry in healthy and lame dairy cows based on 3-dimensional ground reaction force curves following claw trimming. *J Dairy Sci*. 2014;97(12):7679-84.



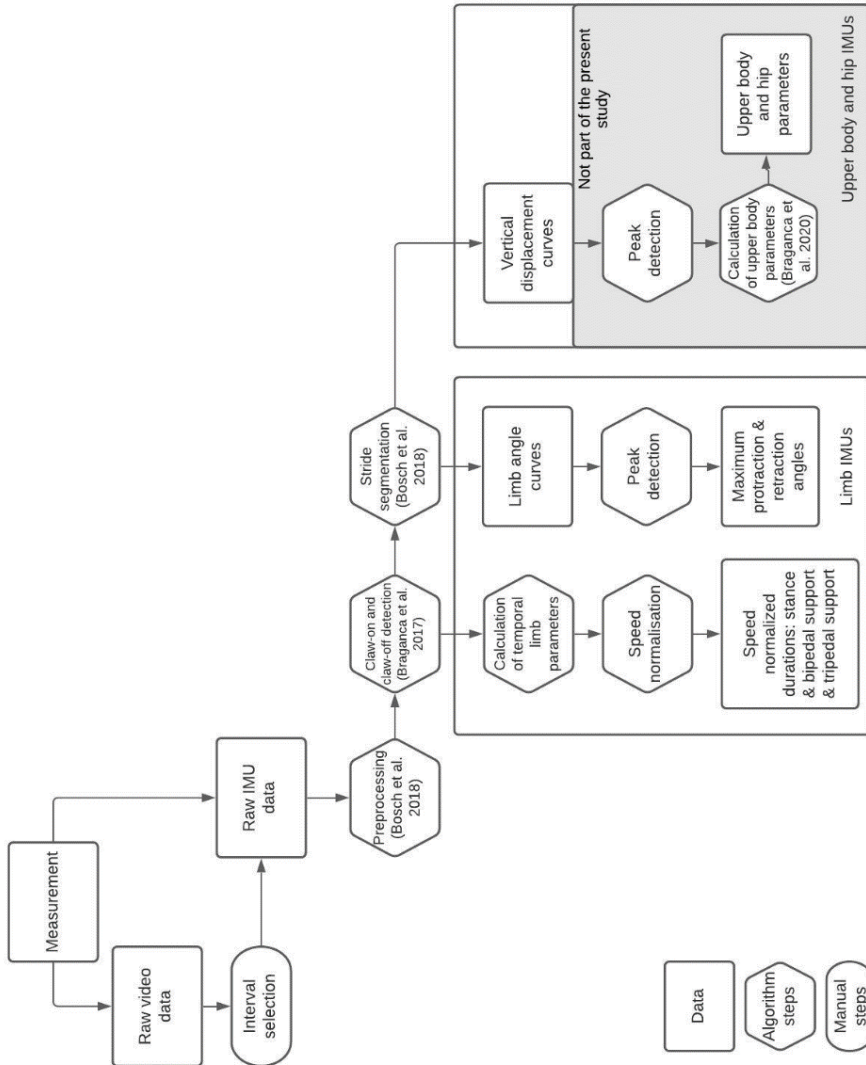
20. Keegan KG, Dent EV, Wilson DA, Janicek J, Kramer J, Lacarrubba A, et al. Repeatability of subjective evaluation of lameness in horses. *Equine Vet J.* 2010;42(2):92-7.
21. Hammarberg M, Egenvall A, Pfau T, Rhodin M. Rater agreement of visual lameness assessment in horses during lungeing. *Equine Vet J.* 2016;48(1):78-82.
22. Arkell M, Archer RM, Guitian FJ, May SA. Evidence of bias affecting the interpretation of the results of local anaesthetic nerve blocks when assessing lameness in horses. *Vet Rec.* 2006;159(11):346-9.
23. Buchner HHF, Savelberg HHCM, Schamhardt HC, Barneveld A. Head and trunk movement adaptations in horses with experimentally induced fore- or hindlimb lameness. *Equine Vet J.* 1996;28(1):71-6.
24. Rhodin M, Persson-Sjodin E, Egenvall A, Serra Braganca FM, Pfau T, Roepstorff L, et al. Vertical movement symmetry of the withers in horses with induced forelimb and hindlimb lameness at trot. *Equine Vet J.* 2018;50(6):818-24.
25. Serra Braganca FM, Hernlund E, Thomsen MH, Waldern NM, Rhodin M, Bystrom A, et al. Adaptation strategies of horses with induced forelimb lameness walking on a treadmill. *Equine Vet Journal.* 2020.
26. Buchner HHF, Savelberg HHCM, Schamhardt HC, Barneveld A. Limb movement adaptations in horses with experimentally induced fore- or hindlimb lameness. *Equine Vet J.* 1996;28(1):63-70.
27. Buchner HHF, Savelberg HHCM, Schamhardt HC, Barneveld A. Temporal stride patterns in horses with experimentally induced fore- or hindlimb lameness. *Equine Vet J Suppl.* 1995;18:161-5.
28. Bosch S, Serra Braganca F, Marin-Perianu M, Marin-Perianu R, van der Zwaag BJ, Voskamp J, et al. EquiMoves: A Wireless Networked Inertial Measurement System for Objective Examination of Horse Gait. *Sensors (Basel).* 2018;18(3).
29. Serra Braganca FM, Broome S, Rhodin M, Bjornsdottir S, Gunnarsson V, Voskamp JP, et al. Improving gait classification in horses by using inertial measurement unit (IMU) generated data and machine learning. *Sci Rep.* 2020;10(1):17785.
30. Braganca FM, Bosch S, Voskamp JP, Marin-Perianu M, Van der Zwaag BJ, Vernooij JCM, et al. Validation of distal limb mounted inertial measurement unit sensors for stride detection in Warmblood horses at walk and trot. *Equine Vet J.* 2017;49(4):545-51.
31. Valenti RG, Dryanovski I, Xiao J. Keeping a Good Attitude: A Quaternion-Based Orientation Filter for IMUs and MARGs. *Sensors (Basel).* 2015;15(8):19302-30.
32. Back W, Clayton HM. *Equine Locomotion.* 2nd Edition ed: Saunders Ltd.; 2013 6th June 2013. 528 p.
33. Pfau T, Witte TH, Wilson AM. A method for deriving displacement data during cyclical movement using an inertial sensor. *J Exp Biol.* 2005;208(Pt 13):2503-14.
34. Bates D, Mächler M, Bolker B, Walker S. Fitting Linear Mixed-Effects Models Using lme4. *Journal of Statistical Software.* 2015;67(1).
35. R Foundation for Statistical Computing. *R: A Language and Environment for Statistical Computing.* Vienna, Austria: R Core Team; 2018.
36. Weishaupt MA, Hogg HP, Auer JA, Wiestner T. Velocity-dependent changes of time, force and spatial parameters in Warmblood horses walking and trotting on a treadmill. *Equine Vet J Suppl.* 2010(38):530-7.
37. Byström A, Egenvall A, Roepstorff L, Rhodin M, Braganca FS, Hernlund E, et al. Biomechanical findings in horses showing asymmetrical vertical excursions of the withers at walk. *PLoS One.* 2018;13(9):e0204548.
38. Starke SD, May SA, Pfau T. Understanding hind limb lameness signs in horses using simple rigid body mechanics. *J Biomech.* 2015;48(12):3323-31.



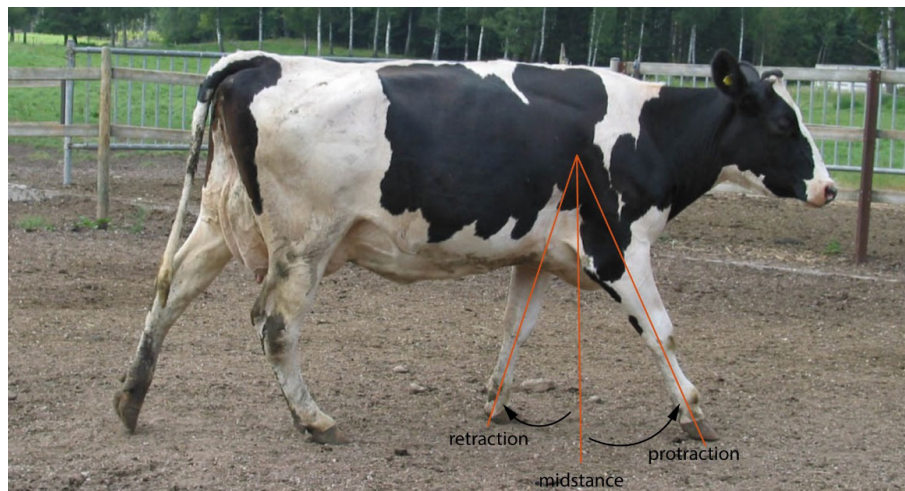
39. Keegan KG, Pai PF, Wilson DA, Smith BK. Signal decomposition method of evaluating head movement to measure induced forelimb lameness in horses trotting on a treadmill. *Equine Vet J.* 2001;33(5):446-51.
40. Peham C, Scheidl M, Licka T. A Method of Signal Processing in Motion Analysis of the Trotting Horse. *Journal of Biomechanics.* 1996;29(8):1111-4.
41. Audigié F, Pourcelot P, Degueurce C, Geiger D, Denoix JM. Fourier analysis of trunk displacements: a method to identify the lame limb in trotting horses. *Journal of Biomechanics.* 2002;35:1173-82.
42. Loscher DM, Meyer F, Kracht K, Nyakatura JA. Timing of head movements is consistent with energy minimization in walking ungulates. *Proc Biol Sci.* 2016;283(1843).



## Supporting Information



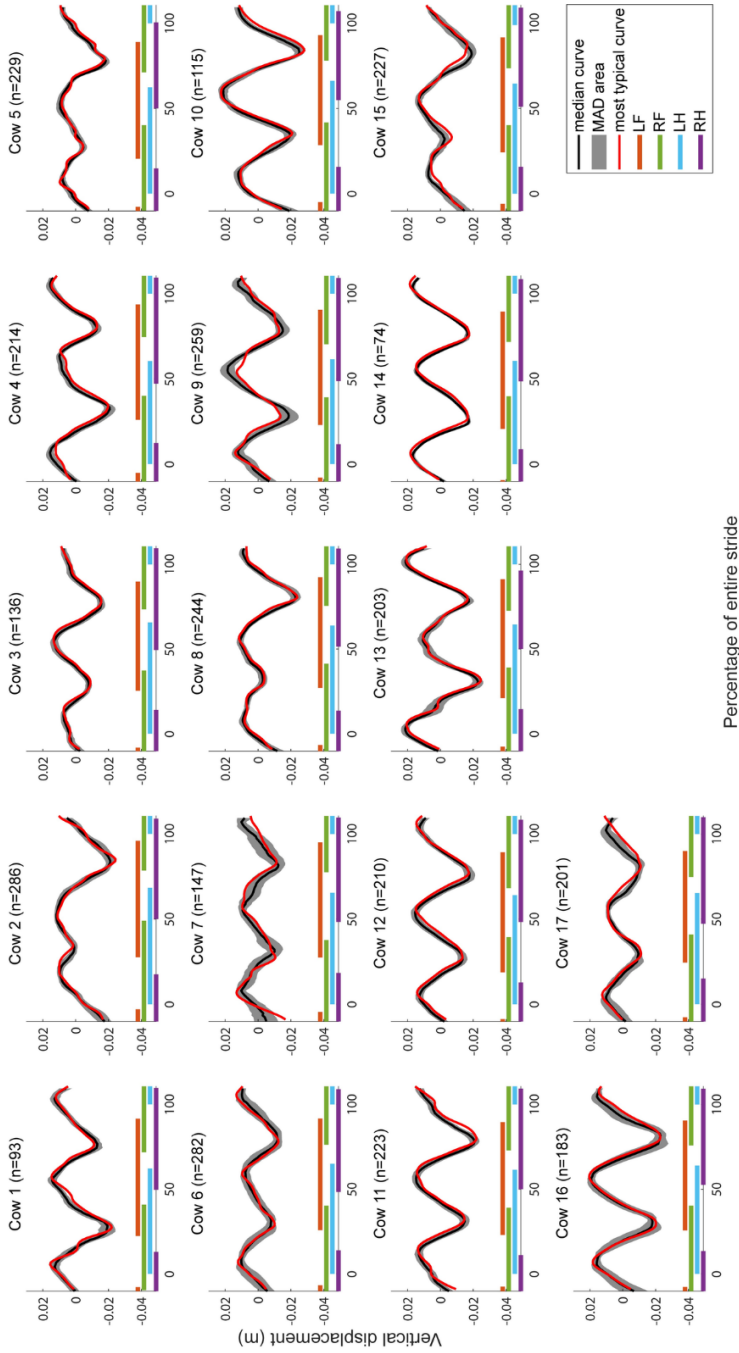
S1 Figure. Schematic representation of analysis steps performed.



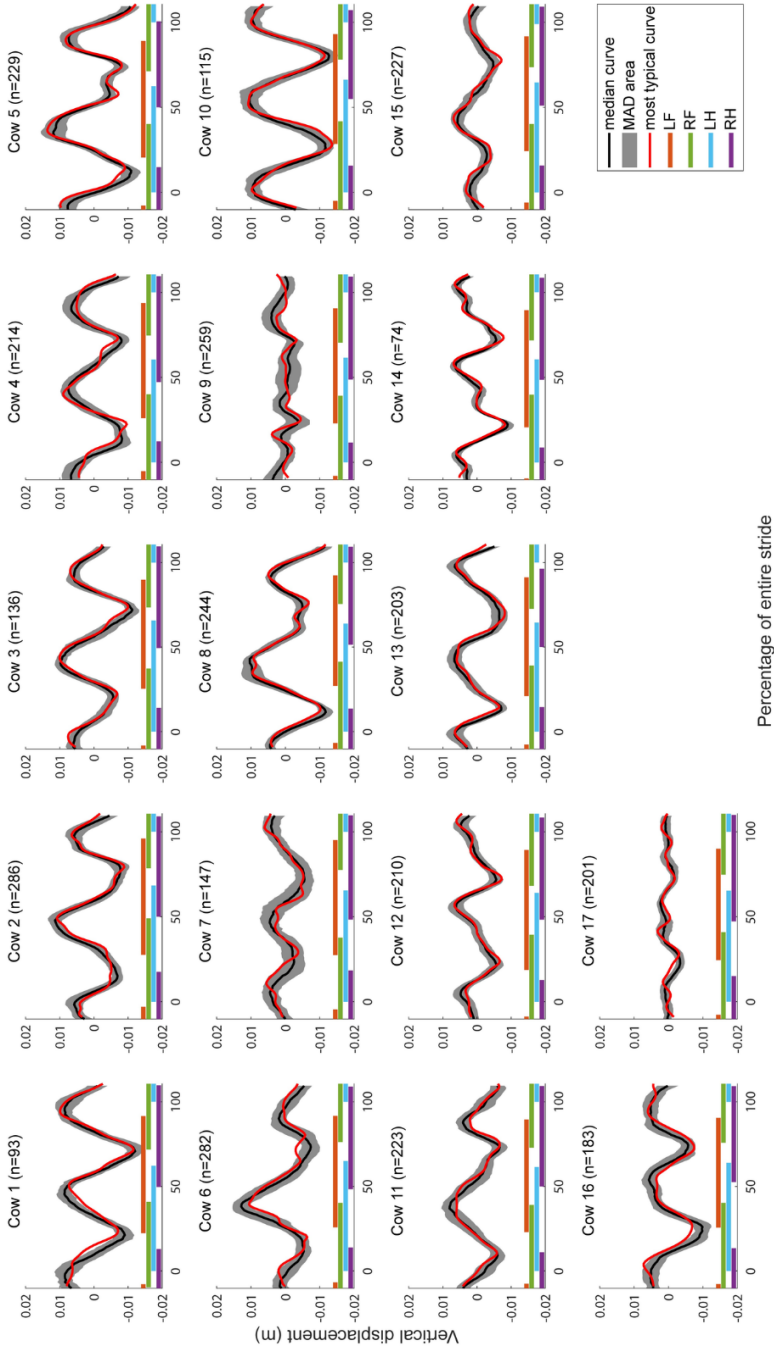
**S2 Fig. Definition of distal limb angles.** Maximal protraction is the maximal forward protraction (positive angle) from midstance and maximal retraction is the maximal backward retraction (negative angle) from midstance measured at the metacarpus/-tarsus in the sagittal plane, as adapted from horses (28, 32).

**S1 Table. Cow Characteristics** (SR stands for the Swedish Red and SH stands for the Swedish Holstein breed).

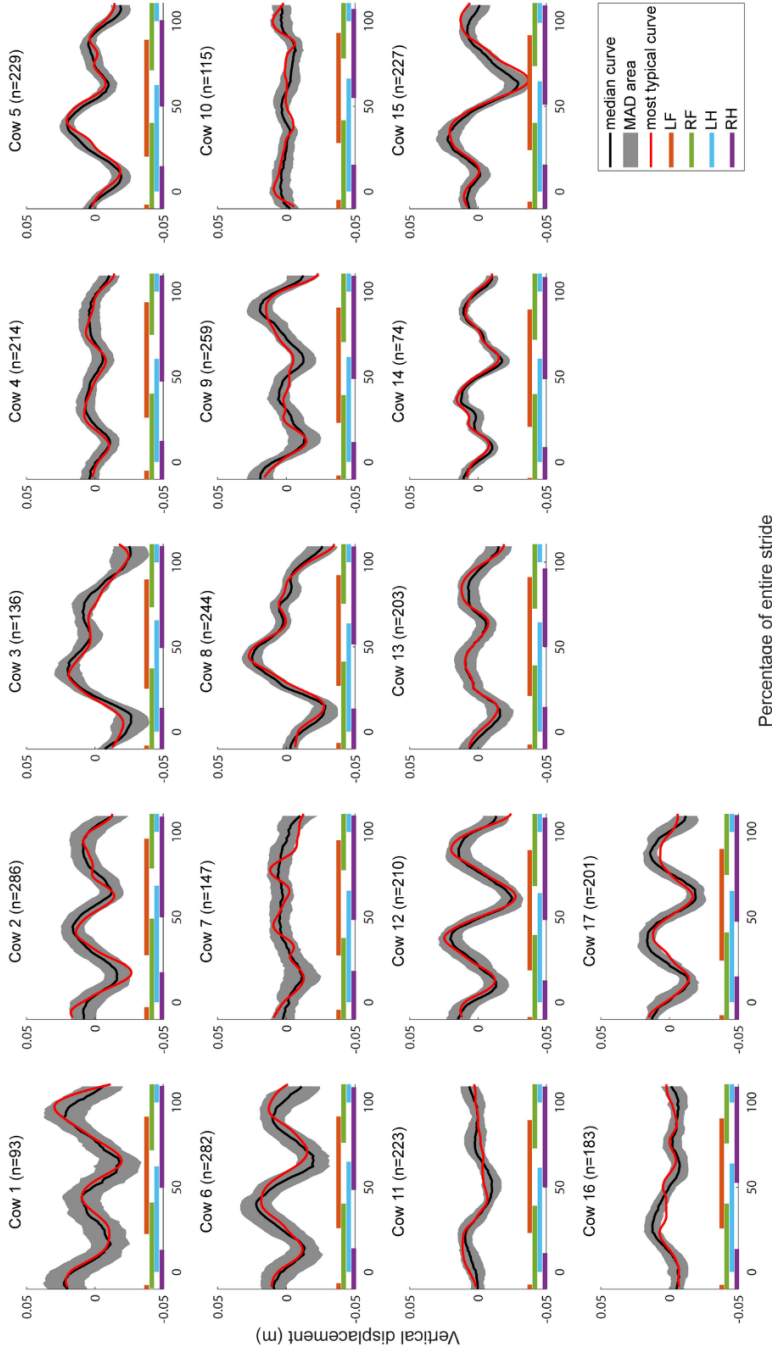
Cow	Number of measurements	Breed	Lactation cycle	Last calving	Insemination date	Start dry-period	Last claw trimming	Findings at claw trimming
1	1	SH	2	9-6-2019	5-8-2019		12-6-2019	Sole hemorrhage
2	2	SH	2	10-8-2019			16-8-2019	
3	1	SR	1	23-2-2019	22-8-2019		16-8-2019	Sole hemorrhage
4	2	SH	1	3-12-2018	16-3-2019	25-10-2019	12-6-2019	Dermatitis, Sole hemorrhage
5	2	SH	1	18-1-2019	18-4-2019	27-11-2019	16-8-2019	
6	2	SH	1	13-1-2019	18-3-2019	27-10-2019	16-8-2019	
7	2	SR	1	30-1-2019	16-4-2019	25-11-2019	16-8-2019	
8	2	SR	1	29-1-2019	11-7-2019		16-8-2019	
9	3	SH	1	6-6-2019			12-6-2019	
10	1	SH	1	9-6-2019	20-8-2019		16-8-2019	
11	2	SR	1	30-6-2019	17-8-2019		10-7-2019	
12	2	SH	1	3-8-2019			16-8-2019	
13	2	SR	1	12-7-2019			10-7-2019	
14	1	SH	1	12-7-2019			19-7-2019	Sole hemorrhage
15	2	SR	1	29-6-2019			3-8-2019	
16	2	SR	1	13-7-2019			16-8-2019	
17	2	SR	1	31-7-2019			16-8-2019	



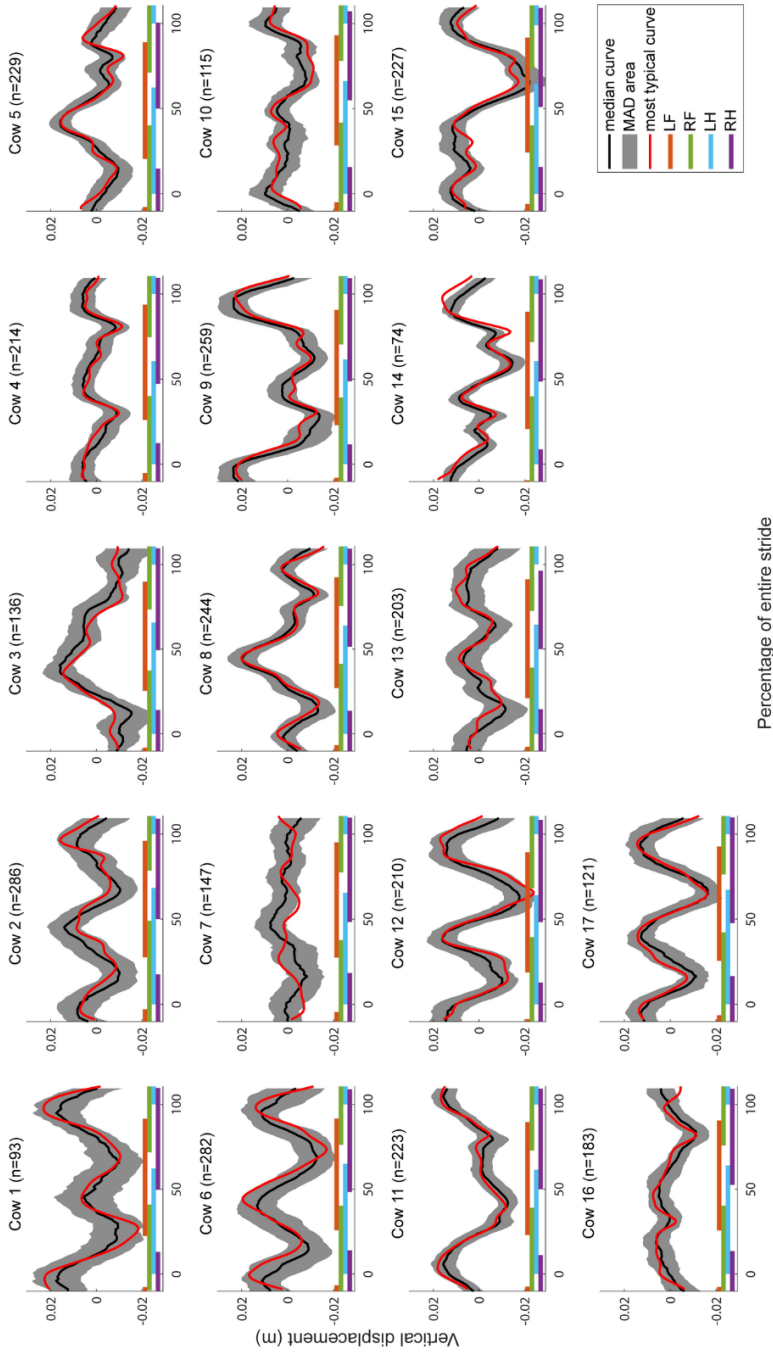
**S3 Figure. Vertical displacement curves of the withers.** Per cow, the median curve (black), the MAD area (grey), and the most typical curve (red) is shown on a scale from zero to 100 % of the entire stride duration. The stance phases of the limbs are indicated by the horizontal lines underneath the curves (orange: LF, green: RF, blue: LH, purple: RH).



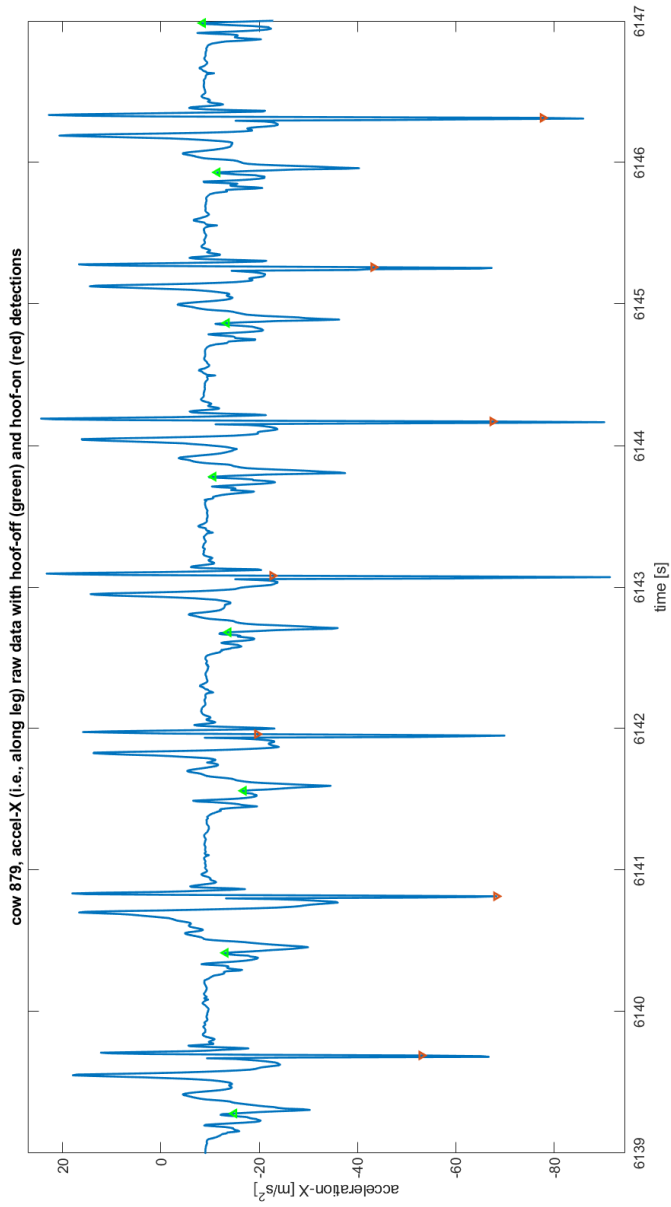
**S4 Figure. Vertical displacement curves of the back.** Per cow, the median curve (black), the MAD area (grey), and most typical curve (red) is shown on a scale from zero to 100 % of the entire stride duration. The stance phases of the limbs are indicated by the horizontal lines underneath the curves (orange: LF, green: RF, blue: LH, purple: RH).



**S5 Figure. Vertical displacement curves of the head.** Per cow, the median curve (black), the MAD area (grey), and the most typical curve (red) is shown on a scale from zero to 100 % of the entire stride duration. The stance phases of the limbs are indicated by the horizontal lines underneath the curves (orange: LF, green: RF, blue: LH, purple: RH).

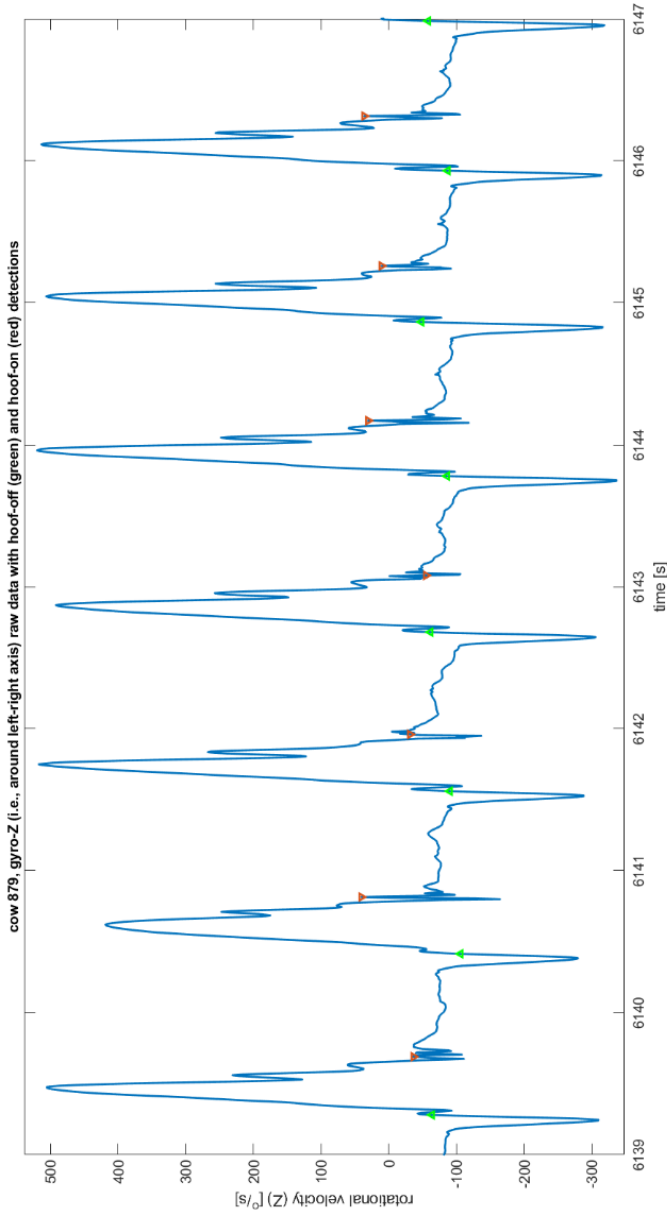


**S6 Figure. Vertical displacement curves of the collar.** Per cow, the median curve (black), the MAD area (grey), and the most typical curve (red) is shown on a scale from zero to 100 % of the entire stride duration. The stance phases of the limbs are indicated by the horizontal lines underneath the curves (orange: LF, green: RF, blue: LH, purple: RH).



**S7 Figure. Claw-on and claw-off detection relative to the acceleration signal along horizontal axis.** Raw acceleration data of the LF limb of cow 16 was used to show the claw-on (red) and claw-off (green) detections.





**S8 Figure. Claw-on and claw-off detection relative to the gyroscope signal along the left-right axis.** Raw gyroscope data of the LF limb of cow 16 was used to show claw-on (red) and claw-off (green) detections.





# 5

## **Kinematic gait characteristic changes in induced hind limb lameness in dairy cows**

In preparation

Marij Tijssen  
Katrina Ask  
Filipe M. Serra Bragança  
Pia Haubro Andersen  
Evgenij Telezhenko  
Christer Bergsten  
Mirjam Nielen  
Elin Hernlund  
Marie Rhodin

## Abstract

The aim of this study was to determine the most informative kinematic gait characteristic and sensor location for the identification of induced hindlimb lameness in cows during straight line walk. We hypothesized that differences in kinematic gait characteristics due to lameness induction can be identified with Inertial Measurement Units.

Measurements were performed by letting 17 cows walk on a straight line at their own chosen speed while wearing Inertial Measurement Unit (IMU) sensors on tuber sacrale, thoraco-lumbar junction of the back, withers and all four limbs. Baseline measurements were performed when cows were clinically sound, followed by hind limb lameness inductions and a second measurement. Data was selected based on analysis of video data. For the limb sensors, preselected parameters were calculated, while for the upper body sensors, parameters commonly used in equine kinematic were computed.

Most apparent gait related changes due to hind limb lameness induction were found in the pro- and retraction angles of the front limbs and the RoM of the back, located at the thoraco-lumbar junction. This coheres well with the visual lameness descriptor “arching of the back” as, for instance, assessed using the Sprecher lameness scale.

This is the first study to provide extensive information about gait adaptation strategies during induced lameness using a large number of IMUs attached to many different anatomical locations of the cow. This knowledge might be useful for the development of an automatic recognition method as an early warning system, although more insight in the development of the gait related changes over time with different degrees of lameness and of more anatomical locations (such as the hip) is needed.



## Introduction

Lameness evaluation is an essential part of cattle management and can be performed by visual assessment of cattle locomotion by the farmer, the veterinarian or animal caretakers. This assessment can be challenging since the scoring systems might not be sensitive enough to detect subtle orthopedic disorders and experience of the observer may determine the reliability of the lameness evaluation (1-4).

Kinematic gait characteristics are important features for lameness evaluation in dairy cattle. Gait characteristics displayed by dairy cattle due to orthopedic disorders, are described in the literature as arching of the back, decreased stride length, reluctance to bear weight on one limb, increased head bobbing, placement of hind limbs behind previous placement of ipsilateral front limbs (also known as insufficient tracking up), decreased joint angles due to joint stiffness, asymmetric gait and alignment of the tubera coxae (5-8). However, a more in-depth exploration of gait characteristics might provide more detailed information and help to discover other gait related changes that could improve visual gait assessment.

Gait characteristics can be studied by objective gait analysis such as video image analysis and limb-mounted accelerometers (9). Using video image analysis, reduced step length together with increased tripod support duration, and higher stride frequency were reported in relation to lameness in cattle (10-13). Using limb-mounted accelerometers, clinically lame cows showed an increase in movement asymmetry and significant lower walking speed (14, 15). Also, differences in stance phase duration between the sound and lame hindlimb were measured with this method (16).

Quantitative gait analysis is becoming increasingly popular in equine veterinary practice, and some of the motion parameters used for horses could potentially aid lameness assessment also in cows. Vertical displacement of the head, withers and pelvis (including tuber sacrale and tubera coxae) are commonly used to objectively assess lameness at trot in horses (17), while head and withers can identify front limb lameness at walk (18). In a recent study, sound cows were equipped with body-mounted accelerometers, attached to the head, withers, back, the sacrum between tubera sacrale and tuber coxae, to evaluate vertical displacement (19). Hence, evaluation of asymmetry of the vertical displacement of the head, withers and pelvis may also contribute to lameness detection in dairy cattle.

The aim of this study was to determine the most informative kinematic gait characteristic and sensor location for the identification of induced hindlimb lameness in cows during straight line walk. Gait characteristics and sensor locations followed from previous work (19). We hypothesized that differences in kinematic gait characteristics due to lameness induction can be identified with Inertial Measurement Units.

## **Materials and Methods**

### **Ethical statement**

These experiments were approved by the Swedish Ethics Committee and performed according to the Swedish legislation on animal experiments (diary number 5.8.18-10570/2019).

### **Study protocol**

Measurements were performed by letting cows walk on a straight line at their own chosen speed while wearing Inertial Measurement Unit (IMU) sensors on different anatomical landmarks. The first measurement was always performed when the cow was clinically sound. Thereafter, hind limb lameness was induced, and the same measurements were repeated. Data of the IMUs was selected based on analysis of video data. For analysis, preselected parameters were calculated for every sensor location.

### **Animals**

For the experiments, 17 milk producing cows were selected from the Field Research Station Lövsta of the Swedish University of Agricultural Sciences (for more details see Table 2). The cows had to meet the following criteria: i. They were claw trimmed at least than three months prior to the measurements during which no major finding was found, ii. Cows were in their first or second lactation, to lower the risk of chronic orthopedic disease), iii. Cows showed no signs of pain, nervous or stressed behavior, iv. Cows were clinically healthy and scored zero on the Sprecher lameness scale (6) (evaluated by two experienced raters, CB and ET), v. Cows had a body exterior within normal range, vi. Udder was not below hock angle and cows had a limb conformation without major visible deviations.

### **Experimental setup**

The measurements were performed with the equine gait analysis system EquiMoves® ([www.equimoves.nl](http://www.equimoves.nl)). The cows were equipped with 11 ProMove-



mini wireless IMU sensors (Inertia-Technology B.V., Enschede) on predefined anatomical landmarks; the highest point of the withers (further called withers), the spinal process of the 13th thoracic vertebra (further called back), the cranial part of sacrum or between the left and right sides tuber sacrale (further called sacrum), right and left tuber coxae (further called, respectively, RTC and LTC or, when combined, hip) and lateral aspect of the metatarsus/metacarpus of each limb (further called limb or LF (left front), RF (right front), LH (left hind), RH (right hind)). The sensors on the upper body (sacrum, back and withers) were attached to the skin with cyanoacrylate glue and the limb sensors with straps. After the measurements, the sensors were removed with acetone from the upper body.

The sensors were all set to a sampling rate of 200 Hz and synchronized in time with an accuracy of < 100 ns (for more details see (19)). All measurements were started with a period of five seconds of silent signal in which the cow was completely standing still for calibration of the EquiMoves system. After each measurement, the acceleration and angular velocity data were wirelessly transmitted via the Inertia Gateway to the Inertia Studio software (version 3.5.2).

During the measurements, video recordings were made from the side by a researcher walking alongside the cow with a handheld camera (Canon Legria HF R78, Canon, Tokyo, Japan). The handheld camera had a frame rate of 50 fps and a resolution of 1280x720 pixels. The camera was synchronized with the EquiMoves system by tapping the wither sensor twice at the start of the measurement while filming.

### **Lameness induction**

An appropriate induction method had to be designed to induce a consistent degree of lameness. A pilot study was executed to test the lameness induction method and identify the optimal way of inducing a mild and moderate degree of hind limb lameness in two cows. An optimal induction method is easy to apply, creates a constant pressure to the claw without sliding, and induces a fully reversible and constant hind limb lameness.

Two different induction methods were used to induce lameness by increasing the pressure on the sole of the claw or on the interdigital space. The pressure on the sole used two different materials either a wooden cylinder, with a diameter of 10 mm and height between 5 – 14 mm, or a plastic bulb, with a diameter of 10 mm and height between 5 – 15 mm. Both objects were glued to the predilection “typical” site for sole ulcer (directly below the flexor tuberosity of the pedal bone),



which is in the caudal third and axial half of the lateral sole of the hind limb. The second method consisted of a rectangular piece of a rubber mat with a height between 30 – 50 mm and a thickness of 17 mm. This rubber mat was placed in the interdigital space and fixated with self-adhesive elastic bandage to give a pressure to the interdigital skin. The interdigital skin was protected from chafing by a plastic film. The height difference between the sole and the end of the rubber mat was measured for every induction to make sure that all cows experienced similar levels of discomfort.

### **Measurement setup**

At the day of the measurement, two cows were moved to the stable where the measurements took place and had access to food and water ad libitum.

During the measurements, a single cow was walked through a 72-meter-long corridor with diamond grooved concrete flooring and turned around at the end of the corridor to walk back. Per measurement, the cows had to walk this corridor up and down twice (in total 288 meters) with a calm and constant pace chosen by the cow itself to obtain data of a natural walking flow. The cows were driven from a distance by one or two researchers to prevent the cows from turning around, with handling the cows as little as possible to not disturb the measurements. No other animals were present in the corridor during measurements.

For every cow, multiple measurements were performed. The first measurement was a baseline measurement before lameness induction. Thereafter, induction of one hind limb was performed in the trimming chute. It was randomly assigned which hind limb was induced and induction of a mild and a moderate degree of lameness was performed sequentially, always aiming for a mild degree of lameness with the first induction. The same two experienced raters (CB and ET) evaluated the degree of lameness using the Sprecher scale (6).

### **Data processing**

IMU data was exported to MATLAB (version R2017a, The MathWorks Inc., Natick, Massachusetts, USA) and a maximum of four intervals was selected per measurement and preprocessing analysis steps were performed as described by (20) and claw-on and claw-off timings were detected as described by (21). Thereafter, the preprocessed data was stride segmented by cutting the data in epochs from the LH claw-on to the consecutive LH claw-on (further called stride). For every stride, parameters adapted from horses were calculated (18). All processing steps are depicted in Fig 1.

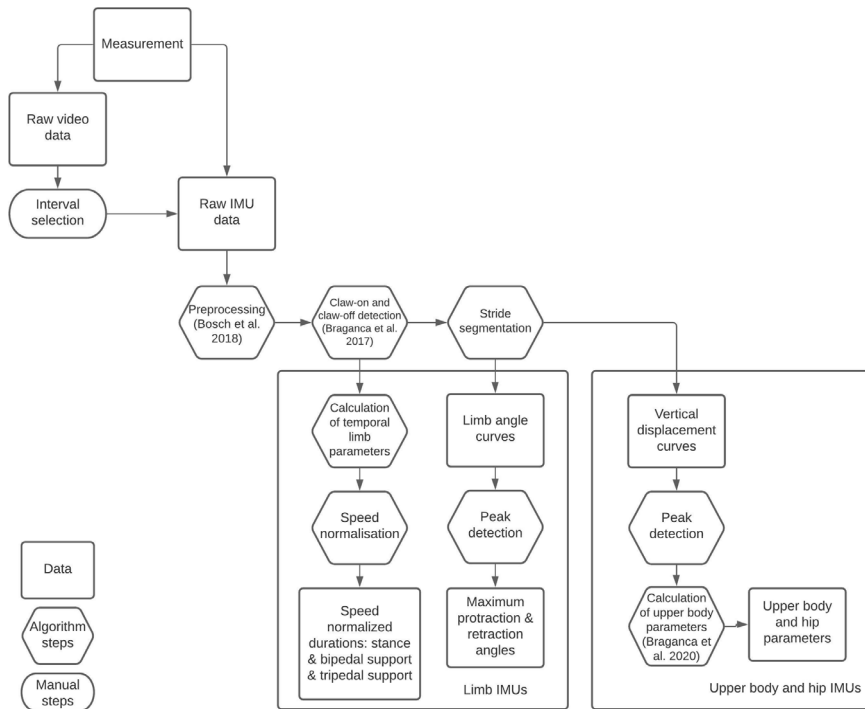


**Figure 1. Schematic representation of analysis steps performed.**

For the limb sensors, speed normalized durations were calculated for stance, bipedal support and tripedal support durations, as well as the maximum protraction angles and maximum retraction angles were calculated as described previously (19). For cows with a LH limb induction, limb parameters, of sound and induction measurements, were shifted between right and left limbs to make sure that induction effects were standardized between all cows to an RH limb induction, as previously described (18).

For the upper body sensor, scripts developed for horses were adjusted to detect peaks and valleys from the vertical displacement signals (20). From these peaks and valleys, the difference in minima (MinDiff), difference in maxima (MaxDiff), the range of motion (RoM), symmetry up index ( $SI_{up}$ ) and symmetry down index ( $SI_{down}$ ) were calculated for every stride and cow. For cows with a LH induction, these parameters were multiplied by minus one to standardize the induction effects between all cows. The definitions of these parameters can be found in Table 1 and a schematic representation is given in Fig 2. For all parameters,

boxplots were made to visualize the distributions. The percentage of successfully calculated parameters was determined per sensor location relative to the total amount of collected strides over all cows.

### Statistical analysis

For all parameters, the difference between the sound and induction condition were statistically evaluated by linear mixed model analysis with the “lme4” package (22) in R (version 1.1.442, RStudio Inc., Boston, Massachusetts, USA).

**Table 1. Detailed description of the calculated parameters in this study.** Each parameter is calculated per stride. Limb parameters and limb angles are calculated for LF (left front), RF (right front), LH (left hind) and RH (right hind). Upper body parameters are calculated for sacrum, back and withers. These definitions are adapted from horses (18).

Name	Abbreviation	Description
<b>Limb parameters</b>		
Relative stance duration (fraction between 0 and 1)		Time between claw-on and subsequent claw-off divided by entire stride duration of LH
Relative bipedal support duration (fraction between 0 and 1)		Duration of simultaneous stance phase of two limbs divided by entire stride duration of LH:
	Diagonal limb pairs	LF-RH and RF-LH
	Ipsilateral limb pairs	LF-LH and RF-RH
Relative tripedal support duration (fraction between 0 and 1)		Duration of simultaneous stance phase of three limbs divided by entire stride duration of LH:
	Single front limb involvement	LF-LH-RH and RF-LH-RH
	Single hind limb involvement	LF-RF-LH and LF-RF-RH
<b>Limb angles</b>		
Max protraction angle (degrees)		Maximal forward protraction of the limb measured at the metacarpus/metatarsus in the sagittal plane
Max retraction angle (degrees)		Maximal backward retraction of the limb measured at the metacarpus/metatarsus in the sagittal plane
<b>Upper body parameters</b>		
Difference maxima (MaxDiff) (mm)		Difference in vertical displacement between the two maxima (Max <sub>1</sub> and Max <sub>2</sub> ) of the vertical displacement signal (Fig 2)
Difference minima (MinDiff) (mm)		Difference in vertical displacement between the two minima (Min <sub>1</sub> and Min <sub>2</sub> ) of the vertical displacement signal (Fig 2)
Range of Motion (RoM) (mm)		Vertical displacement from the absolute maximum to the absolute minimum of the vertical displacement signal (Fig 2)
Symmetry up index (SI <sub>up</sub> )		Difference between RangeUp <sub>1</sub> and RangeUp <sub>2</sub> divided by the absolute maximum of those two
Symmetry down index (SI <sub>down</sub> )		Difference between RangeDown <sub>1</sub> and RangeDown <sub>2</sub> divided by the absolute maximum of those two

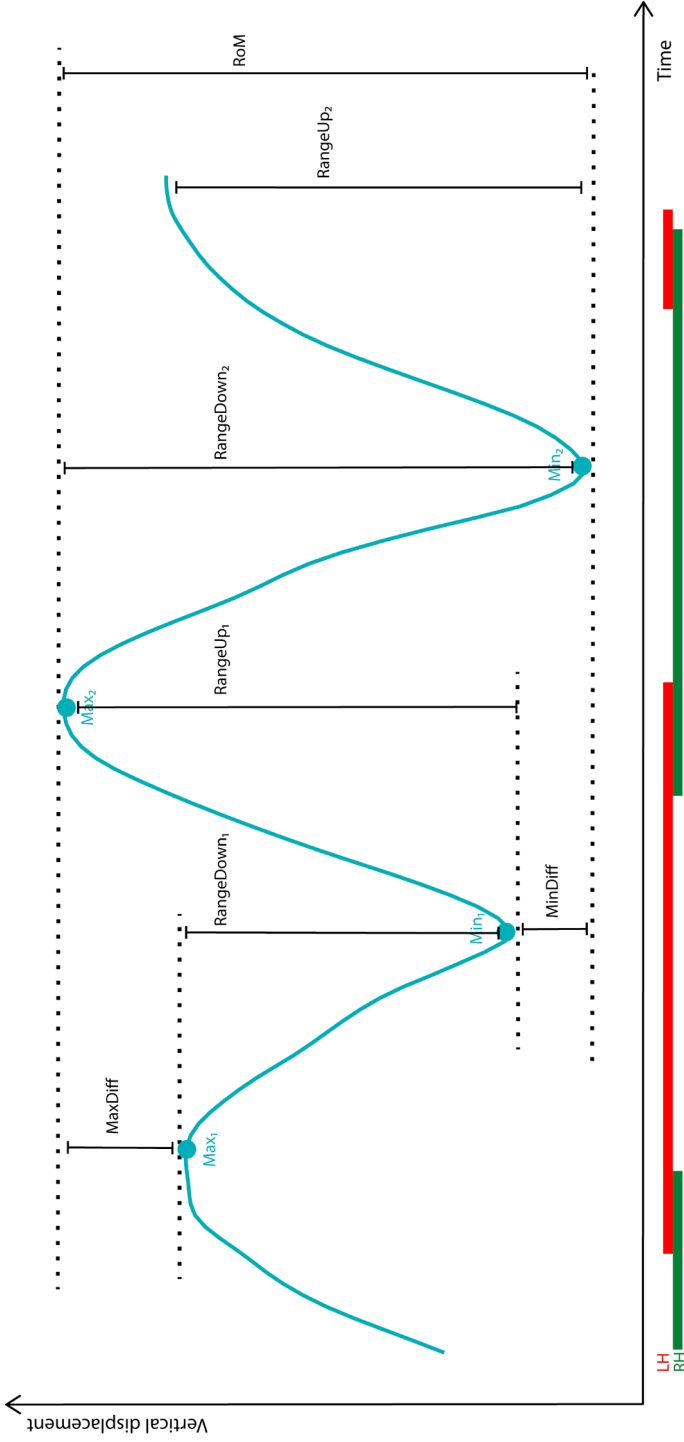


**Figure 2. Schematic representation of the upper body parameters (sacrum, back and withers).** For illustrative purposes, the vertical displacement signal of one upper body sensor of one stride is shown with the calculated parameters indicated. Underneath, the corresponding footfalls of the LH and RH are shown.

For the limb parameters, two models were developed; one model to evaluate the difference between the sound and induction condition (model 1) and another model to evaluate the difference between the induced limb (RH) and the non-induced limbs within the induction data (model 2). Model 1 contained fixed effects for the condition (sound vs induction) and limb pairs (front vs hind, left vs right, diagonal vs ipsilateral and single front limb and single hind limb involvement, as described in (19)). For this model, an interaction term between all fixed effects was used and cow was added as random effect. In model 2, all limbs were added as fixed effect and cow was set as random effect. In both models, the induced limb (RH) was set as the reference limb against which the effects were evaluated.

For the upper body, one model was developed to evaluate the difference between the sound and induction condition, which was equal to model 1 of the limb parameters. For the upper body parameters, the model contained fixed effects for the different sensor locations (sacrum, back and withers) and the condition (sound vs induction). Furthermore, an interaction term between the fixed effects was added and cow was set as random effect.

For all models, the residuals were checked with normal probability plots. Model reduction was applied with the Akaike's information criterion and the model with the lowest Akaike's information criterion values was selected according to Occam's Razor principle. Thereafter, 95% profile likelihood confidence intervals (CI) were evaluated with the "confint" package (23) and used for hypothesis testing. For model 1, it was assumed that the parameter did not differ between the two conditions when the 95% CI contained zero. For model 2, it was assumed that the limb parameter did differ between the RH and other limbs if 95% CIs did not overlap.

## **Results**

### **Data description**

In total, 71 measurements were performed, of which 31 were baseline measurements and 40 hind limb induction measurements. Inductions were successful (n=27) when a stable and clear lameness was seen, and when the wooden cylinder or plastic bulb was still intact after the measurement. All measurements with unsuccessful inductions were excluded from further analysis (n=13) for which the majority was caused due to crushing of the wooden cylinder



or loss of the plastic bulb. An overview of the cow characteristics, the number of measurements per cow and the induction methods can be found in Table 2.

**Table 2. Cow characteristics, number of measurements performed per cow and induction methods** (SR stands for the Swedish Red and SH stands for the Swedish Holstein breed, DIM is days in milk, PB is plastic bulb, WC is wooden cylinder, RM is rubber mat). \*All cows were first parity, except cow 1 and 2 (second parity)

Cow	Breed	DIM	Pregnancy (yes/no)	Days since last claw trimming	Findings at claw trimming	Sound / induction measurements (#)	Induction method
1	SH	93	yes	90	Sole hemorrhage	1 / 2	PB 10 and 15mm
2	SH	31	no	25		2 / 1	PB 15mm
3	SR	198	yes	25	Sole hemorrhage	1 / 1	PB 10mm
4	SH	281	yes	90	Dermatitis, Sole hemorrhage	2 / 2	PB 10 and 15mm
5	SH	235	yes	25		2 / 1	PB 15mm
6	SH	240	yes	25		2 / 2	PB 10 and 15mm
7	SR	223	yes	25		2 / 1	WC 5mm
8	SR	224	yes	25		2 / 1	PB 15mm
9	SH	96	no	90		3 / 2	PB 8 and 10mm
10	SH	93	yes	25		1 / 2	PB 10 and 15mm
11	SR	72	yes	62		2 / 3	PB 11 and 15mm and RM 5mm
12	SH	38	no	25		2 / 1	RM 5mm
13	SR	60	no	62		2 / 1	PB 15mm
14	SH	60	no	53	Sole hemorrhage	1 / 2	WC 6 and 10mm
15	SR	73	no	38		2 / 1	PB 10mm
16	SR	59	no	25		2 / 2	PB 5 and 10mm
17	SR	41	no	25		2 / 2	WC 6mm and PB 10mm

## Statistical analysis

For all parameters, the residuals of the models were approximately normally distributed, except for the RoM for which a log transform was used due to non-normality of the original values. For all parameters, the cow variance was 4 to 5 times smaller than the residual variance.

For all limb parameters, differences between the sound and induction condition were evaluated with model 1. For the relative stance duration, a front-hind limb effect was found, for the relative bipedal support duration a diagonal-ipsilateral limb effect was found, and for the relative tripod support duration no effect for single front limb and single hind limb involvement was found. For the limb angles,

**Table 3. Results for the limb parameter and angle analysis (model 1).** On the left side, the mean absolute values (95% likelihood CI) and the absolute difference (%) between the limb pairs are shown for all limb parameters and angles. On the right side, the difference between induction and sound condition is shown for all limb pairs relative to its own sound condition with the percentage. \*95% CI does not contain zero.

	Absolute values for sound condition		Difference between induction and sound condition	
	Mean (95% CI)	Difference between limb pairs (%)	Mean (95% CI)	Difference between conditions (%)
Relative stance duration (fraction of entire stride duration)	Hind (ref)	0.64 (0.63 – 0.65)	0.005 (0.002 – 0.008) *	0.8%
	Front	0.68 (0.67 – 0.70)	0.04 (6.3%)	0.5%
Relative bipedal support duration (fraction of entire stride duration)	Diagonal (ref)	0.11 (0.10 – 0.12)	-0.003 (-0.005 – -0.002) *	-2.7%
	Ipsilateral	0.14 (0.13 – 0.15)	-0.027 (-24.5%)	-2.7%
Relative tripedal support duration (fraction of entire stride duration)	All limbs	0.16 (0.15 – 0.16)		
Maximal retraction angle (degree)	Hind (ref)	-30.8 (-32 – -29.5)	1.37 (1.16 – 1.57) *	-4.5%
	Front	-45.6 (-46.9 – -44.1)	-14.8 (48%)	-2.8%
Maximal protraction angle (degree)	Right (ref)	-30.8 (-32 – -29.5)	1.36 (1.16 – 1.57) *	-4.5%
	Left	-32.8 (-33.8 – -31.7)	-0.81 (-1.01 – -0.60) *	-2.8%
Relative bipedal support duration (fraction of entire stride duration)	Hind (ref)	23.5 (22.6 – 24.3)	-0.74 (-0.9 – -0.6) *	-3.2%
	Front	26.4 (25.4 – 27.4)	2.96 (12.6%)	-6.4%
Relative tripedal support duration (fraction of entire stride duration)	Right (ref)	23.5 (22.6 – 24.3)	-0.74 (-0.89 – -0.6) *	-3.2%
	Left	22.4 (21.6 – 23.1)	-0.83 (-0.96 – -0.67) *	3.5%

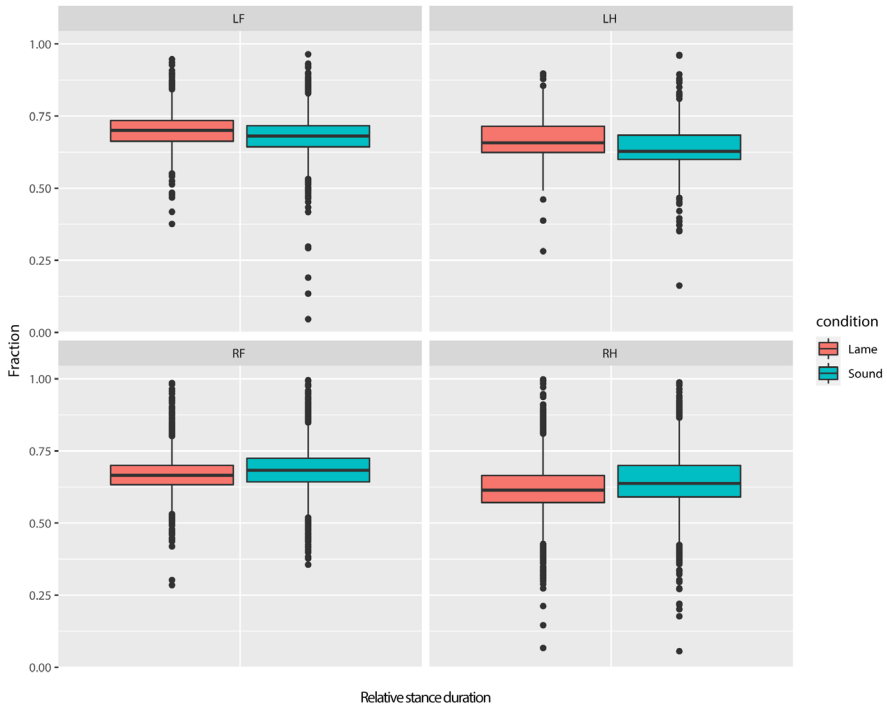


**Figure 3. Distribution of relative stance duration for every limb as fraction of entire stride duration.**

a front-hind and left-right limb effect was found. The results of this analysis can be found in Table 3 and Fig 3-5.

For the sound condition, Table 3 shows that the relative stance duration was 6.3% longer for the front limbs (0.68) compared with the hind limbs (0.64). After induction, this duration increased by 0.005 (0.8%) in the hind limbs, relative to its own duration in the sound condition, In the front limbs an increase of 0.003 (0.5%) was found relative to its own duration in the sound condition. The bipedal support was shorter for ipsilateral limb pairs (-24.5%) in the sound condition, and both diagonal and ipsilateral limb pairs decreased by 2.7% after induction condition. The 95% CI indicate that there are no systematic condition effects for both the relative stance and bipedal support duration. The tripedal support duration did not show any limb pair effects nor differences between sound and induction condition.



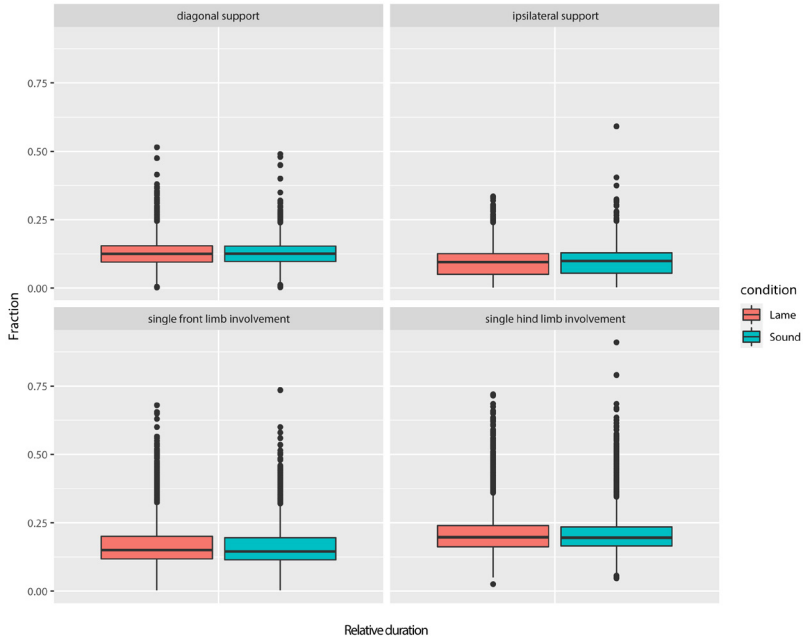


**Figure 4. Distribution of relative bipedal and tripodal support durations as fraction of entire stride duration.** For the bipedal support durations, the diagonal and ipsilateral limb pair durations are shown. For the tripodal support durations, the durations for the single front limb and single hind limb involvement are shown.

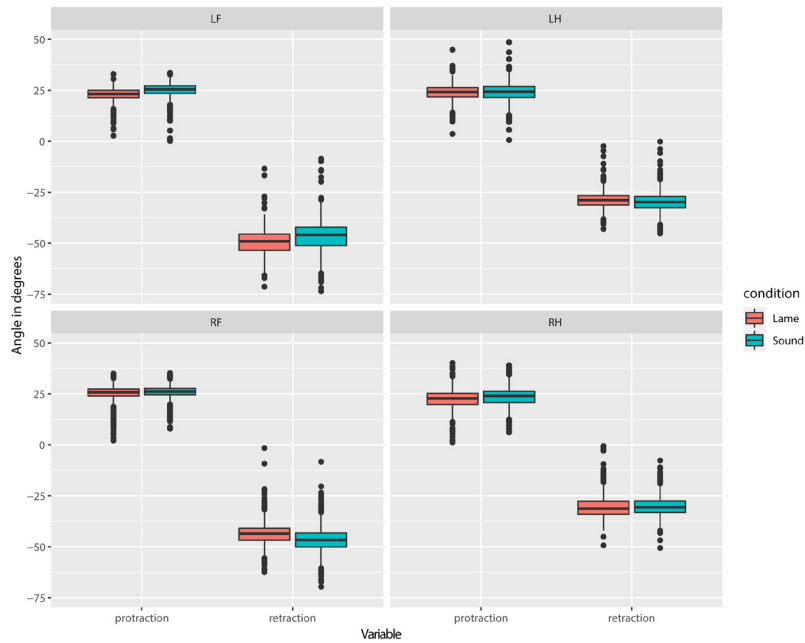


**Figure 5. Distribution of protraction and retraction angles are shown for every limb.**



For the maximal retraction angle, bigger angles were found for the front limbs (48%) and a smaller angles were found for the left limbs (-6.3%) compared with the reference limbs. For the induction condition, smaller retraction angles were found for all limbs. For the maximal protraction angle, bigger angles were found for the front (12.6%) and left (4.7%) limbs compared with the reference limbs. For the induction condition, the angles decreased (-3.2% and -6.4%) except for the left limbs (3.5%). The 95% CI indicate that there are no systematic condition and limb effects for both the retraction and protraction angles.

Differences between limbs within the induction data were evaluated with model 2 for all limb parameters. For the relative stance duration, relative bipedal support duration and relative tripedal support duration, no limb effect was found. For the limb angles, a front-hind and a left-right limb effect was found. The results of this analysis can be found in Table 4.

**Table 4. Results for the limb effects within the induction condition (model 2).** Mean (95% likelihood CI) are shown for all limb parameters with the absolute values for all limbs (if there was a limb effect) on the left and the difference (percentage) with the induced limb (RH) on the right. \*95% CI do not overlap with the reference (RH).

Limb pair effect within induction condition			
		Mean (95% CI)	Difference between not-induced limbs with induced limb (RH) (%)
Relative stance duration (fraction of entire stride duration)	All limb pairs	0.67 (0.65 – 0.68)	
Relative bipedal support duration (fraction of entire stride duration)	All limb pairs	0.09 (0.89 – 0.10)	
Relative tripedal support duration (fraction of entire stride duration)	All limb pairs	0.16 (0.15 – 0.16)	
Maximal retraction angle (degree)	RH (ref)	-30.1 (-31.3 – -28.9)	
	RF	-43.4 (-44.8 – -41.9) *	-13.3 (44%)
	LF	-49 (-50.4 – -47.5) *	-18.9 (63%)
	LH	-28.34 (-29.78 – -26.89)	1.76 (-5.9%)
Maximal protraction angle (degree)	RH (ref)	22.34 (21.3 – 23.36)	
	RF	25.29 (24.08 – 26.46) *	2.95 (13%)
	LF	22.93 (21.72 – 24.12)	0.59 (2.6%)
	LH	24.09 (22.87 – 25.28)	1.75 (7.8%)

Within the induction data, both front limbs showed larger retraction angles compared with the induced limb (RH), particularly LF. Smaller differences were found for the maximal protraction angle with a largest angle for RF.

For the upper body parameters, the percentage of successfully calculated parameters was high. As can be seen in Table 5, the RoM is calculated 99.8% correctly for all sensor locations, while the Symmetry Indices are least successfully calculated with 91.3% for the wither sensor.

**Table 5. Percentage correctly calculated parameters for upper body sensors.** Percentage is calculated relative to total amount of collected strides.

Parameter	Sacrum	Back	Withers
MinDiff	99%	95.9%	99.5%
MaxDiff	95.9%	95.8%	99.5%
Symmetry Index Up	98.5%	93.5%	91.3%
Symmetry Index Down	98.5%	93.5%	91.3%
Range of Motion	99.8%	99.8%	99.8%

**Table 6. Results for the upper body parameter analysis.** For all upper body parameters, the absolute values within the sound condition are given for the different sensor locations on the left side. The mean (95% likelihood CI) of every parameter is shown for all parameters, except for the RoM were median difference was shown. For the condition effect (induction versus sound), the difference between the induction and sound condition per sensor location is given relative to its own location. \*95% CI does not contain zero.

		Absolute values for sound condition	Difference between induction and sound condition
		Mean (95% CI)	Mean (95% CI)
MaxDiff (mm)	Sacrum	-0.65 (-1.82 – 0.53)	-0.14 (-0.82 – 0.53)
	Back	-2.20 (-3.53 – -0.87)	3.41 (2.71 – 4.10) *
	Withers	-0.86 (-2.61 – 0.88)	-1.11 (-1.77 – -0.45) *
MinDiff (mm)	Sacrum	3.97 (1.30 – 6.63)	0.63 (-0.48 – 1.74)
	Back	2.27 (0.22 – 4.32)	6.61 (5.48 – 7.75) *
	Withers	5.00 (1.51 – 8.50)	-0.46 (-1.54 – 0.63)
RoM (mm)	Sacrum	37.97 (33.96 – 42.44)	1.03 (1.00 – 1.05) *
	Back	21.22 (18.96 – 24.10)	1.17 (1.14 – 1.20) *
	Withers	38.5 (34.97 – 42.48)	1.14 (1.11 – 1.16) *
Symmetry Index Up	Sacrum	0.12 (0.05 – 0.19)	-0.01 (-0.06 – 0.03)
	Back	0.21 (0.09 – 0.34)	0.05 (0.01 – 0.10) *
	Withers	-0.12 (-0.22 – -0.02)	0.09 (0.04 – 0.13) *
Symmetry Index Down	Sacrum	0.07 (0.00 – 0.15)	-0.05 (-0.10 – -0.01) *
	Back	-0.01 (-0.07 – 0.05)	0.12 (0.07 – 0.17) *
	Withers	-0.13 (-0.25 – 0.02)	-0.04 (-0.09 – 0.00)

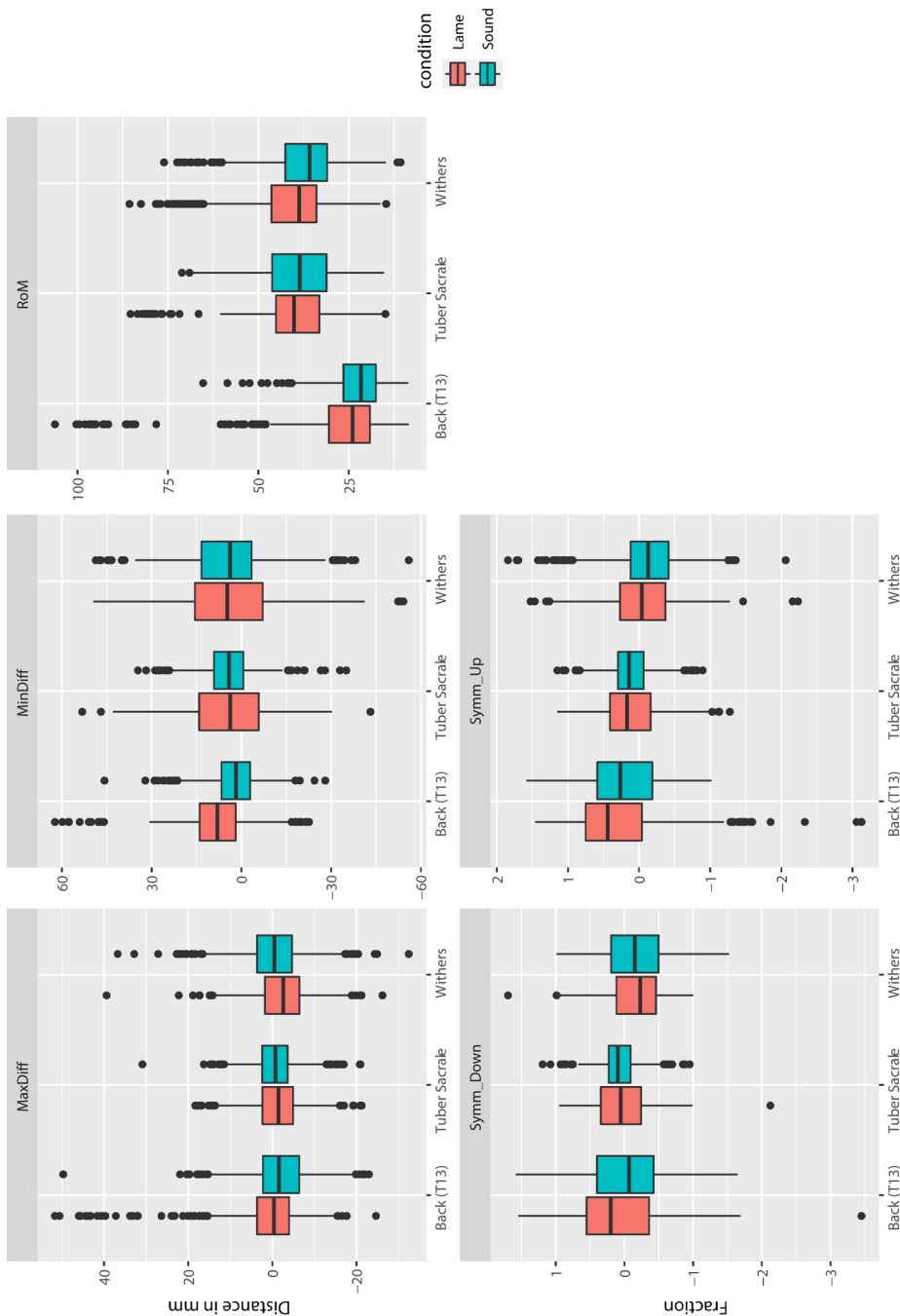
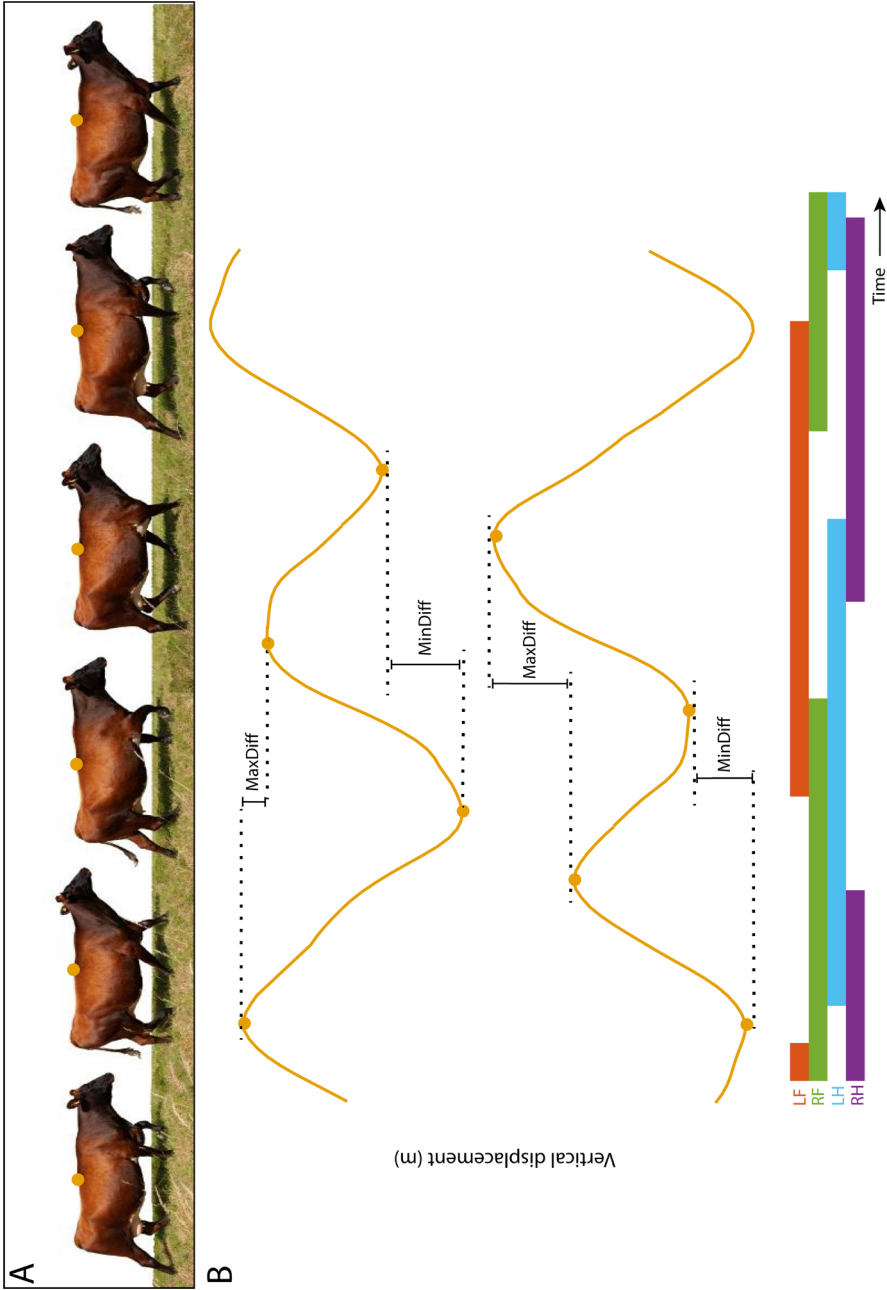


Figure 6. Distribution of upper body parameters for all sensor locations.



**Figure 7. Schematic representation of the vertical displacement signal relative to cow walking motion.** For illustrative purposes, the vertical displacement signal of one stride is shown with the MinDiff and MaxDiff parameters indicated. Underneath, the corresponding footfalls of all limbs are shown.



Differences between the sound and induction condition were evaluated with model 1 for all upper body locations. For all parameters, a location effect and a condition effect were found (Table 6).

As can be seen in Table 6, the back sensor showed systematic differences between the two conditions for all parameters indicated by the 95% CI. For the sacrum sensor, systematic differences were only found for the RoM and Symmetry Index Down. For the withers, systematic differences were found between the two conditions for the MaxDiff, RoM and Symmetry Index Up. The systematic differences found for the sacrum and wither sensor were smaller compared to the back sensors, except for the Symmetry Index Up obtained from the wither sensor. An overview of these results is given in Fig 6.

Overall, the MaxDiff of the back sensor shows the biggest difference compared to the other locations. As can be seen in Fig 7, the MaxDiff is increasing because the second peak of the vertical displacement signal increases in height which indicates that the back is arching (ventral flexion). This peak occurs when the lame limb is placed on the ground (RH). The MinDiff is increasing because the second valley is less deep which happens when the lame limb is lifted of the ground resulting in hollowing of the back (dorsal flexion).

## Discussion

In this study, multiple kinematic gait characteristics were obtained from the upper body and the limbs measured with IMUs. This is the first study where a large number of IMUs were attached to different anatomical locations of a cow to provide extensive information about gait adaptation strategies due to lameness induction. Most apparent gait related changes due to hind limb lameness induction were found in the pro- and retraction angles and the RoM of the back, located at the thoraco-lumbar junction.

The limb angle of the lame hind limb was less protracted (measured by the angle of the metatarsus) around claw impact and less retracted at the end of stance, without a decrease in relative stance duration. Furthermore, the front limbs are less retracted, while the protraction angle is kept similar in the LF and is prolonged in the RF limb. The LH limb does show a slight increase both angles, which might be necessary for the cow to keep walking in a straight line and maintaining a similar relative stance duration. The limb angle show that the limbs have a

different compensatory mechanism to the induction. This mechanism is most clearly visible when comparing the limb angles within the induction condition. In this study, a very small increase was found for the bipedal support duration in the induction condition. The results of the statistical analysis of the limb parameters showed similar absolute values in sound condition as previous described (19) which indicated that the statistical approach seemed valid for this analysis.

From the upper body sensors, the back sensor showed differences for all parameters. This coheres well with the visual lameness descriptor “arching of the back” as assessed with the Sprecher scale (5, 6). Flower and Weary (2006) also found back arch to be a significant tool to detect sole ulcer, which our induction method with pressure to the claw sole aimed to imitate (5). The MinDiff parameter showed only a systematical difference between the two conditions for the back sensor, while for the withers and sacrum no systematic differences were found. Furthermore, the RoM of the back sensor showed the biggest differences between the two conditions with the highest percentage of successfully calculated parameters. Therefore, the back might be a more informative location compared to the sacrum and withers.

It was expected from similar studies with horses that clinically sound cows would have symmetry indices close to zero. This was however only true for MinDiff for the back and fairly true for the sacrum and withers. The Symmetry Index Up was more away from zero compared to the Symmetry Index Down. This might be caused by motor laterality of the cows, environmental distractions in the stable, walking speed differences or anatomical asymmetry due to a filled rumen. Since this is a novel method for the assessment of walking in cows, it should be pointed out that reference values are needed for clinical sound walking conditions, including knowledge about expected variability within each individual (24).

For the upper body, the analysis scripts were modified to detect all peaks and values needed for the calculation of the upper body parameters. These scripts are property of Inertia BV and described elsewhere (20). Following these modifications, high percentages of correctly calculated parameters were obtained, ranging between 99.8% and 91.3%. The relatively small percentage of the wither sensors might be caused due to vertical displacement signals that showed completely different signal patters from vertical displacement signals obtained from other locations as previous described (19). Despite of the withers’ signals, the percentages are high enough to conclude that the scripts are sufficient for the analysis of cow data.



The lameness induction model used during this study was adapted from principles used in horses (25). When the induction method was successfully applied it caused a constant and extensive pressure over the sensitive point beneath the flexor tuberosity of the claw bone (P3). The locomotion was visually assessed with the Sprecher lameness scale for all cows (6). The Sprecher scale evaluates walking patterns for clinical signs of pathologic lameness. The measurement was included for analysis if a stable lameness, e.g. no deterioration or weakening of the clinical signs, was seen. Furthermore, the lameness caused by the induction ranged between zero and two for all cows, which in horses is considered associated to a mild to moderate lameness. We included only measurements from cows without shaking its claw, no itching behavior, or without kicking movements. This resulted in a reliable comparison of the kinematic characteristic, as also supported by the small cow variance in the statistical analysis. Effects of the different induction methods could not be analyzed due to the limited amount of data although this might be important for future research.

The high number of sensors used in this study is not a realistic method for clinical use. However, this method will allow us to gain extensive knowledge about the adaptation strategies of multiple body locations made by cows with discomfort in the hind limbs. The analysis steps performed can be used to distinguish the most informative anatomical locations and selection of parameters. In this study, hip movement parameters such as the roll, yaw and pitch of the tuber coxae were not analyzed. However, these parameters might be informative for the detection of hind limb lameness since the hip movements might reveal more adaptation strategies used by cows. This knowledge might be useful for the development of an automatic recognition method, which can also be used as an early warning system. However, for such a system more research is needed to gain insight in the development of the gait related changes over time with different degrees of lameness and of more anatomical locations.

## Conclusion

IMUs can be utilized to detect hind limb lameness in cows. The most important limb parameters are the front limb angles, in particularly the retraction angle. The thoraco-lumbar junction of the back proved to be the most informative upper body location to measure, where multiple parameters showed systematical and clear differences between sound and induction condition.



## **Acknowledgments**

We acknowledge that cooperation of the cows was vital to collect these data. Furthermore, we would like to thank J. Lundblad, C. Frisk and the animal caretakers of the Swedish Livestock Research Centre Lövsta for their contribution to the data collection. And J. van den Broek who greatly helped with statistical guidance.



## References

1. Tadich N, Flor E, Green L. Associations between hoof lesions and locomotion score in 1098 unsound dairy cows. *Vet J.* 2010;184(1):60-5.
2. Schlageter-Tello A, Bokkers EAM, Koerkamp PWGG, Van Hertem T, Viazzi S, Romanini CEB, et al. Comparison of locomotion scoring for dairy cows by experienced and inexperienced raters using live or video observation methods. *Animal Welfare.* 2015;24(1):69-79.
3. Dyer RM, Neerchal NK, Tasch U, Wu Y, Dyer P, Rajkondawar PG. Objective determination of claw pain and its relationship to limb locomotion score in dairy cattle. *J Dairy Sci.* 2007;90(10):4592-602.
4. Van Nuffel A, Zwertvaegher I, Pluym L, Van Weyenberg S, Thorup VM, Pastell M, et al. Lameness Detection in Dairy Cows: Part 1. How to Distinguish between Non-Lame and Lame Cows Based on Differences in Locomotion or Behavior. *Animals (Basel).* 2015;5(3):838-60.
5. Flower FC, Weary DM. Effect of hoof pathologies on subjective assessments of dairy cow gait. *J Dairy Sci.* 2006;89(1):139-46.
6. Sprecher DJ, Hostetler DE, Kaneene JB. A lameness scoring system that uses posture and gait to predict dairy cattle reproductive performance. *Theriogenology.* 1997;47(6):1179-87.
7. Whay H. Locomotion scoring and lameness detection in dairy cattle. In *Practice.* 2002;24(8):444-9.
8. Telezhenko E. Measurement of spatial gait parameters from footprints of dairy cows. *Animal.* 2009;3(12):1746-53.
9. O'Leary NW, Byrne DT, O'Connor AH, Shalloo L. Invited review: Cattle lameness detection with accelerometers. *J Dairy Sci.* 2020;103(5):3895-911.
10. Poursaberi A, Bahr C, Pluk A, Van Nuffel A, Berckmans D. Real-time automatic lameness detection based on back posture extraction in dairy cattle: Shape analysis of cow with image processing techniques. *Computers and Electronics in Agriculture.* 2010;74(1):110-9.
11. Viazzi S, Bahr C, Van Hertem T, Schlageter-Tello A, Romanini CEB, Halachmi I, et al. Comparison of a three-dimensional and two-dimensional camera system for automated measurement of back posture in dairy cows. *Computers and Electronics in Agriculture.* 2014;100:139-47.
12. Blackie N, Bleach EC, Amory JR, Scaife JR. Associations between locomotion score and kinematic measures in dairy cows with varying hoof lesion types. *J Dairy Sci.* 2013;96(6):3564-72.
13. Flower FC, Sanderson DJ, Weary DM. Hoof pathologies influence kinematic measures of dairy cow gait. *J Dairy Sci.* 2005;88(9):3166-73.
14. Pastell M, Tiusanen J, Hakojärvi M, Hänninen L. A wireless accelerometer system with wavelet analysis for assessing lameness in cattle. *Biosystems Engineering.* 2009;104(4):545-51.
15. Chapinal N, de Passille AM, Pastell M, Hanninen L, Munksgaard L, Rushen J. Measurement of acceleration while walking as an automated method for gait assessment in dairy cattle. *J Dairy Sci.* 2011;94(6):2895-901.
16. Alsaood M, Luternauer M, Hausegger T, Kredel R, Steiner A. The cow pedogram-Analysis of gait cycle variables allows the detection of lameness and foot pathologies. *J Dairy Science.* 2017;100(2):1417-26.
17. Buchner HHF, Savelberg HHCM, Schamhardt HC, Barneveld A. Head and trunk movement adaptations in horses with experimentally induced fore- or hindlimb lameness. *Equine Vet J.* 1996;28(1):71-6.
18. Serra Braganca FM, Hernlund E, Thomsen MH, Waldern NM, Rhodin M, Bystrom A, et al. Adaptation strategies of horses with induced forelimb lameness walking on a treadmill. *Equine Vet Journal.* 2020.
19. Tijssen M, Serra Bragança FM, Ask K, Rhodin M, Andersen PH, Telezhenko E, et al. Kinematic gait characteristics of straight line walk in clinically sound dairy cows. *PLoS One.* under review.

20. Bosch S, Serra Braganca F, Marin-Perianu M, Marin-Perianu R, van der Zwaag BJ, Voskamp J, et al. EquiMoves: A Wireless Networked Inertial Measurement System for Objective Examination of Horse Gait. *Sensors* (Basel). 2018;18(3).
21. Braganca FM, Bosch S, Voskamp JP, Marin-Perianu M, Van der Zwaag BJ, Vernooij JCM, et al. Validation of distal limb mounted inertial measurement unit sensors for stride detection in Warmblood horses at walk and trot. *Equine Vet J*. 2017;49(4):545-51.
22. Bates D, Mächler M, Bolker B, Walker S. Fitting Linear Mixed-Effects Models Using lme4. *Journal of Statistical Software*. 2015;67(1).
23. R Foundation for Statistical Computing. R: A Language and Environment for Statistical Computing. Vienna, Austria: R Core Team; 2018.
24. Hardeman AM, Serra Braganca FM, Swagemakers JH, van Weeren PR, Roepstorff L. Variation in gait parameters used for objective lameness assessment in sound horses at the trot on the straight line and the lunge. *Equine Vet J*. 2019;51(6):831-9.
25. Merkens HW, Schamhardt HC. Evaluation of equine locomotion during different degrees of experimentally induced lameness. I: Lameness model and quantification of ground reaction force patterns of the limbs. *Equine Vet J Suppl*. 1988(6):99-106.





# 6

## General discussion

The increasing number of possibilities to monitor both physical and mental health in animals comes with an increasing amount of data that needs to be processed and analyzed. In this thesis, I focused on biomechanical gait characteristics of horses and cows measured with Inertial Measurement Units (IMUs) and the application of different signal processing procedures for this type of data.

In the first part of this discussion, I will address challenges related to the studies performed, and the advances made in this thesis. The potential use of automatic monitoring for animal health and welfare is much broader but also generally technically more challenging and less well developed than for the applications studied here. In the second part of this discussion, I will illustrate this by addressing two applications that we studied in the initial explorative phase of my PhD-research. I will conclude the discussion with the lessons learned in the thesis and the future outlook.

## Discussion of the thesis

This thesis consists of two parts. In the first part, development of signal analysis procedures for gait analysis in horses is described and evaluated. In the second part, the horse signal analysis procedures are applied to the study of biomechanical gait characteristics in cows.

### Part 1: Development of signal analysis procedures

In **Chapters 2 and 3**, the development of different algorithms was described for the automatic detection of hoof-events from hoof-mounted IMUs. Subsequently, the performance of these algorithms was evaluated with the force plate and optical motion capture system. The results of this performance evaluation showed that the angular velocity signal was the most accurate for hoof-on detection while the acceleration signal was the most accurate for the hoof-off and break-over phase onset detection. The hoof-off event was detected with the highest accuracy and precision. These studies are innovative because they are the first to describe signal analysis procedures for the automatic detection of hoof-events from IMU data. Moreover, these procedures were evaluated with different measurement methods. These algorithms can improve gait classification in horses and enhance the application of hoof-mounted IMUs for clinical purposes. The challenges that came with these studies were (1) the development of a suitable signal analysis procedure and (2) the performance evaluation of these algorithms against methods that measure different properties.



### ***Development of a suitable signal analysis procedure***

Selecting the proper signal characteristic from the IMU data can be challenging because different environmental circumstances during the collection of the data may alter the signal appearance. Such differences in circumstances can be in the type of flooring, in the gait and speed of the horses or in the attachment method of IMUs to the hooves (2-4). In addition, there can be different stimuli around the measurement area such as other animals or people walking around. It is of importance to be aware of the effects of the measurement and environmental circumstances on the data as well as the effect of signal analysis procedures on the signal appearance. Furthermore, the application for which the signal analysis procedure is being developed also plays an important role in choosing specific procedures over others.

For the studies performed in **Chapter 2 and 3**, a robust measurement and signal analysis procedure had to be developed in order to detect the right characteristics under different circumstances. The data analyzed in these studies had already been obtained and preprocessed by Inertia BV and no alterations could be made on this part. These preprocessing steps included calculating the sensor orientation, which was performed by aligning the z-axis of the sensor with the gravitational force (5), and combining the low-*g* and high-*g* acceleration signals, which reduced the data from two tri-axial signals into one tri-axial signal (6). Furthermore, hoof-on and hoof-off events were detected and used for stride segmentation. Although, information about the preprocessing steps was available, no alterations could be made and all the algorithms to perform these processing steps were processed with proprietary software from EquiMoves System which might limit the applicability under different circumstances and for other animal species.

After the preprocessing steps were performed, the data were made available for further analysis and a signal analysis procedure was performed that did not alter the signal's appearance, meaning that no filtering of the signals was performed during which certain frequencies are removed from the signal (7). The signal analysis procedure included calculating the Euclidean norm after which peak detection was performed to collect the time points for certain hoof-events. The benefits of the calculation of the Euclidean norm were that effects due to different attachment methods were canceled out and that calculating a horse specific rotation matrix became unnecessary which led to a reduction of the calculation time and reduction of the data from a tri-axial signal to a single-axial signal. A disadvantage of calculating the Euclidean norm was that the information about the orientation of the sensor was lost and only the magnitude of the signal was



obtained. Information about the orientation of the sensor was not needed for detecting the hoof-events, because only the time points of these hoof-events were needed for the specific application of gait analysis. Furthermore, the data reduction and faster calculation speed were important since large amounts of data need to be analyzed for gait analysis in horses. However, for other applications in which one direction of the data need to be studied, for example vertical displacement, this calculation is not beneficial.

### ***Performance evaluation by comparison with methods that measure different properties***

Evaluating the performance of the developed algorithms with the force plate and optical motion capture system was challenging because the data of both methods are not directly comparable. The algorithms used the angular velocity and acceleration signal, measured with IMUs, while the force plate measured the force exerted underneath the hoof and the optical motion capture system measured the displacement of infra-red markers attached to the horse. This challenge was overcome by formulating clear definitions of the hoof-events and by adapting these definitions to the specific measurement methods.

In **Chapter 2 and 3**, the definitions of different hoof-events were developed as follows. The break-over phase onset was defined as the start of the rotational movement of the hoof around the toe. A straightforward method to measure the break-over phase onset is to measure the angle of the heel around the toe of the hoof. The hoof-off event was defined as the moment in time where the hoof was completely lifted off the ground which can be measured with kinetic methods as a drop in force or pressure, and with kinematic measures as a change in displacement or increase in acceleration. The hoof-on event is the reverse of the hoof-off event and can be measured by an incline in force or pressure measured with the force plate or a by a decrease in acceleration.

All measurement methods used in these studies are able to capture these hoof-events, although the properties they measure differ. The IMUs measure both acceleration and angular velocity, which are the second derivative of displacement and the first derivative of angle with respect to time, respectively. The optical motion capture system measures displacement and angle over time and therefore allows direct comparison with the IMUs, in contrast to the force plate. The force plate measures the force over time and therefore no direct comparison with the optical motion capture system and IMUs can be made. As a result, it is necessary to make an adaptation to the measurements captured by the force plate, to allow



for a comparison with the measurements taken with the IMUs and optical motion capture system.

For the studies in **Chapter 2 and 3**, this adaptation was made by calculating the first derivative of the force with respect to time, to determine the change in force over time. The rationale employed here was that the force will change when the hoof starts rotating, thus exerting less force on the force plate. This allowed a comparison between the detection of the break-over phase onset by the force plate and the displacement and angle measured by the IMUs and optical motion capture system. And therefore, performance evaluation of these algorithms with the gold standards for the kinematic and kinetic measurement methods became possible.

## **Part 2: Application of signal analysis procedures to another species**

In **Chapter 4 and 5**, explorative studies with IMUs attached to multiple anatomical locations of cows were described. These studies evaluated the changes in biomechanical gait characteristics with (induced) lameness, as well as the feasibility of different attachment locations of the sensors. These studies are innovative for two reasons: firstly, the relatively large number of IMUs attached to the cows, which is normally not feasible on farms, and secondly the novel use of lameness inductions to compare the changes in biomechanical gait characteristics within the same cows. In these studies, the signal-analysis procedures and measurement method developed for horse data were applied to data from cows.

### ***Challenges that came with adaptation between species***

Although horses and cows are both quadrupeds, small differences in the signal pattern between the two species were observed which might be caused by differences in movements and structure of the limbs and hooves (**Chapter 4**). These small differences affected the hoof-on and hoof-off event detection needed for the stride segmentation (8). In stride segmentation, the signal is divided into epochs corresponding to the strides made by the animal. The hoof-on and hoof-off event detection led to small time shifts when making this division. This resulted in the epochs not starting exactly on the hoof-on event. Modifications in the procedures had to be made in order to successfully remove this time shift from the signal.

Another modification was made in the measurement method for the studies in **Chapter 4** and **Chapter 5**. Extra sensors were attached to the back and the collar of the cows. The collar offers an accessible attachment site. This location is often

used by conventional sensors for measuring behavior (9). The back is known as an important landmark for visual lameness detection (10). Therefore, arching of the back was considered an important feature to objectively investigate. For clinical use, the relatively large number of sensors used in these studies is not feasible and should be reduced. However, it will provide a very thorough investigation into both the biomechanical gait characteristics and the attachment locations that are needed to develop an objective lameness detection method for cows.

Adaptation of measurement methods from one animal species to another will be possible when anatomical differences between the species are considered and when the measurement purposes are fairly similar. In **Chapter 4** and **Chapter 5**, adapting the measurement methods and signal analysis procedures between animal species was justified because both cows and horses were measured for the purpose of lameness detection. But even then, modifications in the measurement setup were performed to be able to study specific traits such as arching of the back. Furthermore, the signal analysis procedure had to be modified to account for the differences in feet structure. I expect that modification in the signal analysis procedure are necessary when measuring animals with different limb height, different feet structure (e.g., claws or paws) and different gaits (e.g., walking of a cow, gallop of a horse and running of a dog). Adaptation and application of these methods to different species may lead to interesting insight into differences in biomechanical gait and behavior characteristics (11, 12).

When these measurement and analysis methods are applied for another purpose, it might be that different anatomical attachment locations are important, as well as different signal analysis algorithms to be able to detect characteristics specific for that purpose. For this, more extensive modifications to the measurement method and signal analysis procedures need to be made or completely new methods need to be developed.

## **Two additional case studies**

In the last couple of decades, new biosensors and wearable technologies have become very popular in human health care and are increasingly adapted to the field of veterinary medicine. For animals, these new developments are mainly used for health management and welfare by automatically detecting changes in physiological and behavioral variables, such as locomotion, of individuals or of animals living in a group (13). When sensor technologies applied in human



medicine are adapted in the veterinary medicine field, the specifications in design and attachment methods need to be modified in addition to the measurement method and signal analysis procedures. For example, wearables don't have to be aesthetically designed, but should have the right properties for their purpose and target animals in order to become applicable. Two case studies were performed at the start of this PhD that illustrate the challenges that come with the application of new technologies in different fields of veterinary medicine.

### ***First case study: parturition detection in sows***

The first case study concerns the development of a sensor to monitor the parturition in sows and automatically identify the start of farrowing and birth-interval lengths. Piglet mortality has an incidence ranging from 16 to 20% and is therefore an important concern in the pig industry. The major causes of piglet mortality are stillbirth, crushing and starvation (14-16). Stillbirth is caused by asphyxia and dystocia with an incidence ranging from 2 to 9%. A direct relation between increased farrowing duration and risk of stillbirths exists, although it remains unclear whether this is a result or cause of longer birth-intervals lengths (16-18).

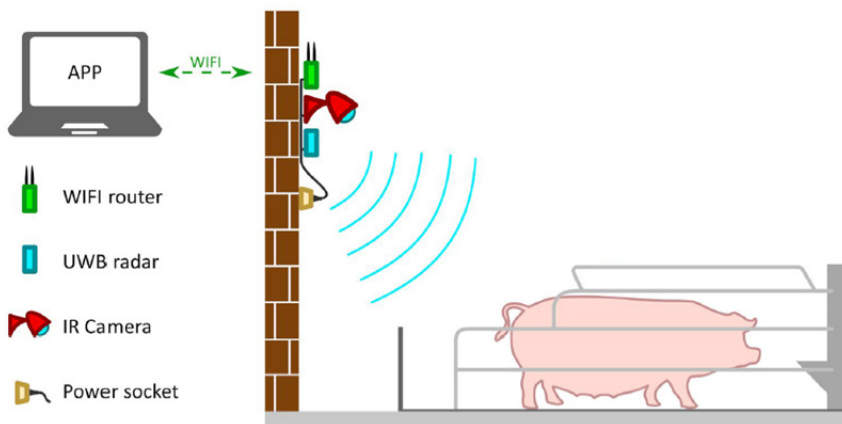


**Figure 1. Measurement setup with ultrawide-band signal sensor and infra-red camera placed on the wall behind the sow.**

Timely intervention by the farmer during parturition may decrease the risk of stillbirth, but farrowing duration and birth-interval lengths are hard to observe and manage for farmers. A potential technology to monitor the parturition is an ultra-wideband signal sensor which can be used for short-range positioning

applications (19). The ultrawide-band signal contains a broad range of frequencies and short pulses of this signal are sent out by the sensor to the sow. The sow absorbs part of the signal with certain frequencies and reflects the other part back to the sensor. The sensor picks up this reflected signal and sends this information to the cloud where it is stored for analysis. The reflected signal can be compared with the baseline signal, and information such as posture and breathing frequency can be determined with advanced signal analysis techniques.

This sensor was initially developed for a fall detection system in elderly people by the company FACTIC B.V. and was modified for parturition detection in sows. The sensor was placed on the wall behind the farrowing pen at the University farm Tolakker as can be seen in Fig 1. Major changes were made to the exterior of the sensor because pigs' excretion of ammonia abrades metals and plastics. Furthermore, the signal analysis techniques had to be adapted for sows to be able to detect variables such as change in posture, restless behavior (defined as the number of changes in posture) and frequency of breathing in time. After data collection, signal analysis procedures would need to be performed to measure characteristics such as the start of farrowing, farrowing duration and birth-interval lengths. Video recordings were made with an infrared camera for validation of the variables needed for automatic monitoring of parturition.

This case study was ended due to the high costs which came with further development of the hardware required for this technique and the labor needed for the development of signal analysis procedures.

### ***Second case study: monitoring movement directions in squirrel monkeys***

In the second case study, it was investigated whether a semi-free ranging squirrel monkey group could be monitored with use of radiofrequency identification (RFID) technology in the monkey zoo Apenheul in the Netherlands. A large group of more than 90 Bolivian squirrel monkeys (*Saimiri boliviensis*) is housed in a semi-free wooden enclosure to mimic their natural environment. The monkeys can roam freely and can spend their species-specific time budgets on travelling, foraging and other spatial related activities (20, 21). The large group consists of several subgroups which sometimes compete over their indoor enclosure during feeding time in the afternoon or during the night. On some occasions, this competition excludes individuals from the feeding or from sleeping inside the enclosure at night, which can result in cold related trauma. It is therefore of importance for the Apenheul zoo to monitor which individuals sleep outside



during the night and which individuals are potentially excluded from the feeding. Like most zoo animals, the squirrel monkeys are chipped with a passive RFID chip to allow identification of individuals for medical and management purposes. The passive chips are able to receive energy from electromagnetic waves that are sent out by an RFID antenna. When the passive chip is activated, they will send out their unique identification number which is measured by the antenna. A custom-made corridor equipped with two antennas was built by the company Dorset Identification BV and placed inside a corridor through which the squirrel monkeys have to move to enter and leave the indoor enclosure. These antennas measure the unique code of the RFID chip of the monkeys and send this information to an attached USB-logger which stores the received identification number and the corresponding time and date of this registration, as can be seen in Fig 2. Two antennas were used to be able to measure the walking direction of the monkeys in the corridor.

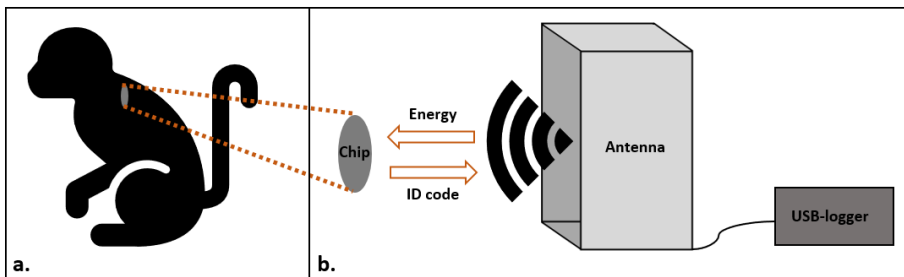


**Figure 2. Illustration of squirrel monkey with RFID chip (a) and RFID chip and antenna.** In Figure a, the passive RFID chip located between the shoulder blades of the squirrel monkey is shown. In Figure b, the antenna and radio waves sent out by the antenna are shown. These radio waves activate the chip causing it to send its unique identification number back to the antenna which is then stored by the USB-logger. Figure is used from student report (1) and designed by M. Weima.

The custom-made corridor should not hinder the squirrel monkeys from entering or exiting the enclosure. Furthermore, the construction should be robust and strong enough to not be damaged by the monkeys and should also not distract the monkeys which potentially can result in measurement noise. Also, the antennas should meet certain criteria to allow for accurate measurements. Therefore, different properties and construction methods were tested during this case study. For example, the direction of the coil inside the antenna was adapted to be able to measure all monkeys accurately and the distance between the two antennae was adapted to perform better with different movement speeds. Moreover, different

registration settings of the antennas were tested to investigate which settings were most beneficial to measure the monkeys entering and exiting the enclosure.

This case study was ended after two years due to the high costs which came with further development of the custom-made corridor and the limited possibilities of the RFID chips to measure stress related variables that were deemed important for biological conclusions.

### ***In summary***

For both case studies challenges with the sensor placement were encountered. Sensor attachment to the body of an animal can provoke stress because it hinders the animal in its movements or draws the attention of other animals which might lead to hurtful situations for the animal wearing the sensor. Most zoo animals, pets and laboratory animals are chipped with RFID chips which overcome this problem although the purposes are limited since no physiological parameters, such as heart rate, stress and body temperature, can be measured with this technique. When applying sensors invasively, the size of the sensor will limit its purposes due to the battery life span. The size of the battery is limited because the weight of the sensor should not exceed 5% of the body mass of the animal (22, 23). Furthermore, invasive sensors in wildlife animals are challenging since these animals should be captured and brought under general anesthesia to equip the animals with the sensor. Therefore, it's more logical to place sensors in the natural environment to measure these animals.

In both studies, measurement methods were chosen based on the fact that these techniques were easy applicable and were already available. The squirrel monkeys were already chipped with the RFID chips and the antenna technique was already used for behavioral research in poultry and pigs. Also, the ultra-wideband sensor was already under development for elderly people. However, other measurement methods might also be applicable or even more suitable for these two purposes. It is of importance to carefully consider which method is suitable and to evaluate all the advantages and disadvantages before modifying and applying such method.



For these two case studies, imaging methods could also be used for these purposes in combination with computer vision algorithm for automatic detection of specific traits. The benefits of imaging methods are that they can be applied from a distance, no attachment of sensors is coming into play and sometimes cameras are already available at the farm. However, for every new application new computer vision algorithms need to be developed or modified from another application which will also cost time and money.

## **Conclusion and outlook perspective**

The development of signal analysis procedures for automatic detection of hoof-events from IMU signals was successful and can improve gait classification in horses and enhance the clinical application of IMUs for both horses and cows. The preprocessing and selection of the signal characteristics should be appropriate for the procedures to work for signals collected under different circumstances, keeping in mind the specifics of the intended application.

The modification of measurement methods of horses to cows was successful with some minor modifications. These analysis procedures were used for the description of gait characteristics of clinically sound cows and to describe changes in the characteristics resulting from hind limb lameness. The adaptation of measurement methods and signal analysis procedures for horses to other animal species might be beneficial in the future since they benefit animal health and welfare and also will be more cost effective and time efficient compared with developing completely new methods.

In the future, machine learning algorithms might facilitate the use of IMU sensors for clinical applications and make IMUs easier to apply for training and exercises evaluation. Machine learning algorithms can automatically detect a certain event, for example hoof-on or hoof-off, from the signal without the need of extensive signal analysis procedures. In addition, these algorithms can also automatically detect lameness under different circumstances (24, 25). However, some of these machine learning algorithms act as a 'black box' and do not offer transparency needed for later adaptations. It is therefore of importance to first gain insight into the different machine learning algorithms and to carefully determine which signal characteristics is of importance for a specific application. Another technique that will be more often used in the future is computer vision, which eliminate the use of sensors or markers attached to the animal itself. Therefore, these techniques



might be even more easily applied in clinical settings. Furthermore, also for this video imaging, the development of computer vision analysis procedures is needed to detect specific hoof-events or gait characteristics.

In the general, the financial costs that come with sensor development and research can be substantial while the financial gains by using the sensors will depend on the application, the size of the market (i.e., the species) and the willingness of animal owners to pay. For some animals, such as horses and companion animals, the gains may justify the high costs due to the role of the animal in our community. Horses are very valuable in sport and as athletic companions, and companion animals such as dogs and cats find strong emotional attachment in the human owners. This is in contrast to farm animals, such as cows, pigs and chickens. These are kept in large numbers for food production and the emotional attachment to individual animals is less. Financial gains here should come from increased production at lower total cost.

Sensor application in veterinary medicine is exciting and will open many possibilities which were not yet available. In this thesis, various aspects and challenges are described that come with the application of sensors and the development of signal analysis procedures. By performing these studies, knowledge about hoof placement and unrollment pattern were obtained which will support the farrier and provide an objective analysis procedure for companies that develop tools to analysis hoof motion. Furthermore, explorative studies to the biomechanics of cows were performed to improve lameness detection and hence offer prevention tools that allow early detection and treatment in cows with claw conditions. The two cases studies presented in this thesis, illustrated some non-trivial challenges that come into play when adapting and applying sensor to animals or when adapting measurement methods between animal species.



## References

1. Weima M. Monitoring Bolivian squirrel monkeys (*Saimiri boliviensis*) with RFID technology. Dept. Animal Behaviour & Cognition, Utrecht University; 2020.
2. Hernlund E. Sport Surfaces in Show Jumping [Doctoral Thesis]. Uppsala: Swedish University of Agricultural Sciences; 2016.
3. Thomason JJ, Peterson ML. Biomechanical and mechanical investigations of the hoof-track interface in racing horses. *Vet Clin North Am Equine Pract.* 2008;24(1):53-77.
4. Telezhenko E. Effect of Flooring System on Locomotion Comfort in Dairy Cows. Skara: Swedish University of Agricultural Sciences; 2007.
5. Valenti RG, Dryanovski I, Xiao J. Keeping a Good Attitude: A Quaternion-Based Orientation Filter for IMUs and MARGs. *Sensors (Basel).* 2015;15(8):19302-30.
6. Bosch S, Serra Braganca F, Marin-Perianu M, Marin-Perianu R, van der Zwaag BJ, Voskamp J, et al. EquiMoves: A Wireless Networked Inertial Measurement System for Objective Examination of Horse Gait. *Sensors (Basel).* 2018;18(3).
7. Serra Bragança FM, Roepstorff C, Rhodin M, Pfau T, van Weeren PR, Roepstorff L. Quantitative lameness assessment in the horse based on upper body movement symmetry: The effect of different filtering techniques on the quantification of motion symmetry. *Biomedical Signal Processing and Control.* 2020;57:101674.
8. Braganca FM, Bosch S, Voskamp JP, Marin-Perianu M, Van der Zwaag BJ, Vernooij JCM, et al. Validation of distal limb mounted inertial measurement unit sensors for stride detection in Warmblood horses at walk and trot. *Equine Vet J.* 2017;49(4):545-51.
9. Alsaad M, Fadul M, Steiner A. Automatic lameness detection in cattle. *Vet J.* 2019;246:35-44.
10. Sprecher DJ, Hostetler DE, Kaneene JB. A lameness scoring system that uses posture and gait to predict dairy cattle reproductive performance. *Theriogenology.* 1997;47(6):1179-87.
11. Hildebrand M. Motions of the running cheetah and horse. *Journal of Mammalogy.* 1959;40(4).
12. Hildebrand M. The Quadrupedal Gaits of Vertebrates. *BioScience.* 1989;39(11):766-75.
13. Neethirajan S. Recent advances in wearable sensors for animal health management. *Sensing and Bio-Sensing Research.* 2017;12:15-29.
14. Pandolfi F, Edwards SA, Robert F, Kyriazakis I. Risk factors associated with the different categories of piglet perinatal mortality in French farms. *Prev Vet Med.* 2017;137(Pt A):1-12.
15. Edwards SA, Baxter EM. 11. Piglet mortality: causes and prevention. 2015:253-78.
16. Vanderhaeghe C, Dewulf J, de Kruijff A, Maes D. Non-infectious factors associated with stillbirth in pigs: a review. *Anim Reprod Sci.* 2013;139(1-4):76-88.
17. Oliviero C, Heinonen M, Valros A, Peltoniemi O. Environmental and sow-related factors affecting the duration of farrowing. *Anim Reprod Sci.* 2010;119(1-2):85-91.
18. Vallet JL, Miles JR, Brown-Brandl TM, Nienaber JA. Proportion of the litter farrowed, litter size, and progesterone and estradiol effects on piglet birth intervals and stillbirths. *Anim Reprod Sci.* 2010;119(1-2):68-75.
19. Alarifi A, Al-Salman A, Alsaleh M, Alnafessah A, Al-Hadhrani S, Al-Ammar MA, et al. Ultra Wideband Indoor Positioning Technologies: Analysis and Recent Advances. *Sensors (Basel).* 2016;16(5).
20. Brambell FWR. Report of the technical committee to enquire into the welfare of animals kept under intensive livestock husbandry systems. London: University College of North Wales; 1965.
21. Melfi VA, Feistner ATC. A Comparison of the Activity Budgets of Wild and Captive Sulawesi Crested Black Macaques (*Macaca nigra*). *Animal Welfare.* 2002;11:213-22.

22. Portugal SJ, White CR, Börger L. Miniaturization of biologgers is not alleviating the 5% rule. *Methods in Ecology and Evolution*. 2018;9(7):1662-6.
23. Jepsen N, Schreck C, Clements S, Thorstad EB. A brief discussion on the 2% tag/bodymass rule of thumb. *Proceedings of the Fifth Conference on Fish Telemetry; Rome2005*.
24. Taneja M, Byabazaire J, Jalodia N, Davy A, Olariu C, Malone P. Machine learning based fog computing assisted data-driven approach for early lameness detection in dairy cattle. *Computers and Electronics in Agriculture*. 2020;171:105286.
25. Yigit T, Han F, Rankins E, Yi J, McKeever K, Malinowski K. Wearable IMU-based Early Limb Lameness Detection for Horses using Multi-Layer Classifiers. 2020:955-60.





# Nederlandse samenvatting

Het doel van dit proefschrift is het ontwikkelen en analyseren van de signaal analyseprocedures voor het meten van hoefplaatsingen van paarden en het toepassen van signaal analyseprocedures van paarden voor de kreupelheid detectie bij koeien.

Paarden en koeien zijn gedomesticeerde vierbenige dieren waarvoor het goed functioneren van hun locomotie systeem een belangrijk aspect is voor het bevorderen en behouden van hun gezondheid, welzijn en prestatie. Het functioneren van het locomotie systeem kan worden bestudeerd door het observeren van de bewegingen en het gangpatroon van zowel paarden als koeien. Er zijn verschillende soorten methodes om deze bewegingen en het gangpatroon te bestuderen. De meest voorkomende en gebruikelijke methode is het visueel bestuderen van het gangpatroon. Echter, dit is een subjectieve methode waarvan de nauwkeurigheid afhankelijk is van de beoordelaar.

Objectievere methodes kunnen worden onderverdeeld in kinetische en kinematische methodes. De gouden standaard van de kinetische methodes is de *krachtplaat*. Deze methode meet de krachten onder de voeten als een paard of koe over de plaat loopt. De gouden standaard van de kinematische methodes is het *“optical motion capture systeem”*. Dit systeem meet de bewegingen van reflecterende bolletjes waarmee het dier wordt uitgerust. Deze reflecterende markers kunnen overal op het lichaam geplakt worden waardoor zowel de hoeken van gewrichten als de bewegingen van het boven- en onderlijf gemeten kunnen worden.

Een andere kinematische methode is de *“Inertial Measurement Units”* (IMUs). Het voordeel van deze IMUs is dat ze relatief goedkoop zijn en draadloos, waardoor ze ook buiten in het open veld te gebruiken zijn. Deze IMUs meten zowel de acceleratie als de hoekversnelling in 3 verschillende richtingen. Hierdoor wordt er veel data verzameld tijdens een meting. Deze data moeten eerst verwerkt worden voordat het geanalyseerd kan worden voor de studie van de bewegingen en het gangpatroon van paarden en koeien.

Er zijn signaal analyseprocedures ontwikkeld voor de automatische detectie van bewegingsaspecten van de hoef gemeten met IMUs. De uitkomst van deze signaal analyseprocedures zijn vervolgens vergeleken met de gouden standaard, krachtplaat en optical motion capture system. In **hoofdstuk 2** zijn er signaal analyseprocedures ontwikkeld voor het automatisch detecteren van twee kenmerkende bewegingsaspecten van de hoef. De eerst is de hoef plaatsing

("hoof-on") en de tweede is het optillen van de hoof ("hoof-off"). Voor deze beide zijn twee signaal analyseprocedures ontwikkeld. De eerste procedure detecteert de hoof events op basis van het acceleratie signaal en de tweede procedure op basis van het hoekversnellingssignaal. De uitkomst van deze twee signaal analyseprocedures is in dit onderzoek vergeleken met de uitkomst van de krachtplaat en geëvalueerd ten opzichte van elkaar.

In **hoofdstuk 3** zijn er twee signaal analyseprocedures ontwikkeld voor het detecteren van de start van het afrollen van de hoof voorafgaand aan het optillen ("break-over phase onset"). De eerste procedure werkt op basis van het acceleratie signaal en de tweede procedure op basis van het hoekversnellingssignaal. De uitkomst van de twee procedures is in dit onderzoek vergeleken met de uitkomst van de krachtplaat en "optical motion capture system" en geëvalueerd ten opzichte van elkaar.

In **hoofdstuk 2 en 3** vielen twee dingen op: 1) de hoof plaatsing ("hoof-on") werd beter gedetecteerd met de procedure die werkt op basis van het hoekversnellingssignaal, 2) het optillen van de hoof ("hoof-off") en de start van het rolmoment ("break-over phase onset") werden beter gedetecteerd met de procedure die werkt op basis van het acceleratie signaal. De resultaten van deze studies lieten zien dat het mogelijk is om signaal analyseprocedures te ontwikkelen voor het automatisch detecteren van specifieke bewegingsaspecten van de hoof en het afrollen van de hoof met goede nauwkeurigheid. Deze signaal analyseprocedures kunnen worden gebruikt om gangpatronen te bestuderen bij paarden en koeien.

In **hoofdstuk 4** wordt beschreven hoe de signaal karakteristieken van looppatronen van een niet kreuple koe eruitzien. Deze looppatronen zijn gemeten met 11 IMUs die geplakt zijn op verschillende anatomische locaties van een koe. De signalen, gemeten met deze IMUs, zijn geanalyseerd met signaal analyseprocedures die ontwikkeld zijn voor paarden. Deze procedures bleken ook te kunnen werken voor signalen gemeten op koeien, waarbij kleine aanpassingen konden worden gemaakt om de procedures iets nauwkeuriger te maken.

In **hoofdstuk 5** is er onderzoek gedaan naar de signaal karakteristieken van kreuple koeien. Er is een begin gemaakt met het analyseren van IMU-data gemeten op koeien die kreupel zijn en onderzocht welke karakteristieke bewegingspatronen veranderen als een koe kreupel is. Dit is onderzocht door eerst gezonde koeien een stukje te laten lopen en daarna deze koeien tijdelijk



kreupel te maken door een blokje onder hun klauw te plakken en deze na de meting weer te verwijderen. Dit was een geheel nieuwe methode om kreupelheid te simuleren. Ook voor deze studie zijn er procedures gebruikt die oorspronkelijk voor paarden ontwikkeld zijn.

In **hoofdstuk 4 en 5** bleek dat signaal analyseprocedures die ontwikkeld zijn voor paarden ook te gebruiken zijn voor koeien met wat kleine modificaties. Het hergebruiken van signaal analyseprocedures voor een andere diersoort lijkt daarom efficiënt, want dan hoeven er geen nieuwe analyseprocedures ontwikkeld te worden. Het hergebruik van signaal analyseprocedures zou in de toekomst ook op andere diersoorten kunnen worden toegepast.

Het toepassen van sensortechnologieën vanuit de humane naar de veterinaire gezondheidszorg kan op verschillende manieren. Twee voorbeelden zijn hier beschreven aan de hand van twee casestudies.

De **eerste casestudie** gaat over de ontwikkeling van een geboorte sensor voor zeugen om de hoge biggensterfte te verlagen. Deze sensor zendt "ultrawide-band" signalen (d.w.z. signalen met veel verschillende frequenties) uit. Een deel van de signalen wordt geabsorbeerd door de zeug, terwijl een ander deel wordt gereflecteerd naar de sensor. Deze gereflecteerde signalen kunnen worden geanalyseerd om de lichaamshouding en de ademhalingsnelheid van de zeug te meten. Daarnaast kan er ook worden bekeken of de zeug contracties heeft. Deze geboorte sensor zou in de toekomst, na een validatie proces, kunnen worden door ontwikkeld naar een beveiligings- en alarmeringssysteem voor de boer. Helaas is deze casestudie na één pilot meting stopgezet vanwege een tekort aan financiering.

De **tweede casestudie** gaat over het bestuderen van de groepsdynamiek binnen een groep doodshoofdaapjes. Deze groep doodshoofdaapjes leeft in de Apenheul en bestaat uit 90 individuen. Binnen deze groep zijn er subgroepen ontstaan die strijden om voedsel en een plek in het nachtverblijf. De Apenheul wilde daarom graag kunnen meten welke aapjes het verblijf binnengaan en/of verlaten, zodat zij zicht krijgen op het ontstaan van subgroepen en welke subgroepen met elkaar strijden om voedsel en het nachtverblijf. De doodshoofdaapjes waren gechipt met een RFID-chip en de code op deze chip kon worden uitgelezen met een antenne. Voor deze casestudie was er een tunneltje gebouwd met 2 antennes waardoor met data analyse te zien was welke aap in welke richting door het tunneltje beweegt. Helaas is ook deze casestudie na een validatie en twee pilot metingen stopgezet vanwege een tekort aan financiering.

In dit proefschrift zijn een aantal verschillende studies beschreven over het toepassen van sensoren in het veterinaire veld en de data-analyse van de verzamelde data. Het ontwikkelen van signaal analyseprocedures voor de automatische detectie van hoef plaatsingen, het afrollen van de hoef en karakteristieke bewegingspatronen kan de objectiviteit vergroten en de analysetijd verlagen. Dit is van belang omdat het gebruik van sensoren in het veterinaire veld veel mogelijkheden biedt met betrekking tot het monitoren van diergezondheid en -welzijn. In de toekomst kunnen "machine learning algoritmes" helpen om de data sneller te analyseren. Daarnaast zijn beeldvormende methodes zoals "computer vision analysis" ook veel belovende methodes voor toepassingen in een klinische setting.



# Dankwoord

Dit proefschrift was er niet geweest zonder het bonte gezelschap van heel veel koeien, paarden en een grote groep mensen.

Allereerst wil ik mijn begeleiders, **Hans** en **Mirjam**, bedanken voor de kans om als technisch geneeskundige te promoveren bij diergeneeskunde. Dankzij jullie enthousiasme en steun heb ik mij vanaf het begin welkom gevoeld en heb ik deze thesis tot een goed einde gebracht. De combinatie van jullie expertise en persoonlijkheden heb ik vanaf het begin een interessante en leuke combinatie gevonden.

Secondly, I would like to thank my daily supervisors, **Filipe** and **Elin**, who showed me what it really means to be a great researcher with their passion and endless enthusiasm, creativity and perseverance.

Daarnaast wil ik graag alle mensen met wie ik heb samengewerkt in dit traject bedanken voor hun inbreng en support.

In de periode van mijn PhD heb ik veel leuke en leerzame momenten beleefd met de vele collega's. Een paar wil ik extra benoemen: **Sanne** en **Ellen**. Wij hebben een hele fijne en goede sfeer weten te creëren met elkaar op de werkkamer. Ik zal deze fijne en grappige momenten nooit vergeten en in mijn achterhoofd houden als voorbeeld van hoe een goede werksfeer hoort te voelen. Verder wil ik **Jesse**, **Annika** en **Annelies** bedanken voor de fijne en leuke tijd. Ik heb mij altijd erg welkom en gesteund gevoeld bij jullie.

De **andere collega's** wil ik graag bedanken voor de gezellige koffie- en lunchpauzes. Jullie verscheidenheid en persoonlijkheid heeft mijn horizon verbreed en een inkijk gegeven in de veterinaire wereld met zijn merkwaardige trekjes die daarbij horen. Ik zal deze ervaring zeker meenemen in het vervolg van mijn carrière.

I also would like to thank all the **PhD student from abroad**, for sharing their cultures and insight with me during the coffee and lunch breaks. And of course, I want to thank all the lovely **Swedish people** who showed me their beautiful country and their Swedish hospitality. I think back with utter joy to our sushi evenings, trips and fika's. I'm honored that you all let me in so easily and made me feel at home.

Aan alle lieve mensen die mij hebben bijgestaan, ik wil jullie allemaal bedanken voor de momenten die wij hebben gedeeld, of ze nu kort of lang waren, ze hebben allemaal bijgedragen aan waar ik nu sta.

Allereerst **mijn ouders**, zonder hen was mijn bestaan sowieso niet aan de orde geweest. Zij hebben een zeer grote bijdrage geleverd aan mijn ontwikkeling en een stempel gedrukt op de persoon die ik ben geworden. Zonder hen had ik niet de discipline gehad die mij gebracht heeft waar ik nu sta en niet het doorzettingsvermogen om dit prachtige einddoel te bereiken.

**Mijn oma** heeft hier zeker ook aan bijgedragen. Zonder haar en oplossingsgerichtheid, eeuwige geduld en kracht om mij weer moed in te spreken, was ik al lang en breed afgehaakt.

Natuurlijk ook **mijn zusje** want zussen zijn is iets speciaals. Je doorloopt samen een hele periode van je leven waarin je zusterlijke momenten deelt op een eigen unieke zussen manier. Het moment dat wij onze eigen, meer afzonderlijke, levens gingen leiden was even lastig, ook omdat de hemelsbrede afstand tussen ons opeens een stuk groter werd. Gelukkig werd bleef onze persoonlijke afstand nog steeds even klein door de jaren heen.

En uiteraard **Reina**, die steeds meer in ons gezin gegroeid is en al onze eigenaardig- en lastigheden heeft weten te trotseren. Jouw rol en invulling in ons gezin en leven weet ik steeds meer te waarderen.

Als laatste wil ik **Wil** enorm bedanken voor haar coaching en steun waarop ik kon terugvallen toen het einde naderde en ik het overzicht verloor.

Naast deze familieleden zijn er natuurlijk mijn vriendinnen, in het speciaal **Marie** en **Eleonora**, jullie ken ik het al super lang en we delen een hele intieme en speciale band. Ik hecht erg veel waarde aan onze vriendschap, ontwikkeling, groei en steun die wij door de jaren heen hebben gemaakt en ervaren. Bij jullie kan ik mij echt thuis voelen en mezelf laten zien in alle momenten.

Van de vele roeigenootjes die ik heb versleten is er eentje gek genoeg geweest om mij al een aantal jaren met open armen te ontvangen. Lieve **Niki**, ik vind het ontzettend leuk dat wij weer samen in een roeiteam roeien en vriendinnen zijn geworden. **Hella** wil ik bedanken voor de vroege ochtenden in het park en fietstochtjes met hilarische afloop. De rest van **Nooitgedacht** wil ik graag

bedanken voor alle mooie roeimomenten die wij hebben beleefd en ik hoop dat wij nog vele overwinningen mogen vieren.

Verder wil ik Moeders Overste, **Nicole**, bedanken voor haar tomeloze inzet en steun. Voor de bitterballen, bier, chocolade en arancini tijdens mijn quarantaine want zonder jou zou ik uitgehongerd zijn voordat ik kon sneuvelen aan COVID-19. En daarnaast heb ik met jou hele “milky ways” gevormd met sterren en vervolgens weer opgedronken met koffie.

Ook wil ik **Machteld** bedanken voor haar boeiende en leerzame gesprekken. Ik hoop dat ik nog jaren van jou kan blijven leren en kan blijven bewonderen over hoe jij alfa, bèta en gamma samenbrengt in het leven. Jij bent veelte bescheiden over wat jij ons, heel Nederland en daarbuiten, te bieden hebt. Jij bent mijn Al-Wahid!

Ook **Esmée** en **Ikaika** wil ik bedanken voor al hun sportieve support en steun in deze moeilijk corona winter en daarna. Zelfs met temperaturen onder nul bleven we de kou trotseren om fit te blijven en mentale struggles te overwinnen.

Dan wil ik **Seline** bedanken voor alle reflecties en relativerende gesprekken met de kopjes thee tijdens de lockdown en de drankjes op de terrasjes. En **Paul**, **Hannah** en **Ellis** voor alle etentjes en lunch wandelingen.

Als laatste wil ik **Ouissal** bedanken voor haar warme momenten in de koude wintertijd. Bij jou ging ik altijd weg vol schoonheid van binnen en van buiten!

Het grootste gevaar van een dankwoord is dat je iemand vergeet bij naam te noemen. Dit neemt echter niet weg dat ik dankbaar ben voor de momenten die wij gedeeld hebben. En ik hoop dat ik jullie mijn dankbaarheid en waardering heb kunnen laten merken in de momenten die wij hebben gedeeld met elkaar.

De meeste mensen eindigen dan hier vaak hun leven... Oh nee, hun dankwoord met het beschrijven van de hoeveelheid steun die hun levenspartner, ook wel geliefde, aan hen gegeven heeft tijdens het afronden hun promotie. Echter, deze partner is niet op tijd in mijn leven opgedoken en ik heb geen katten of geraniums om me achter te verschuilen... It's just me







# Authors affiliations

- P. H. Andersen** Department of Anatomy, Physiology and Biochemistry, Swedish University of Agricultural Sciences, Uppsala, Sweden
- K. Ask** Department of Anatomy, Physiology and Biochemistry, Swedish University of Agricultural Sciences, Uppsala, Sweden
- C. Bergsten** Department of Clinical Sciences, Swedish University of Agricultural Sciences, Uppsala, Sweden
- S. Bosch** Inertia Technology B.V., Enschede, The Netherlands & Department of Computer Science, Pervasive Systems Group, University of Twente, Enschede, The Netherlands
- E. Hernlund** Department of Anatomy, Physiology and Biochemistry, Swedish University of Agricultural Sciences, Uppsala, Sweden
- M. Nielen** Department Population Health Sciences, Faculty of Veterinary Medicine, Utrecht University, Utrecht, The Netherlands
- M. Rhodin** Department of Anatomy, Physiology and Biochemistry, Swedish University of Agricultural Sciences, Uppsala, Sweden
- F.M. Serra Bragança** Department Clinical Sciences, Faculty of Veterinary Medicine, Utrecht University, Utrecht, The Netherlands
- E. Telezhenko** Department of Biosystems and Technology, Swedish University of Agricultural Sciences, Alnarp, Sweden
- M. Tijssen** Department Population Health Sciences, Faculty of Veterinary Medicine, Utrecht University, Utrecht, The Netherlands
- J.P. Voskamp** Rosmark Consultancy, Wekerom, The Netherlands





# Curriculum Vitae

## **Curriculum Vitae**

Marij Tijssen was born on the 7<sup>th</sup> of January 1988 in Amsterdam, the Netherlands.

In 2007, she finished high school (VWO) at the Montessori Lyceum Amsterdam and travelled through Thailand and Laos for 6 months. In Nong Khai, she volunteered in an English teaching program for high school children and monks.

In 2008, she moved house to study Technical Medicine at Twente University (Enschede). She obtained her bachelor's degree in 2012 and subsequently enrolled in the specialization track Medical Sensing & Stimulation. For this specialization track, she performed four clinical internships in different medical areas throughout the Netherlands. In 2016, she graduated at the University Medical Center Utrecht at the Clinical Neurophysiology department with the thesis called "Development of automatic detector for Single Pulse Electrical Stimulation data based on template detection".

After completing her Master's, Marij started her PhD at the faculty of Veterinary Medicine at the Utrecht University. During a period of 4 and a half years, she worked on two projects; the development of different signal analysis procedures to study the hoof motion in horses and the study of the kinematic characteristics of dairy cattle based on measurement and signal analysis procedures that had been adapted from horses. The results of these two projects are presented in this thesis.

## List of Publications

**Tijssen M**, Ask K, Braganca FM, Andersen PH, Telezhenko E, Bergsten C, Nielen M, Hernlund E, Rhodin M. (In preparation). "Biomechanical gait characteristic changes in induced hind limb lameness in dairy cows."

**Tijssen M**, Serra Braganca FM, Ask K, Rhodin M, Andersen PH, Telezhenko E, Bergsten C, Nielen M, Hernlund E. (2021). "Kinematic gait characteristics of straight line walk in clinically sound dairy cows." PLOS One 16(7)

**Tijssen M**, Hernlund E, Rhodin M, Bosch S, Voskamp JP, Nielen M, Serra Braganca FM. (2020) "Automatic hoof-on and -off detection in horses using hoof-mounted inertial measurement unit sensors." PLOS One 15(6)

**Tijssen M**, Hernlund E, Rhodin M, Bosch S, Voskamp JP, Nielen M, Serra Braganca FM. (2020) "Automatic detection of break-over phase onset in horses using hoof-mounted inertial measurement unit sensors." PLOS One 15(5).

Farag F, Koens M, **Tijssen M**, de Jong S, Fabius T, Tromp J, van Breda H, Smeets J, Feitz W, Heesakker J. (2016). "Electroanatomical Mapping of the Urinary Bladder." International Neurourology Journal 20(2): 164-167.